JYVÄSKYLÄ STUDIES IN COMPUTING
146

Tero Tuovinen

Analysis of Stability of Axially Moving Orthotropic Membranes and Plates with a Linear Non-homogeneous Tension Profile

JYVÄSKYLÄN YLIOPISTO

JYVÄSKYLÄ STUDIES IN COMPUTING 146

Tero Tuovinen

Analysis of Stability of Axially Moving Orthotropic Membranes and Plates with a Linear Non-homogeneous Tension Profile

Esitetään Jyväskylän yliopiston informaatioteknologian tiedekunnan suostumuksella
julkisesti tarkastettavaksi yliopiston Agora-rakennuksen salissa AgAud3
joulukuun 17. päivänä 2011 kello 12.

Academic dissertation to be publicly discussed, by permission of
the Faculty of Information Technology of the University of Jyväskylä,
in building Agora, auditorium AgAud3, on December 17, 2011 at 12 o'clock noon.

UNIVERSITY OF JYVÄSKYLÄ

JYVÄSKYLÄ 2011

Analysis of Stability of Axially Moving Orthotropic Membranes and Plates with a Linear Non-homogeneous Tension Profile

JYVÄSKYLÄ STUDIES IN COMPUTING 146

Tero Tuovinen

Analysis of Stability of Axially Moving Orthotropic Membranes and Plates with a Linear Non-homogeneous Tension Profile

UNIVERSITY OF JYVÄSKYLÄ

JYVÄSKYLÄ 2011

Editors
Timo Männikkö
Department of Mathematical Information Technology, University of Jyväskylä
Pekka Olsbo, Ville Korkiakangas
Publishing Unit, University Library of Jyväskylä

URN:ISBN:978-951-39-4578-7
ISBN 978-951-39-4578-7 (PDF)

ISBN 978-951-39-4577-0 (nid.)
ISSN 1456-5390

Jyväskylä University Printing House, Jyväskylä 2011

ABSTRACT

Tuovinen, Tero
Analysis of Stability of Axially Moving Orthotropic Membranes and Plates with a Linear Non-homogeneous Tension Profile
Jyväskylä: University of Jyväskylä, 2011, 104 p.
(Jyväskylä Studies in Computing
ISSN 1456-5390; 146)
ISBN 978-951-39-4577-0 (nid.),
ISBN 978-951-39-4578-7 (PDF)
Finnish summary
Diss.

The topic of this thesis relates to the classical problem of the stability of moving materials. We have studied problems of dynamics and stability of a moving web, travelling between two rollers at a constant velocity using analytical and numerical approaches. The stability of the plate is investigated with the help of studies of small out-of-plane vibrations. The influence of linearly distributed in-plane tension on the characteristics of the web vibrations is studied as well.

Our analysis is based on models of axially moving orthotropic membranes and plates. The static forms of instability are investigated using numerical methods, and an estimate for the divergence speed of a membrane is expressed with the help of in-plane strain and material parameters. The original dynamic plate problem is reduced to a two-dimensional spectral problem and solved using analytical techniques. As a result, the minimal eigenvalue and the corresponding buckling mode are found. This study has been extended to consider a linear non-homogeneous tension profiles as well.The materials based on published articles have been extended and re-written and new results have been introduced for the thesis.

The conclusion of this thesis is that the effect that originates from the orthotropic material is moderate, while the tension profile plays an important role in the shaping of the buckling mode. It can be concluded that inhomogeneities in the applied tension may significantly decrease the critical web velocities, and even small inhomogeneities in the tension may have a large effect on the divergence forms. In particular, the effect of the localization of transverse displacements in the vicinity of free boundaries is illustrated. The obtained results match the experimental knowledge; they can be used for an effective estimation of the critical velocity as a function of mechanical and geometric problem parameters.

Keywords: Stability, Axially Moving Plates, Orthotropic Material, Paper Web, Critical Velocity

Author

M.Sc. Tero Tuovinen
Department of Mathematical Information Technology
University of Jyväskylä
Finland

Supervisors

Professor Pekka Neittaanmäki
Department of Mathematical Information Technology
University of Jyväskylä
Finland

Professor Nikolay Banichuk
Institute for Problems in Mechanics
Russian Academy of Sciences
Russia

Professor Raino Mäkinen
Department of Mathematical Information Technology
University of Jyväskylä
Finland

Reviewers

Professor Gennadij Leonov
Institute of Problems of Mechanical Engineering
Russian Academy of Sciences
Russia

TkT Kari Juppi
Metso Paper Inc.
Finland

Opponents

Professor Heikki Koivo
Department of Automation and Systems Technology
Aalto University
Finland

TkT Kari Juppi
Metso Paper Inc.
Finland

ACKNOWLEDGEMENTS - KIITOKSET

First of all, I want to thank my supervisors. I would like to thank Professor Nikolay Banichuk; you have taught me how to do science. I would like to thank Professor Pekka Neittaanmäki for all the trust he has had in me. I would also like to express my gratitude to Professor Raino Mäkinen and Professor Timo Tiihonen; your comments have been valuable and you have acted as a dynamic counterforce during my studies. I would also like to thank Gennadi Leonov, Kari Juppi, and Heikki Koivo for participating in the research process as preliminary examiners or opponents. This work has been financially supported by Tekes (MASI, FiDiPro, and Digital Product Process), Academy of Finland, European Social Fund, and COMAS graduate school, which are hereby acknowledged.

Tutkimuksen tekeminen on joukkuepeliä ja olen saanut työskennellä aivan mahtavassa joukkueessa kuluneiden vuosien aikana. Nikolay Banichuk, Juha Jeronen, Tytti Saksa, Matti Kurki ja Maria Tirronen, kiitos kaikesta, ilman teitä en olisi tässä tilanteessa. Tahdon kiittää myös Matti Nurmiaa sekä Ilona Riikosta väitöskirjan oikolukemisesta.

Tahdon kiittää seuraavia henkilöitä laitokselta, tiedekunnan palvelukeskuksesta, IT-tuesta sekä Agora Centeristä: Katia, Juhoa, Ilkkaa, Auria, Timoja, Villejä, Tommia, Tuomoja, Sameja, Sannoja, Kirsiä, Jacquesia, Ollia, Immanuelia, Mariaa, Juliaa, Jussia, Jonnea, Antti-Juhania, Jaanoja, Veskua, Kaisaa, Tuomaksia, Paavoa, Pekkaa, Ilpoa, Sergeytä, Saulia, Jukkia, Jukka-Pekkaa, Hongia, Annemaria, Tapaneja, Juhania, Santeria, Joukoa, Petriä, Petteriä, Leaa, Outia, Marja-Leenaa, Tiinaa, Johannaa, Seijaa, Jaria, Anttia, Niinoja, Mikkoa, Esaa, Anua ja Päiviä. Lisäksi tahdon kiittää myös sinua, joka olet työskennellyt kanssani ja huomasit, että nimesi puuttuu listalta; olet aina ollut meistä se tarkempi. Kiitos teille kaikille siitä, että olette auttaneet minua jaksamaan työssäni ja mahdollistaneet tutkimuksen tekemisen.

Tahdon kiittää Savikylän Tapiola Ry:tä sekä Korpilahden Erämiehet Ry:tä keskeisen tutkimusympäristön järjestämisestä sekä Korpilahden VPK Ry:n väkeä tuesta ja kannustavasta suhtautumisesta akateemiseen harrastukseeni liittyen.

Tahdon muistaa ja kiittää Paavo Murasta sekä Helvi Rysää niistä lukuisista keskusteluista, joilla tietoa ja kokemuksia siirrettiin sukupolvilta seuraaville. Tahdon kiittää Tarja ja Markku Ollilaista, Paula ja Emma Ollilaista, Piia ja Jyri Leppästä, Tiina ja Mikko Jokista, Jouni Korhosta, Merja ja Ilkka Myllyperkiötä, Päivi ja Pauli Murasta, Senja ja Markku Baljaskinia, Petteri Hakasta, Osmo Tuovista, Marja Tuovista, Mika Baljaskinia, Antti Saastamoista, sekä Anna Sarkkista siitä, että olette tukeneet minua eri tavoin elämäni aikana.

Tahdon kiittää vanhempiani, Arvo ja Leena Tuovista, kaikesta siitä rakkaudesta, jonka he ovat minulle antaneet. Tahdon kiittää sisariani Saria ja Jonnaa, joiden kautta olen oppinut tutkimuksen vaatimaa kärsivällisyyttä.

Ennen kaikkea tahdon kiittää vaimoani Tanjaa sekä Ronjaa, Eemeliä ja Oskaria. Te olette elämäni ja tahdon omistaa tämän kirjan teille.

LIST OF SYMBOLS

α	Skewness parameter for a non-homogenous tension profile
a	Acceleration
A, B	Constants
β_i	Mechanical parameters for isotropic and orthotropic materials
$a(f, g)$	Bilinear form of functions f and g
b	Width of the membrane or plate
C	Wave speed in a string
C_{ij}	Elastic moduli
D	Bending rigidity
D_0	Characteristic bending rigidity
D_1	Component of the D along the x-axis
D_2	Component of the D along the y-axis
D_3	Component of the D along the z-axis
ε	Small parameter
η	Dimensionless parameter y/b
$\in \Omega$	Belong to Ω
E	Young's modulus
E_1	Component of E in the x-direction
E_2	Component of E in the y-direction
F	Force
f^a	Function, antisymmetric with respect to the x-axis
f^s	Function, symmetric with respect to the x-axis
$\bar{g}$	Complex conjugate of function g
γ	$\sqrt{\lambda}$
γ_*	Square-root from the lowest eigenvalue
$\gamma_{\min}$	$\sqrt{\lambda_{\min}}$
G_{12}	Dimensionless shear modulus
G_H	Shear modulus using the Huber quantity (or Huber estimate)
h	Thickness of the material
H_i	Dimensionless bending rigidity
∞	Infinity

$\int_\Gamma$	Integral over the boundary Γ
$\int_\Omega$	Integral over the domain Ω
Im	Imaginary part of the parameter
$()x = 0$	Action location
Δ	Laplace operator
ℓ	Length of the membrane or plate
λ	Eigenvalue
$\lambda_{\min}$	Minimal eigenvalue
$\mathcal{L}^B$	Bending operator
$\mathcal{L}^M$	Membrane operator
μ	Dimensionless constant $\frac{\ell}{\pi b}$
M	Mass
m	Basis weight, mass per unit area
n	Normal component
Ω	Domain of the problem
$\frac{\partial u}{\partial x}$	First partial derivative of u with respect to x
$\frac{\partial^2 u}{\partial t^2}$	Second partial derivate of u with respect to t
$\frac{\mathrm{d}u}{\partial t}$	First total derivative of u with respect to t
P	Force to stability loss
Pe	Euler value of the force to stability loss
Re	Real part of the parameter
σ_{xx}	In-plane stresses
σ_{xy}	In-plane shear stress
σ_{yy}	In-plane stresses
s	Complex characteristic parameter
T	Tension
T_{xx}	Tension coefficients
T_{xy}	Tension coefficients
T_{yy}	Tension coefficients
u	Axial displacement
u_0	Prescribed displacement

ν	Poisson ratio
ν_{12}	Poisson ratio in the xy plane when stretching is applied in the x- direction
ν_{21}	Poisson ratio in the xy plane when stretching is applied in the y -direction
V_0	Constant velocity of the moving material, $\frac{du}{dt}$
V_0^{div}	Value of divergence speed
V_0^{fl}	Value of flutter speed
ω	Frequency of small transverse vibrations
w	Horizontal displacement
x	Coordinate in the machine direction
Y	Airy stress function
y	Coordinate in the co-machine direction

LIST OF FIGURES

LIST OF TABLES

CONTENTS

1 INTRODUCTION

In this thesis, the problems of the dynamics and stability of a moving web are studied using analytical and numerical approaches. More than a simple case study, this thesis is a representation of the real-life problems from the paper industry which can be solved efficiently with the methods of mathematical modeling and numerical analysis. The thesis follows the general monograph style. It offers a more elaborate and extensive review of the previously published articles, and new results have been drawn from them. The monograph style offers the reader an easier way to follow the study as an entity. The self-contained structure of the thesis does not require a particularly comprehensive review of previous research but it introduces the key elements and findings with regard to the moving web.

The key issue of this thesis is how to form the simplest model possible that still yields valuable and reliable information of the nature of the problem. The approaches used are classical and they rely heavily on studies from the 19th century.

Our goal during this study have been to combine classical approaches with the modern numerical methods and to gain a better understanding of even very complex phenomena from the process industry. The objective of this study, as is usual in mathematical modeling, is to find the characteristics of the behaviour of the moving material and to find solutions to practical problems.

1.1 Some remarks about mathematical modeling

Before proceeding to the details of the case, a few words related to mathematical modeling and numerical analysis in general are necessary. As all the experts in the field know, mathematical modeling is an art and like in every form of art, the artist makes the difference. We must combine the ideas from physics and mathematics with the knowledge of numerical analysis and mathematical modeling in a clever way to achieve the best solutions. In addition, we always have to re-

member the objective and the limitations of the models; some of the limitations can be quite tricky. Nevertheless, the best property of this field of science is that mathematical modeling is abstract by its nature and it is possible to use it in many areas, such as engineering and economy (see, for example [61] and [44]). In practice, this means that models from physics or chemistry can be used as a source of ideas for models in economics and vice versa. This abstraction opens up the possibility that the results of a single case can be useful in many other situations as well, and for that reason mathematical modeling, including numerical simulations, has become the third basic method along with theoretical and experimental studies.

It is sometimes hard to remember the limits of mathematical models, especially nowadays, when we have many popular types of software, which provide an easy access to the world of numerical simulations. We have to keep in mind that models are always simplifications of real phenomena, even the most sophisticated or complex ones. Especially, in complex cases where measurements are not available, many restrictions are easily broken by accident. An expert in the field must know how to ask the right questions, how to solve models in a reliable manner, and how to correctly analyze the results.

The field itself has taken a giant leap in the last century. In the past, the researchers had very limited resources for numerical solutions as everything had to be done with pen and paper. In the 20th century and especially during its last decades, we witnessed a technological revolution of an unprecedented scale. Our computing power and facilities have increased dramatically in a very short time. Today, everyone has access to very powerful computing machines, and the computing capacity in total has increased in a nearly unlimited manner. All this has changed the attitude towards solving problems lightly; a temptation to use ”brute force” methods has increased and wasting computing power has become usual. An easy example of this is the finite element field, where discretization is created by meshing the structure. With modern computing power, researchers use much denser meshes than the precision of the model would support. Careless researchers do not notice this and, at the same time, they underestimate the value of decent mathematical modeling principles. It is fortunate that recently attention has turned to this misbehavior, see e.g. book by Neittaanmäki and Repin [64] and Ph.D. thesis by Mali [51].

1.2 Motivation by application

In this thesis, a complex industrial problem is defined and divided into small concrete cases that contain stepwise increasing amounts of information. The idea has been to develop a restricted package which can be implemented later on as a tool for process analysis. We have tried to avoid large steps in theory, while some details have been quite intensively studied. We hope that the readers of this thesis will contribute to our work and inform us about any errors. Ignoring mistakes

and avoiding details easily leads to cumulative errors in the whole research field and corrupts the science.

The impetus for this research came from the industry, more precisely from Metso Paper, Inc., where the runnability in the paper making process is a highly relevant problem. The productivity of the paper mill is strongly dependent on the efficiency and reliability of the running web. The importance of the subject becomes concrete in the following example:

Example Let us consider a middle-sized LWC (lightweight coated) paper mill with a production of about 250,000 t/year with a utilization rate of 87%. The total energy consumption at an LWC paper mill is about 2200 kWh/t. Part of this energy is used as electric power, and the rest is mainly heat (steam) and gas. Let us assume that the utilization rate decreases by 1% due to poor runnability (e.g., the web break rate increases or the quality of paper deteriorates excessively). Note that a paper mill cannot stop running during a web break; instead, it has to continue operating but without any production. The consequence of this 1% decrease in the utilization rate is a loss of 2900 t in production. During breaks (see Figure 1), the paper mill uses about 6400 MWh of energy. The industrial energy price is about 7 cents/kWh (electric power being more expensive and thermal power cheaper). This assumption means a loss of 448,000 euros / year in wasted energy. The price of LWC paper is approximately 700 euros / t and this means a loss of about 2,030,000 euros in sales. A coarse approximation in the total price of a 1 % decrease in the utilization rate is thus 2.5 million / year. Moreover, it is noteworthy that this is the effect in a single paper machine.

At the very beginning of the research project, it was clear that the whole problem with full details cannot be solved even, by using the methods and computing power available today. This kind of fluid-structure interaction problem with turbulent flows and a viscoelastic, nearly plastic material is just too complex. The aim of the research was to create a mathematical model which simplifies the problem sufficiently while still providing an understanding of the phenomenon, qualitatively and quantitatively. A major issue, and a known challenge, was the fact that the measurements of the system were either highly expensive or, as usual, impossible. From Figure 2 on the next page and Figure 3 on page 19 one can get an insight on how complex and large paper machines actually are.

The overall goal of this study is to invent tools for controlling and analyzing such systems and to increase their productivity. From the literature, it can be seen that travelling flexible strings, membranes, beams, and plates are the most common models used in such studies. As the main target of this thesis, we chose to analyze the critical issue of web runnability, i.e. to find the conditions under which the velocity of the web exceeds the safe value and the vibration of the web increases without a limit. For this we need to learn more about the stability of an axially moving web, how disturbances begin, and what the parameters controlling the onset of instability are. This is important because the occurrence of instability can cause, in particular, damage in a paper web and breakage of trans-

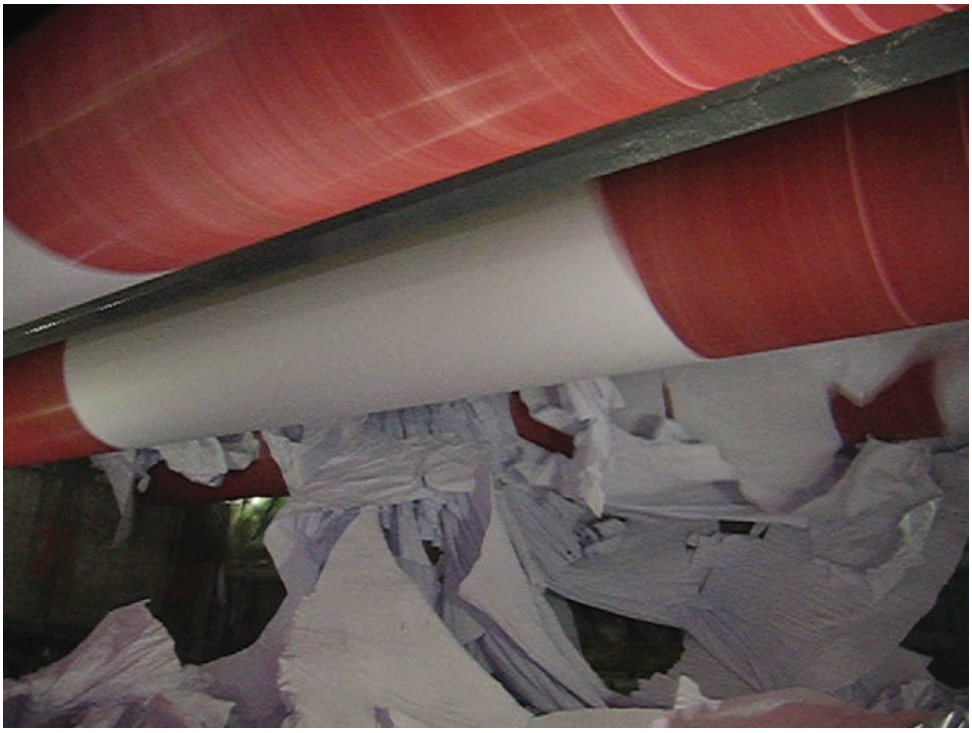

FIGURE 1 The stability has been lost and the web starts to break. (Courtesy of Metso).

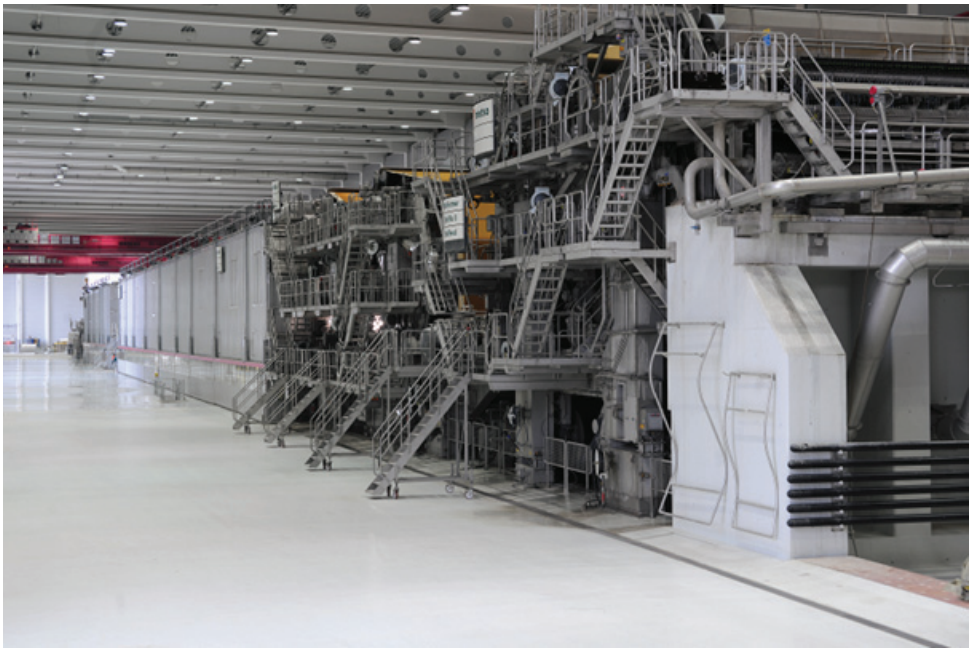

FIGURE 2 The dimensions of a paper machine. The height of the machine is 8 m and the length is 120 m. (Courtesy of Metso).

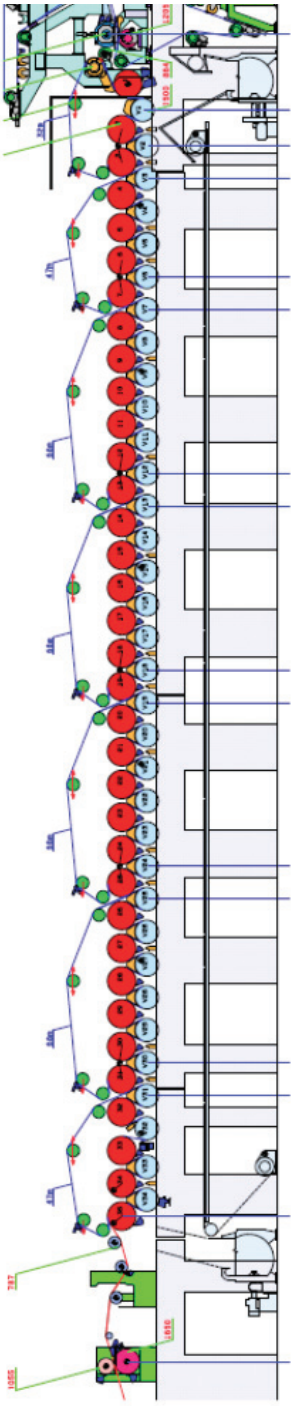

FIGURE 3 A cross-section view of the paper machine. Notice the route of the web through the system. (Courtesy of Metso).(See page 82, in [37].)

mission cables. This study concentrates on cases where the surrounding fluid is neglected; our main focus will be on the in- and out-of-plane tensions and material properties of the web. Our group has studied the effects of the surrounding fluid and that study is briefly described below.

1.3 Background of the research process

In this section, we will present some background of the research process. The research have been done in collaboration with University of Jyväskylä, department of Mathematical Information Technology and the Institute for Problems in Mechanics of the Russian Academy of Sciences. The members of the research team are Prof. Pekka Neittaanmäki, Prof. Nikolay Banichuk, Juha Jeronen, Tytti Saksa, Maria Tirronen, Matti Kurki and Tero Tuovinen. Our history as a research team began in 2007 with the study of the paper web interacting with the surrounding fluid. Later on, studies have been extended in many ways (see Figure 4 on the next page). In the figure, blue boxes are studies which are presented in this thesis and grey boxes represents studies that have been excluded.

We began with an analysis of different instability mechanisms by studying the problem of the moving paper web, modeled as a one-dimensional panel interacting with a two-dimensional flow of an ideal fluid. It was discovered that the web may experience both divergence and flutter instability when its speed exceeds certain critical values. The aerodynamic reaction, i.e., the pressure of the ideal fluid, was found analytically and was used for formulation of the equations governing the behavior of the web. An analysis of the steady-state type of instability and the evaluation of the divergence speed of the moving panel submerged in the ideal fluid was performed by applying the classical concept of elastic stability.

The analysis was performed via a time-dependent eigenvalue problem using an integro-differential equation, describing the instability modes. The solution was derived using complex variable calculus and spectral analysis. The resulting formulae can be used for calculating the divergence speed of the moving web. Furthermore, an important relation was derived for the dependence of the critical divergence speed on the density of the surrounding fluid and the flow velocity. One main objective of our study was the generalization of classical studies into a case with arbitrary fluid velocity: the study supports existing research, confirming that the presence of air reduces eigenfrequencies. In 2008 we extended the study into a non-stationary dynamic analysis of a paper web travelling between two rollers with constant velocity and interacting with the surrounding air. Transverse vibrations of the web were also described by an integro-differential equation that includes a local inertia term, Coriolis and centrifugal forces, the hydrodynamic reaction of the external medium, and some perturbation forces. The Galerkin method was applied to transform the original boundary value problem to a Cauchy problem for a system of coupled ordinary

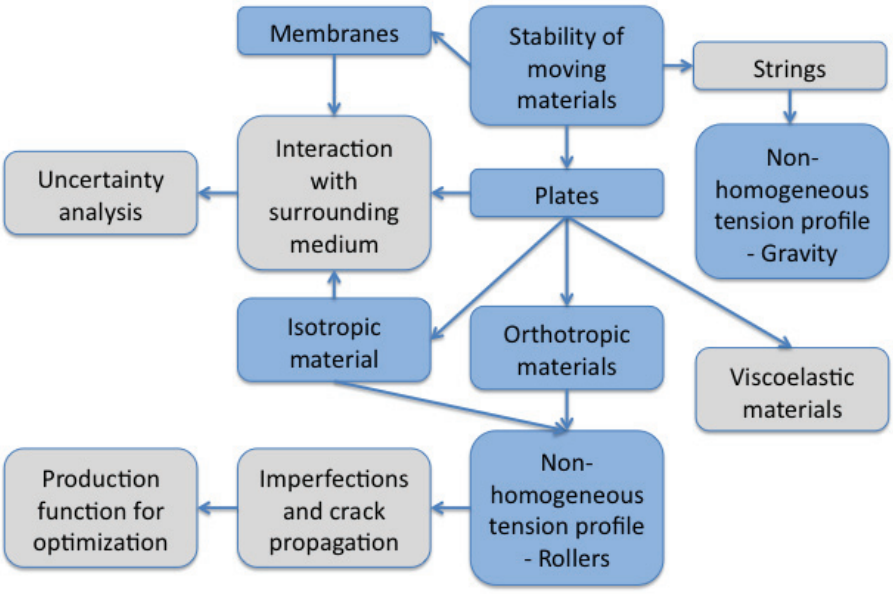

FIGURE 4 The outline of this thesis related to the research done in our group. The blue areas are covered in this study and the grey areas are excluded.

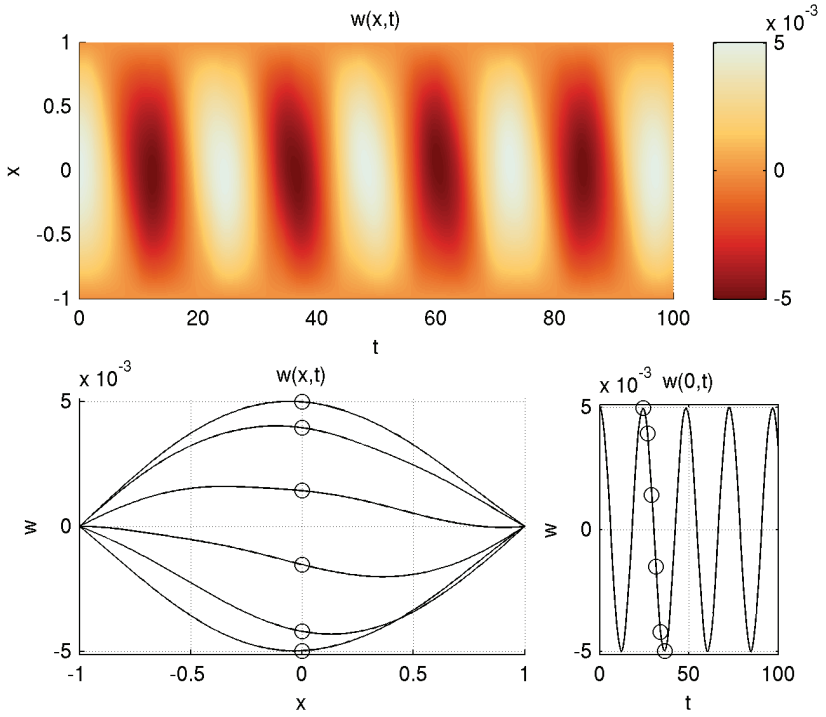

FIGURE 5 The dynamic response of the plate. The topmost graph illustrates a space-time plot of the out-of-plane displacements of the web, and the bottommost graph presents five selected time-steps.

differential equations describing the evolution of the system. An example of the results has been illustrated in Figure 5 where displacements have been presented in a space-time plot. For further information, see the following articles and reports [16, 15, 14, 7, 8, 4, 5, 36, 43, 3, 81].

The other direction of our research, reported in detail in this thesis, is a pure stability analysis of a moving web without considering its interaction with air. As mentioned before, the most common models used by other researchers before us studied cases of travelling flexible strings, membranes, beams, and plates. Previous studies of these models, employing second- and fourth-order differential equations, focus on the aspect of free vibrations including the nature of wave propagation in moving media and the effects of axial motion on the frequency spectrum and eigenfunctions. The first models, mainly developed in the middle of the last century, were one-dimensional string and beam models. The most productive group in the field has been that of Mote et al. and even though not all of their articles have been mentioned here, it is recommended that the reader make himself familiar with them. The literature review in this thesis covers only the most significant papers chosen from many groups. We hope that this helps the reader to build a picture of the activities in this field. The two-dimensional prob-

lem of instability analysis of an axially moving elastic plate is formulated and investigated analytically by Banichuk et al. [6] in the context of an isotropic model. It was observed that the transverse deflection localizes near the free edges (see, [80]). This was found to correspond to the eigenfunctions of stationary plates under in-plane compressive load (Gorman, [30]), and the results matched the results of Lin [46] and Shin [72] for moving plates and membranes mentioned above.

The next step is to generalize the analysis into the case of orthotropic material. Figure 6 on the following page illustrates the corner of a of piece of paper and its orthotropic fiber structure (see the longer fibers in the machine direction[1]). The problem of the stability of an axially moving orthotropic elastic plate travelling between two rollers at a constant velocity, and experiencing small transverse vibrations, is considered in a two-dimensional formulation. The model of a thin, elastic, orthotropic plate subjected to bending and tension is used to describe the bending moment and the distribution of the membrane forces. The static form of instability is investigated and the critical regime is studied as a function of the geometric parameters and the moduli of orthotropicity. It is shown that for some values of the problem parameter, the buckling mode becomes localized in the vicinity of the free boundaries. By using the assumption of Huber the orthotropic case reduces to an isotropic case. This assumption is not widely used in this thesis, but some examples are discussed for the sake of comparison. The results are presented in the article by Banichuk et al. **[2]**[2].

We have extended our study to the analysis of the dynamic behavior and elastic instability of a rectangular plate moving axially at a constant velocity under non-homogeneous tension: we have also investigated the dependence of the solution on the problem parameters. This will provide us with very useful information about the behaviour of a moving web, as can be seen in Figure 7 where the results are compared with actual measurements.

Special attention is given to the analysis of the influence of in-plane tension on the dynamic behavior of the plate and its stability. In the framework of a general dynamic approach, a functional expression for the characteristic index of stability is found in a convenient form that can be effectively used for frequency evaluation and qualitative analysis of dynamic and static modes of instability. The analytical approach allows for a fast solver, which can then be used for applications such as statistical uncertainty and sensitivity analysis, real-time parameter space exploration, and finding optimal values for design parameters. A static investigation of instability is then performed with the help of a qualitative analysis and numerical techniques. The results are presented in the article by Banichuk et al. **[9]**. Under the same topic, but in the longitudinal direction, the tension variations have been studied in a one-dimensional case. The article by Banichuk et al. **[11]** represents the effect of gravitation and validates the simplification where the gravitation effect is neglected. A short illustration of the case is presented in Figure 8 and the resulting buckling modes with respect to the angle

[1] This simple experiment can be done at home by tearing normal paper in different directions and observing the differences between the cuts.

[2] Note that the citations referring to the four main articles of this thesis, have been bolded.

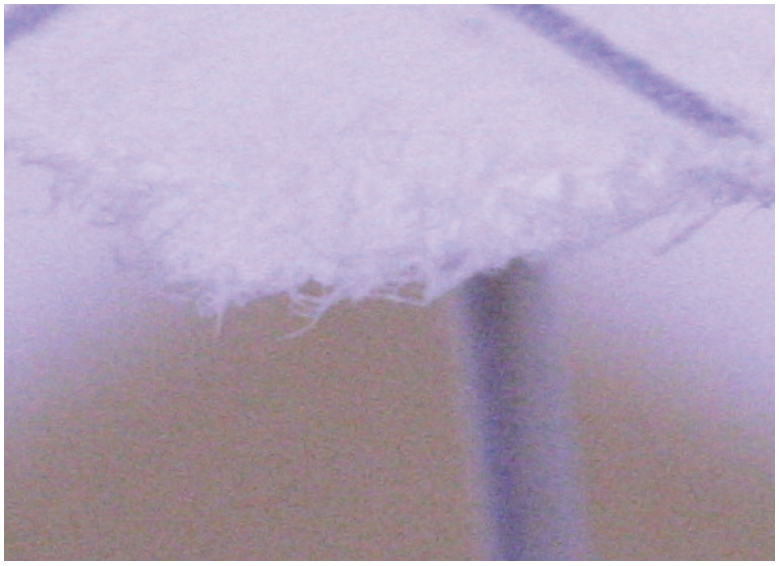

FIGURE 6 This photo represents the fibre structure of the paper sheet. Note the length of fibers with respect to orientation. A similar experimental study can be done by tearing normal paper in different directions. As a result, the torn edges of the paper will look different.

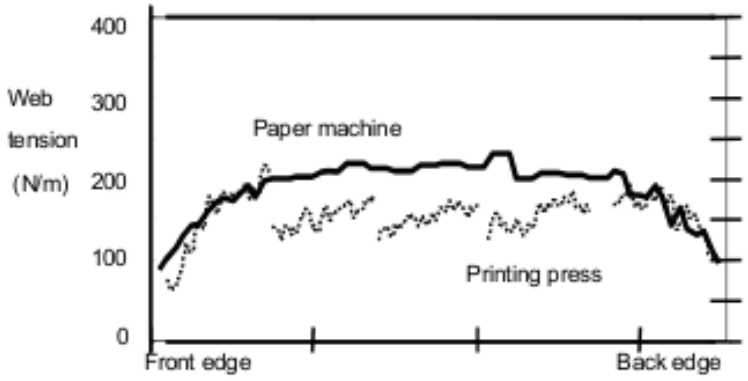

FIGURE 7 The measured tension by web width in a paper machine. Front and back ends correspond to the free boundaries in our model. The measurements have been taken far from the rollers. [49]

to the gravity is presented in Figure 9.

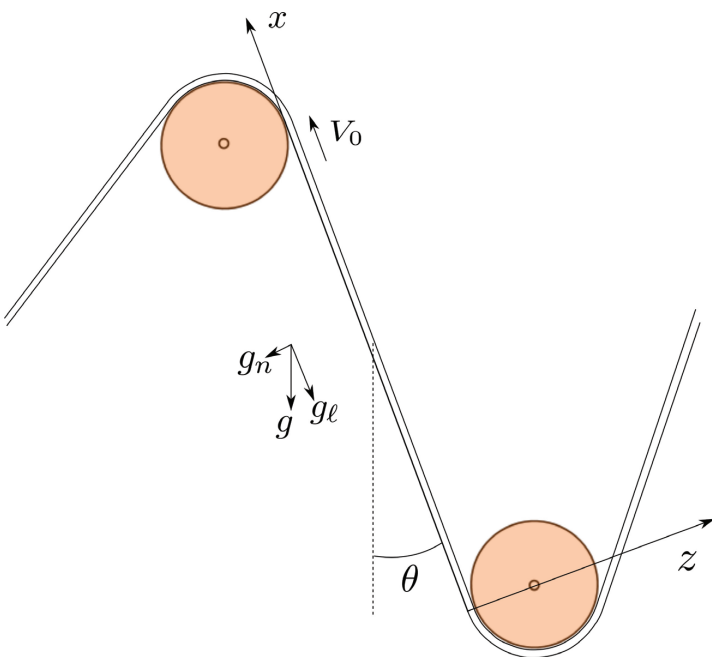

FIGURE 8 The elastic band moving in a non-vertical direction (inclined with respect to the gravity).

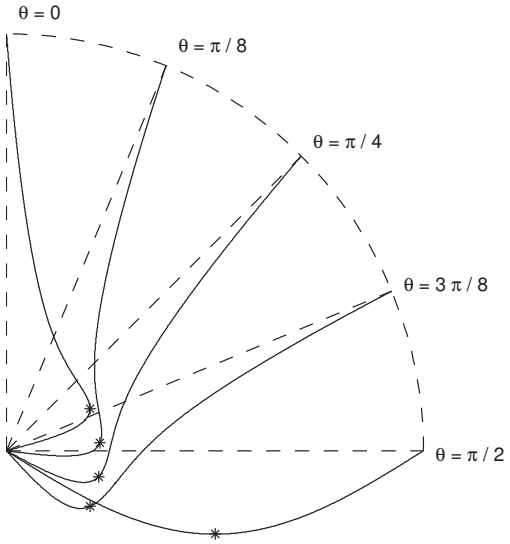

FIGURE 9 The buckling modes of the gravity problem, when the direction of motion of the band is at an angle to the gravity. Graphs of the buckling modes for some selected cases. The displacement maxima are marked by $\star$.

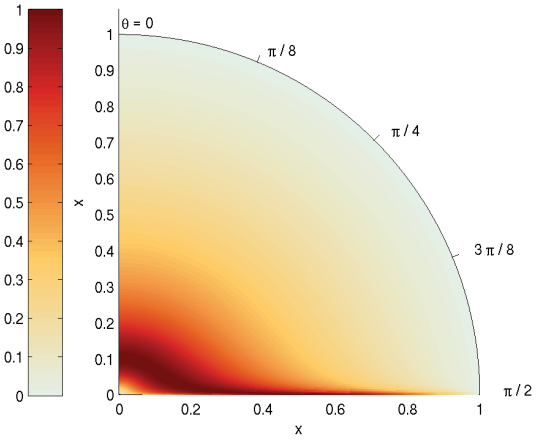

FIGURE 10 The buckling modes of the gravity problem. The colour sheet of the buckling mode for values of θ between 0 and $\pi/2$.

1.4 Literature review

The dynamic and stability considerations discussed here were first reviewed in the article by Mote [62]. The effects of axial motion of the web on its frequency spectrum and eigenfunctions were investigated in the papers by Archibald and Emslie [1] and by Simpson [73]. It was shown that the natural frequency of each mode decreases when the transport speed increases, and that the travelling string and beam both experience divergence instability at a sufficiently high speed. Response predictions were made for particular cases where the excitation assumes special forms, such as a constant transverse point force (see the article by Chonan [26]) or harmonic support motion (see the article by Miranker [60]). Arbitrary excitations and initial conditions have been analyzed with the help of modal analysis and a Green function method in the article by Wickert and Mote [88]. As a result, the associated critical speeds have been explicitly determined. The loss of stability was studied with an application of dynamic and static approaches in the article by Wickert [87]. It was shown by means of numerical analysis that in all cases instability occurs when the frequency is zero and the critical velocity coincides with the corresponding velocity obtained from static analysis.

Two-dimensional studies have also been performed. It is noteworthy that among them are the studies made by Lin and Mote who studied an axially moving membrane in a 2D formulation in their article [47], predicting the equilibrium displacement and stress distributions under transverse loading. In the article by Shin et al. [72], out-of-plane vibrations of an axially moving membrane were studied. They also found by numerical analysis that for a membrane with no-friction boundary conditions in the lateral direction along the rollers, the mem-

brane remains dynamically stable until the critical speed, at which static instability occurs, is reached. Later on, Lin and Mote extended their study in the article [48] where they predicted the wrinkling instability and the corresponding wrinkled shape of a web with small flexural stiffness. Lin continued the studies of stability in his article [46] in 1997.

It is necessary to note that the vibration problem for an axially moving continuum is not the conventional one. Because of the longitudinal continuity of the material, the equation of motion for transverse vibration contains additional terms, representing a Coriolis force and a centripetal force acting on the material. As a consequence, the resonant frequencies are dependent on the longitudinal velocity of the axially moving continuum (see the article by Mujumdar and Douglas [63]). Another important factor that affects the instability of the axially moving continuum is the interaction between the elastic continuum and the surrounding medium. The interaction between the travelling web and the surrounding air is known to influence the critical velocity (see the articles by Pramila [68] and by Frondelius et al. [27]) and the dynamical response of the web (discussed in the article by Kulachenko et al. [41]), possibly also affecting the buckling shape. These effects are ignored in the in-vacuum model used in this thesis, but should be noted here. The simplest approach to taking the interaction into account is to assume potential flow; that is, the surrounding air is assumed to be incompressible and inviscid, and the flow is assumed to be irrotational (like in their articles by Niemi and Pramila [65]). Experimental studies and some theoretical estimations (see, e.g., the article by Pramila[68]) indicate that in the case of normal vibration, a comparison of experimental and theoretical results shows that predictions based on the potential flow theory are within approximately 10 % of the measured results. To solve the external hydrodynamic problem, and to find the reaction of the surrounding medium, the finite element method has been used [65]. Note that dynamical properties of moving plates have been studied by Shen, Sharpe and McGinley [71] and by Shin et al. [72], and the properties of a moving web have been studied by Kulachenko, Gradin, and Koivurova in both their articles [40, 41]. Critical regimes and other problems of instability analysis have been studied by [85] and [75]. From experimental studies and some theoretical estimations (see e.g. the article by Pramila [68]), it can be concluded that mechanical instability of a travelling paper web can arise at some critical velocities and that the instability may occur in either dynamic, i.e. flutter, or static, i.e. divergence, forms. These critical velocities are of both theoretical and practical interest as they set an upper limit for the running speed of paper machines, and consequently, for the rate of paper production that can be achieved. Some previous investigations (see e.g., Lin [46]) show that for an axially moving elastic paper web under a homogeneous tension profile along the rollers and certain other conditions, the value of divergence speed V_0^{div} is less than the value of flutter speed V_0^{fl}, i.e.,

$$V_0^{\text{div}} < V_0^{\text{fl}}. \tag{1}$$

Thus, the speed V_0 for a reliable, stable movement of the paper web must satisfy

the condition

$$V_0 < V_0^{\mathrm{Div}}. \tag{2}$$

Corresponding results have been obtained also for axially moving beams interacting with external media; see, e.g. the articles by Chang and Morretti [21], and the articles by N. Banichuk and P. Neittaanmäki [16, 15, 14]. The same authors with Tero Tuovinen and Juha Jeronen have extended the study in the article [6] to a two-dimensional model of the web, considered as a moving plate under homogeneous tension but without external media.

The mechanical behavior of the paper web under a non-failure condition is adequately described by the model of an elastic orthotropic plate. The rigidity coefficients of the plate model that describe the tension and bending of the paper sheet have been estimated for various types of paper in many publications (see, for example the articles by Gottsching and Baumgarten [31], by Thorpe [76], by Skonwronski and Robertson [74] and by Seo [70]). The deformation properties of a sheet of paper under tensile stress or strain are used in simulation of axial movement of a paper web. In particular, these properties are important for the modeling of the instability of the web.

In the article by Hatami et al. [32], the free vibration of a moving orthotropic rectangular plate is studied at sub- and supercritical speeds, and its flutter and divergence instabilities at supercritical speeds. Their study was limited to simply supported boundary conditions at all edges. The free vibrations of orthotropic rectangular plates that are not moving have been studied by Biancolini et al. [18], including all combinations of simply supported and clamped boundary conditions on the edges. Xing and Liu obtained in the article [89] exact solutions for free vibrations of stationary rectangular orthotropic plates; they considered three combinations of simply supported (S) and clamped (C) boundary conditions: SSCC, SCCC, and CCCC. Kshirsagar and Bhaskar [39] studied vibrations and buckling of loaded stationary orthotropic plates. They found critical loads of buckling for all combinations of boundary conditions S, C, and F. For the numerical solving of orthotropic moving material, many necessary fundamentals can be found in the book by Marynowski [55]. In this thesis, we have extended our previous studies including orthotropic material and non-homogeneous tension. The numerical results have not been published before. This addition is relevant for combining all studies for rigorous analysis and conclusions.

It should be noted that when considering a paper material, in order to model the behavior of a wet paper web, we need to include its viscoelastic properties in the model. The first study of transverse vibration of travelling viscoelastic material was carried out by [28] using a string model. Extending their work, they studied the material damping effect in their later research [29]. Later on, viscoelastic strings and beams have been studied exceedingly; see the articles [66, 45], [25], [93], [90, 91, 24], [23], [53, 54, 56, 59, 57, 58]. Our research in that area continues and its results will be published in the future. The further discussion of viscoelastic properties is excluded from this thesis. Therefore, the damping effects resulting from the viscoelastic nature of paper are neglected. This is not a major problem since the introduction of such damping is not expected to change

the critical velocity, although it does modify the postdivergence behavior of the web (see the article by Ulsoy and Mote [82]).

1.5 Highlighted studies, results and related articles

In this thesis, we have studied five cases related to the stability of an axially moving elastic web. The cases are :

- An isotropic plate with a homogeneous tension profile
- An isotropic plate with a non-homogeneous tension profile
- An orthotropic membrane with a homogeneous tension profile
- An orthotropic plate with a homogeneous tension profile
- An orthotropic plate with a non-homogeneous tension profile.

The described cases will cover this part of the field. The main results of this thesis are:

1. In all cases, the value of tension does not affect the buckling shape; however, the tension is the most significant parameter when considering the critical velocity of a moving web.
2. In the case of the moving material with homogeneous tension, it was proved that the buckled plate shape is symmetrical, i.e., the antisymmetric shapes correspond to the higher values of the transport velocity.
3. In the case of the orthotropic moving material, we have noted that by using the Huber quantity, the qualitative behaviour agrees with the isotropic case, as expected. In the analysis we found the effect of the Young modulus ratio E_1/E_2; the smaller the ratio, the more the shape is localized near the free edges.
4. In the case of the orthotropic moving material, we have analyzed the effect of the increasing the ratio G_{12}/G_H and we have found that the zone where the relative strength of localization rapidly increases, shifts to the right towards the larger values of ν_{12}.
5. In the case of the non-homogeneous tension profile, it was seen that inhomogeneities may significantly decrease the critical velocities. For up to a 20 % tension inhomogeneity between the midpoint and the edges, the decrease in the critical velocity is found to be 10 %.
6. In the same study, the critical velocity is not significantly affected by slight inhomogeneities in the tension profile. For up to a 1% tension inhomogeneity between the midpoint and the edges, the largest decrease in the critical velocity is found to be less than 0.5%.
7. Again in the same study, it is also seen that the wider the web is, the more sensitive it is for tension inhomogeneities. Materials with a larger Poisson ratio tend to exhibit a higher degree of sensitivity to inhomogeneities in the tension profile.

8. Finally, we can see that even for the smallest inhomogeneity tested, $1E^{-6}$, the divergence (buckling) mode changes completely for these problem parameters. Thus, from a practical point of view, although studies of the homogeneous tension case can relatively accurately predict the critical velocity. The analysis indicates that the predictions of the divergence shape may be completely inaccurate.

This thesis is a based on the following published articles by the author[3]. Note that the citations referring to these four main articles have been bolded:

- **[6]** Banichuk, N. Jeronen, J. Neittaanmäki, P. and Tuovinen, T. On the instability of an axially moving elastic plate, International Journal of Solids and Structures, 2010
- **[2]** Banichuk, N. Jeronen, J. Kurki, M. Neittaanmäki, P. Saksa, T. and Tuovinen, T. , On the limit velocity and buckling phenomena of axially moving orthotropic membranes and plates, International Journal of Solids and Structures, 2011, pp. 2015–2025
- **[9]** Banichuk, N. Jeronen, J. Neittaanmäki, P. Tuovinen, T. and Saksa, T. Theoretical study on travel ling web dynamics and instability under a linear tension distribution, Reports of the Department of Mathematical Information Technology, 2010
- **[11]** Banichuk, N. Jeronen, J. Saksa, T. and Tuovinen, T. Static instability analysis of an elastic band travelling in the gravitational field, Journal of Structural Mechanics, 2011, pp. 172–185

Some additional information has been collected also from the following articles by the author:

- [7] Banichuk, N. Jeronen, J. Neittaanmäki, P. and Tuovinen, T. Static Instability Analysis for Travelling Membranes and Plates Interacting with Axially Moving Ideal Fluid, Journal of Fluids and Structures, 2010, pp. 274–291
- [8] Banichuk, N. Jeronen, J. Neittaanmäki, P., and Tuovinen, T., Dynamic behaviour of an axially moving plate undergoing small cylindrical deformation submerged in axially flowing ideal fluid, Journal of Fluids and Structures, 2011, pp. 986–1005
- [4] Banichuk, N. Jeronen, J. Neittaanmäki, P. and Tuovinen, T. Nonstationary Dynamics of Travelling Membranes and Plates Interacting with Axially Moving Ideal Fluid. Part I: Theory, Reports of the Department of Mathematical Information Technology, 2008
- [5] Banichuk, N. Jeronen, J. Neittaanmäki, P. and Tuovinen, T. Nonstationary Dynamics of Travelling Membranes and Plates Interacting with Axially Moving Ideal Fluid. Part II: Numerical Results, Reports of the Department of Mathematical Information Technology, 2008

[3] Note that in the group, we have used the policy of alphabetical order in the list of authors where possible.

- [13] Banichuk, N. Kurki, M. Neittaanmäki, P. Saksa, T. and Tuovinen, T. On Axially Moving Webs Under Fracture and Instability Constraints, Reports of the Department of Mathematical Information Technology, 2011
- [35] Jeronen, J. Saksa, T. Tuovinen, T. Banichuk, N. and Neittaanmäki, P. On the Moving Web Dynamics Under Stability Considerations Including Interaction with Surrounding Fluid, Massachusetts Institute of Technology, 2011, pp. 64
- [43] Kurki, M. Jeronen, J. Saksa, T. Tuovinen, T. and Neittaanmäki, P. Liikkuvan paperiradan kriittinen rajanopeus ja stabiilisuusanalyysi paperi- ja kartonkikoneen eri osaprosesseissa, Paperi ja Puu, 2011
- [61] Mönkölä, S. Airaksinen, T. Makkonen, P. Tuovinen, T. and Neittaanmäki, P. Prospectives to tractor cabin design with computational acoustics tools, ECMI newsletter, 2011, pp. 16–19
- [34] Jeronen, J. Banichuk, N. Neittaanmäki, P. and Tuovinen, T. On The Effects Of Bending Rigidity On The Stability Of An Axially Moving Orthotropic Plate, University of Jyväskylä, 2009, pp. 510–521
- [81] Tuovinen, T. and Mönkölä, S. Two Different Approaches for Fluid-Structure Interaction (FSI) Based Flutter Problems in Paper Machine, Reports of the Department of Mathematical Information Technology, 2008

1.6 Author's contributions

The outcome of this thesis is a result of an intensive collaboration between the author and the FSI group. The main problem for the study comes from the industry, more precisely from Metso Paper Inc. (see e.g. the licentiate thesis of Matti Kurki [42]). At the beginning of collaboration, there was an urgent need for modeling runnability in Metso Paper. The author has advanced and extended the studies from the literature into the field of moving materials. The author has written the articles that are the basis of this thesis. The author's main contributions are:

- Structuring the research, planning the steps at the project level, collecting the experts, and organizing the methods in use inside the group.
- Preparing the studies and literature, collecting related articles, defining the cases in the study.
- Developing numerical implementations, partly alone, partly with Juha Jeronen and Tytti Saksa.
- Analysing gained results for publication, improving the cases based on this knowledge, choosing the final cases and results which to publish.
- Publishing the results in international journals.
- Combining and re-writing the published articles, thereby complementing the material to form a full monograph-style thesis.

1.7 Structure of the thesis

This thesis is structured as follows. This thesis is divided into four main parts. In Section 1, we introduce the motivation for this thesis and its background and describe the research process that began in 2005. The literature review found in this section and the main results and the articles that have been the basis of this thesis have been listed shortly. Also the contribution of the author has been presented in a brief manner. In Section 2, we present the theory of this study in detail. The numerical results are presented and analyzed in Section 3, and Section 4 brings all the pieces of this dissertation together and presents some future plans. At the end of this thesis, the reader find a Finnish summary and list of references.

2 MATHEMATICAL MODELING OF WEB DYNAMICS

In this section we present the theoretical background of the problem, including derivations of the equations, solution processes, and pieces of proof that are necessary for analyzing the results. We have included the isotropic examples for the sake of clarity, even though the orthotropic equations also cover the isotropic special case. The membrane is discussed because many classical studies assume a membrane -like behaviour. The implementation of the solver follows directly the structure of this section; therefore, we have avoided using excessively large steps in this section. It is easy to jump over many "technical details" and to create misunderstandings and "guess-based solutions" for the future. The progress of the science is very fast today and one should strive for completeness in laying the foundations for future work.

The preliminary information needed for modeling web dynamics can be found from classical books such as *"Theory of plates and shells"* by Timoshenko and Woinowsky-Krieger [79], and the book by Timoshenko and Gere, *"Theory of Elastic Stability"* [78]. Furthermore, the book by Bolotin, *"Nonconservative Problems of the Theory of Elastic Stability"* [19] is assumed to be known to the reader. The basis of the theory presented in this thesis is described in these books.

2.1 Basic relations for transverse vibration of axially moving elastic plates and membranes

We investigate the elastic stability of a band travelling at a constant velocity V_0 in the x-direction between two rollers located at $x = 0$ and $x = \ell$. Consider, in a Cartesian coordinate system, a rectangular part of the web

$$\Omega = \{(x, y) \mid 0 < x < \ell,\ -b < y < b\},$$

where ℓ and b are prescribed parameters. Domain Ω is considered to be open. Let us also define that Γ is the boundary related to Ω and the union of Ω and

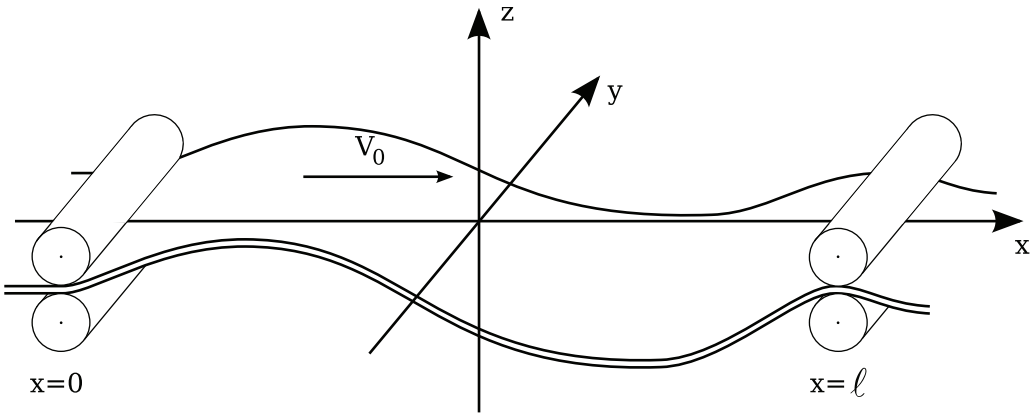

FIGURE 11 An axially moving elastic plate, simply supported at both ends, $x = 0$ and $x = \ell$. The rollers are considered to be unaffected.

Γ is considered to be closed. Additionally, assume that the considered part of the web is represented as a rectangular elastic plate or membrane. We will need the following parameters: constant thickness h, the Poisson ratio ν, the Young modulus E, bending rigidity D, and shear stress G_{12}. In the case of a membrane, we have zero bending rigidities, and in studies of the orthotropic elastic plate we have three bending rigidities D_1, D_2, and D_3. Respectively, instead of ν and E, we have ν_{12} , ν_{21} , E_1, and E_2. The "1" axis of the orthotropic material is aligned with the x-direction, also called the machine direction (MD), while the "2" axis is aligned with the y-direction, also called the co-machine direction (CD) (see Figure 11).

In the studies, the web is subjected to homogeneous or non-homogeneous tension T acting in the x-direction and applied at the boundaries $x = 0$ and $x = \ell$. In-plane distributed forces are defined as

$$k = k(y) = T_0 + \zeta(y), \tag{3}$$

where the constant $T_0 > 0$ and the function $\zeta(y)$ are considered given. In the case of homogeneous tension, $\zeta(y) = 0$. We have assumed that the sides of the bands

$$x = 0, \qquad -b \le y \le b, \qquad \text{and} \qquad x = \ell, \qquad -b \le y \le b \tag{4}$$

are simply supported, and the sides

$$y = -b, \qquad 0 \le x \le \ell \qquad \text{and} \qquad y = b, \qquad 0 \le x \le \ell$$

are free of tractions. The tension profiles are illustrated in Figure 12.

2.1.1 Governing equations of transverse out-of-plane vibrations

In this section we represent the governing equations for transverse out-of-plane vibrations. We begin by considering force balance equations for $x-$, $y-$ and

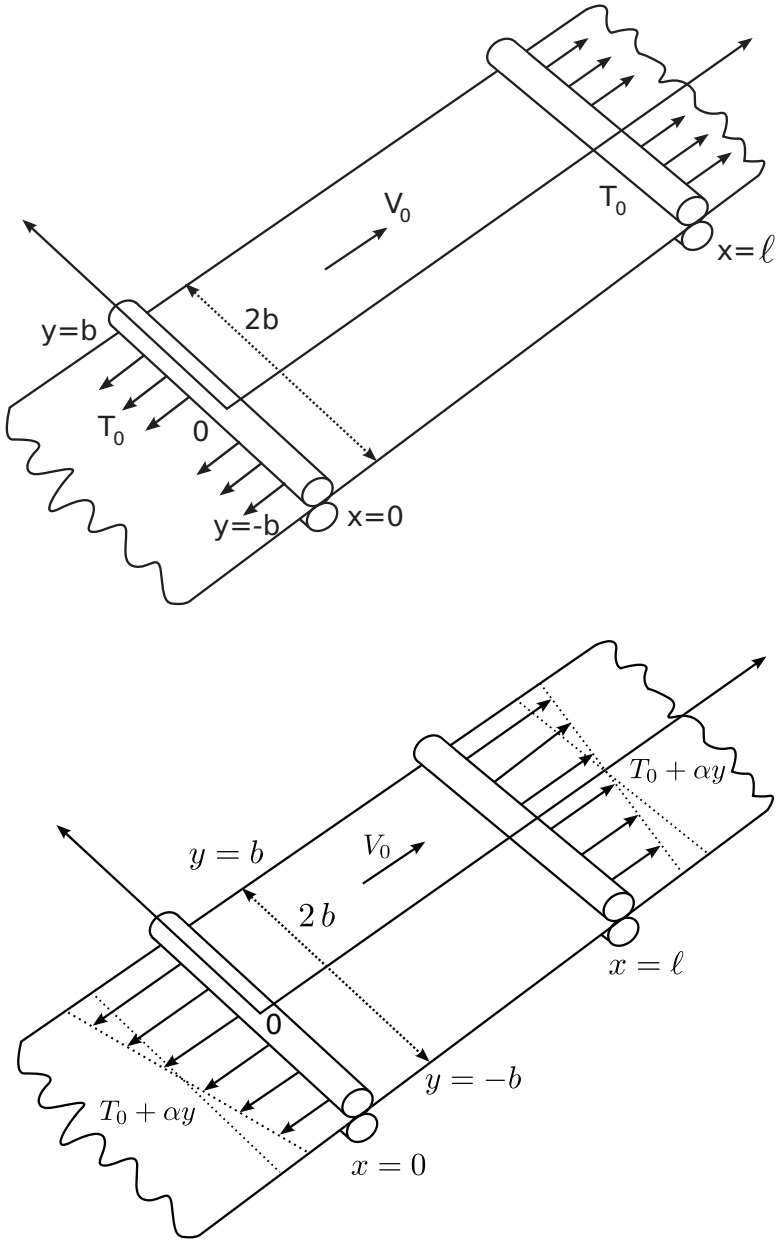

FIGURE 12 An axially moving elastic plate or membrane, simply supported at $x = 0$ and $x = \ell$. Homogeneous and linear non-homogeneous tension forces applied at $x = 0$ and $x = \ell$ have been illustrated qualitatively.

z-directions. The simplest way is to categorize them into external and internal forces. External forces are applied by a force on the web. The most important external forces are the pressure force, gravitation, drag, air friction, and mechanical surface friction. The internal forces are reaction forces that arise in the paper web. The internal forces are usually self-generated or acceleration forces. Typically, rebonding and drying shrinkage of fibres generate negative strains and in-plane tensions inside of a paper web. Another example of an internal force is bending stiffness.

In this thesis, we focus on static analysis and static instabilities of the moving web. As it has been already mentioned, the effects caused by the surrounding medium are neglected. We have studied this interaction with air and the results can be found in our paper [7]. We note very briefly the results for our article **[10]** that the gravitational effects are minimal in this case and can be excluded from the studies presented here. Mechanical friction forces are neglected, because we study an unsupported span. Actually, there is friction in the area where rollers and the web are connected, but because we are using linear models where decoupling between equations of u, v, and w exists, friction can be neglected. Note that u corresponds to the x-direction, v respectively to the y-direction, and w to the z-direction. We have also neglected the adhesion forces, mainly for the sake of simplicity.

First of all, consider the effect of acceleration. The very basic equation for the acceleration is the familiar dependence between force, mass, and acceleration given by Newton's second law,

$$F = Ma = M\frac{\partial^2 u}{\partial t^2}, \tag{5}$$

where F is force and M is mass. Here the small u denotes axial displacement. For the vertical displacement we use the symbol w. We assume that the axial displacement is local and the vertical displacement is global. In this context, we consider that "local" means that the axial displacement of the web "flows through the window", and in vertical displacement "global" means that the displacement describes the overall movement. A similar approach has been presented, for example, by Thurman and Mote in their studies [77]. For the vertical velocity, we obtain

$$\frac{\mathrm{d}w}{\mathrm{d}t} = \frac{\partial w}{\partial t} + \frac{\mathrm{d}u}{\mathrm{d}t}\frac{\partial w}{\partial x}. \tag{6}$$

We will take a total differential of the equation (6),

$$\frac{\mathrm{d}w}{\mathrm{d}t} = \frac{\partial w}{\partial t} + \frac{\partial w}{\partial x}\frac{dx}{dt} = \frac{\partial w}{\partial t} + V_0\frac{\partial w}{\partial x} = \left(\frac{\partial}{\partial t} + V_0\frac{\partial}{\partial x}\right)w, \tag{7}$$

where V_0 is constant. Now, differentiation again gives us the following form:

$$\frac{\mathrm{d}^2 w}{\mathrm{d}t^2} = \left(\frac{\partial}{\partial t} + V_0\frac{\partial}{\partial x}\right)\left(\frac{\partial w}{\partial t} + V_0\frac{\partial w}{\partial x}\right) = \tag{8}$$

$$\frac{\partial^2 w}{\partial t^2} + 2V_0\frac{\partial^2 w}{\partial x \partial t} + V_0\frac{\partial^2 w}{\partial x^2}.$$

Similarly, it is possible to derive the equation for a longitudinal wave. Instead of using the total mass M we are able to use the basis weight m, which is the mass per unit area. The basis weight is more usable from the application point of view. We can present the derivative of tension in the following way (see e.g. Kurki [42]):

$$m\frac{\mathrm{d}^2u}{\mathrm{d}t^2} = \frac{\mathrm{d}T}{\mathrm{d}x}. \tag{9}$$

We assume that

$$\frac{\mathrm{d}x}{\mathrm{d}t} = \frac{\mathrm{d}u}{\mathrm{d}t}. \tag{10}$$

One must note that u is the displacement in a free longitudinal vibration. We denote the constant velocity of the web as

$$V_0 = \frac{\mathrm{d}u}{\mathrm{d}t} \tag{11}$$

and as above, we get the equation

$$\frac{\mathrm{d}^2u}{\mathrm{d}t^2} = \frac{\partial^2u}{\partial t^2} + 2V_0\frac{\partial^2u}{\partial x\partial t} + V_0^2\frac{\partial^2u}{\partial x^2}. \tag{12}$$

We present the differential equation for small transverse vibrations in the following form:

$$m\frac{\mathrm{d}^2w}{\mathrm{d}t^2} = \mathcal{L}^M(w) - \mathcal{L}^B(w). \tag{13}$$

Here m is the mass per unit area of the middle surface of the plate. The total acceleration on the left-hand side of the equation (13) is expressed as

$$\frac{\mathrm{d}^2w}{\mathrm{d}t^2} = \frac{\mathrm{d}}{\mathrm{d}t}\left(\frac{\partial w}{\partial t} + V_0\frac{\partial w}{\partial x}\right) = \frac{\partial^2w}{\partial t^2} + 2V_0\frac{\partial^2w}{\partial x\partial t} + V_0^2\frac{\partial^2w}{\partial x^2}. \tag{14}$$

The right-hand side in the equation (14) contains three terms, representing local acceleration, Coriolis acceleration, and centripetal acceleration, respectively. The membrane operator on the right-hand side of the equation (13) is

$$\mathcal{L}^M(w) = T_{xx}\frac{\partial^2w}{\partial x^2} + 2T_{xy}\frac{\partial^2w}{\partial x\partial y} + T_{yy}\frac{\partial^2w}{\partial y^2}. \tag{15}$$

The coefficients T_{xx}, T_{xy}, and T_{yy} of the linear operator $\mathcal{L}^M$ are related to the corresponding in-plane stresses σ_{xx}, σ_{xy}, and σ_{yy} by the expressions

$$T_{ij} = h\sigma_{ij}. \tag{16}$$

The linear bending operator $\mathcal{L}^B$ is given by the expression

$$\mathcal{L}^B(w) = D\Delta^2w = D\left(\frac{\partial^4w}{\partial x^4} + 2\frac{\partial^4w}{\partial x^2\partial y^2} + \frac{\partial^4w}{\partial y^4}\right) \tag{17}$$

in the case of an isotropic elastic plate. Here,

$$D = \frac{Eh^3}{12\,(1-\nu^2)} \tag{18}$$

is the bending rigidity of the plate, and Δ^2 is the biharmonic operator. When we consider the case of an orthotropic plate, the operator $\mathcal{L}^B$ depends on the three constants, i.e. the operator is

$$\mathcal{L}^B\,(w) = D_1\frac{\partial^4 w}{\partial x^4} + 2D_3\frac{\partial^4 w}{\partial x^2\partial y^2} + D_2\frac{\partial^4 w}{\partial y^4}\,. \tag{19}$$

In the case of a membrane, the bending rigidities are neglected and the entire operator $\mathcal{L}^B$ is omitted ($\mathcal{L}^B \equiv 0$). For the bending rigidities in the equation (19), we have the expressions (see e.g. Timoshenko and Woinowsky-Krieger [79])

$$D_1 = \frac{h^3}{12}C_{11}\,, \quad D_2 = \frac{h^3}{12}C_{22}\,, \quad D_3 = \frac{h^3}{12}\,(C_{12} + 2\,C_{66})\,, \tag{20}$$

where C_{ij} are the elastic moduli. These can be expressed in terms of the Young moduli E_1, E_2, and the Poisson ratios ν_{12}, ν_{21} as (see, e.g., Kikuchi [38]),

$$\begin{gathered} C_{11} = \frac{E_1}{1-\nu_{12}\nu_{21}}, \qquad C_{22} = \frac{E_2}{1-\nu_{12}\nu_{21}}, \\ C_{12} = C_{21} = \frac{\nu_{12}E_2}{1-\nu_{12}\nu_{21}}, \qquad . \\ C_{66} = G_{12}. \end{gathered} \tag{21}$$

In the equation (21), E_1 is the Young modulus in the x-direction, and ν_{12} is the Poisson ratio in the xy plane when the stretching is applied in the x-direction. Respectively, E_2 is the Young modulus in the y-direction, and ν_{21} is the Poisson ratio in the xy plane when the stretching is applied in the y-direction. G_{12} is the shear modulus in the $xy-$ plane.

We assume that the deflection function w and its partial derivatives are small, and that they satisfy the boundary conditions. In the case of an orthotropic plate, the boundary conditions read

$$(w)_{x=0,\ell} = 0, \qquad \left(\frac{\partial^2 w}{\partial x^2}\right)_{x=0,\ell} = 0\,, \qquad -b \le y \le b\,, \tag{22}$$

$$\left(\frac{\partial^2 w}{\partial y^2} + \beta_1\frac{\partial^2 w}{\partial x^2}\right)_{y=\pm b} = 0\,, \qquad 0 \le x \le \ell\,, \tag{23}$$

$$\left(\frac{\partial^3 w}{\partial y^3} + \beta_2\frac{\partial^3 w}{\partial x^2\partial y}\right)_{y=\pm b} = 0, \qquad 0 \le x \le \ell\,, \tag{24}$$

where β_1 and β_2 are mechanical parameters defined as

$$\begin{aligned} \beta_1 &= \nu_{12}\,, \\ \beta_2 &= \nu_{12} + \frac{4\,G_{12}}{E_2}\,(1 - \nu_{12}\nu_{21})\,. \end{aligned} \tag{25}$$

We note that we use the Kirchhoff boundary conditions for the sake of simplicity. From the physical point of view, it is an important and not trivial question which types of boundary conditions to select. However, many other scientists have chosen the same conditions and we have followed their example.

Using the geometric average approximation of G_{12},

$$G_H \equiv \frac{\sqrt{E_1 E_2}}{2\,(1 + \sqrt{\nu_{12}\nu_{21}})}\,, \tag{26}$$

also known as the Huber quantity G_H (see, Huber [33]), the equations for an orthotropic plate reduce to the case of an isotropic plate. It is easy to show that this property is valid for the time-dependent plate problem, including axial motion, as well. Because coordinate scaling is only required in the y-direction (see. [79] for the transformations), the Coriolis term w_{xt} generated by the axial motion of the plate causes no trouble for this approach. However, in the rest of this study, unless otherwise noted, it is assumed that G_{12} is an independent material parameter. This generalization comes from the application point of view, where shear stress generally differs from its geometric average, and can actually be quite variable.

In the case of a membrane, the boundary condition at the rollers reads

$$(w)_{x=0,\,\ell} = 0\,, \quad -b \le y \le b\,. \tag{27}$$

On the free edges, the classical membrane theory asserts (see e.g. [69, 86])

$$\left(\frac{\partial w}{\partial y}\right)_{y=\pm b} = 0,\ (0 \le x \le \ell)\,. \tag{28}$$

Finally, we note that Shin et al. [72] have used a different condition for zero traction, which does not contain the transverse displacement w. We will see below that in our case both choices of the boundary condition on the free edges are possible for a membrane.

2.1.2 In-plane tensions

Our first goal is to describe the stationary representation of in-plane forces, i.e. we assume that the in-plane tensions do not depend on time t. The in-plane tensions T_{xx}, T_{xy}, and T_{yy} are assumed to satisfy the equilibrium equations

$$\frac{\partial T_{xx}}{\partial x} + \frac{\partial T_{xy}}{\partial y} = 0, \quad \frac{\partial T_{xy}}{\partial x} + \frac{\partial T_{yy}}{\partial y} = 0. \tag{29}$$

In the case of a plate, the boundary conditions are

$$T_{xx} = k(y), \quad T_{xy} = 0 \quad \text{at } x = 0,\ |y| \leq b \text{ and } x = \ell,\ |y| \leq b\ , \tag{30}$$

$$T_{yy} = 0, \quad T_{xy} = 0 \quad \text{at } y = \pm b, \quad 0 \leq x \leq \ell\ . \tag{31}$$

Let us begin with the homogeneous tension fields when $k(y)$ degenerates to T_0. For both the plate and membrane cases, in the equation (29), T_{xx}, T_{xy} and T_{yy} the in-plane tensions are related to the corresponding stress tensor components σ_{xx}, σ_{xy} and σ_{yy}. The reader is reminded of the relations between stresses and tensions in the equation (16). Taking into account the behavioral equation of the plane theory of elasticity and the boundary conditions (30) and (31), we have for the orthotropic band considered the tension field

$$T_{xx} = T_0\,, \qquad T_{yy} = T_{xy} = 0\,, \qquad (x, y) \in \Omega\ . \tag{32}$$

The in-plane displacements u, and v, oriented respectively along the axes x and y, are related to the stresses by means of the generalized Hooke's Law:

$$\sigma_{xx} = C_{11}\frac{\partial u}{\partial x} + C_{12}\frac{\partial v}{\partial y}\ , \tag{33}$$

$$\sigma_{xy} = C_{66}\left(\frac{\partial u}{\partial y} + \frac{\partial v}{\partial x}\right) \text{ and} \tag{34}$$

$$\sigma_{yy} = C_{12}\frac{\partial u}{\partial x} + C_{22}\frac{\partial v}{\partial y}\ , \tag{35}$$

where C_{ij} are the elastic moduli; see relations from the equation (21). In the following, we will use Maxwell's relation

$$E_1\nu_{21} = E_2\nu_{12}\ . \tag{36}$$

Note that by using equations (29) and (33) – (35), it is possible to show that if instead of a prescribed tension T_0 we have a prescribed displacement u_0 at $x = \ell$, the generated tension field has the form (32) and its value is

$$T_0 = h\frac{u_0}{\ell}\left(C_{11} - \frac{C_{12}^2}{C_{22}}\right) = h\frac{u_0}{\ell}E_1\ , \tag{37}$$

because

$$C_{11} - \frac{C_{12}^2}{C_{22}} = \frac{E_1}{1-\nu_{12}\nu_{21}} - \frac{\nu_{12}^2 E_2}{1-\nu_{12}\nu_{21}} = E_1. \tag{38}$$

Therefore, our results are applicable to this case as well.

The boundary conditions used in deriving (37) were (31) and the following:

$$\begin{aligned} \sigma_{xy} &= 0 \qquad \text{at } x = 0, \ell, \\ u &= 0 \qquad \text{at } x = 0, \\ u &= u_0 \qquad \text{at } x = \ell. \end{aligned} \tag{39}$$

From (21) and (36) the last form in (37) easily follows. We see that the only material parameter that affects the homogeneous tension field generated by the prescribed displacement is the Young modulus in the longitudinal direction. Compare (37) with

$$T_0 = h\frac{u_0}{\ell}E \tag{40}$$

for an isotropic material.

For non-homogeneous tension we represent tensions T_{xx}, T_{yy}, and T_{xy} with the help of the Airy stress function. The equations are

$$\begin{aligned} T_{xx} &= h\sigma_{xx} &&= \frac{\partial^2 \mathrm{Y}}{\partial y^2} \\ T_{yy} &= h\sigma_{yy} &&= \frac{\partial^2 \mathrm{Y}}{\partial x^2} \\ T_{xy} &= h\sigma_{xy} &&= -\frac{\partial^2 \mathrm{Y}}{\partial x \partial y}. \end{aligned} \tag{41}$$

The Airy stress function Y satisfies the biharmonic equation

$$\Delta^2 \mathrm{Y} \equiv \frac{\partial^4 \mathrm{Y}}{\partial x^4} + 2\frac{\partial^4 \mathrm{Y}}{\partial x^2 \partial y^2} + \frac{\partial^4 \mathrm{Y}}{\partial y^4} = 0\,. \tag{42}$$

The boundary conditions satisfied by Y, corresponding to (30) and (31), are

$$\left(\frac{\partial^2 \mathrm{Y}}{\partial y^2}\right)_{x=0,\ell} = k(y)\,, \quad \left(\frac{\partial^2 \mathrm{Y}}{\partial x \partial y}\right)_{x=0,\ell} = 0\,, \quad -b \le y \le b\,, \tag{43}$$

$$\left(\frac{\partial^2 \mathrm{Y}}{\partial x^2}\right)_{y=\pm b} = 0\,, \quad \left(\frac{\partial^2 \mathrm{Y}}{\partial x \partial y}\right)_{y=\pm b} = 0\,, \quad 0 \le x \le \ell\,. \tag{44}$$

Note that the tensions expressed via the stress function Y in the equation (41) will satisfy the equilibrium equations in (29) for any function Y that is sufficiently smooth. The problem (42) – (44), which must be solved, expresses the condition of compatibility for the tensions (stresses).

In the following we will concentrate on the linear tension distribution, and use the rigorous solution of the boundary value problem (42) – (44) corresponding to the case where $\zeta(y) = \alpha y$, i.e., $k(y) = T_0 + \alpha y$. Here, $\alpha > 0$ is a given constant. We have

$$\mathrm{Y}(x,y) = T_0\,\frac{y^2}{2} + \alpha\,\frac{y^3}{6} + c_1 x + c_2 y + c_0, \quad (x,y) \in \Omega\,. \tag{45}$$

The corresponding tensions will be

$$T_{xx}(x,y) = T_0 + \alpha y, \quad T_{xy}(x,y) = 0, \quad T_{yy}(x,y) = 0, \quad (x,y) \in \Omega\,, \tag{46}$$

where c_0, c_1 and c_2 are arbitrary constants.

2.2 Instability analysis of moving membranes and plates

In this section, the focus is on how to analyze the dynamical problems of instability. We have followed the method described by Bolotin (see, [19]).

First, for the simplicity, we will use the choice $D_0 = D_1$ below. The equation (13) becomes

$$\frac{\partial^2 w}{\partial t^2} + 2V_0 \frac{\partial^2 w}{\partial x \partial t} + \left(V_0^2 - C^2\right) \frac{\partial^2 w}{\partial x^2} + \frac{D_0}{m} \mathcal{L}_0(w) = 0, \qquad C = \sqrt{\frac{T_0}{m}}\,, \tag{47}$$

where

$$\mathcal{L}_0(w) = \frac{D_1}{D_0} \frac{\partial^4 w}{\partial x^4} + \frac{2D_3}{D_0} \frac{\partial^4 w}{\partial x^2 \partial y^2} + \frac{D_2}{D_0} \frac{\partial^4 w}{\partial y^4}\,. \tag{48}$$

Note that the boundary value problem considered (47) – (48), with the boundary conditions (22) – (24), is homogeneous and invariant with respect to the symmetry operation $y \to -y$ and, consequently, all solutions of the problem are either symmetric or antisymmetric functions of y, i.e.

$$w(x, y, t) = w(x, -y, t) \qquad \text{or} \qquad w(x, y, t) = -w(x, -y, t)\,. \tag{49}$$

Let us represent the solution of our dynamic boundary-value problem (47) – (48) as

$$w(x, y, t) = W(x, y) e^{i\omega t}\,, \tag{50}$$

or in the equivalent form

$$w(x, y, t) = W(x, y) e^{st}\,, \tag{51}$$

where ω is the frequency of small transverse vibrations and

$$s = i\omega \tag{52}$$

is the complex characteristic parameter:

$$s = \text{Re}\, s + i\, \text{Im}\, s = s_{\text{re}} + i\, s_{\text{im}}. \tag{53}$$

If this parameter is a purely imaginary, i.e.,

$$\text{Re}\, s = 0, \quad \text{Im}\, s \neq 0, \tag{54}$$

and consequently ω is real, the membrane or plate performs harmonic vibrations of a small amplitude and its motion can be considered stable. If, for some values of the problem parameters, the real part of the characteristic index becomes positive, i.e.,

$$s_{\text{re}} = \text{Re}\, s > 0, \tag{55}$$

the transverse vibrations grow exponentially and consequently the behaviour is unstable (See Figure 13).

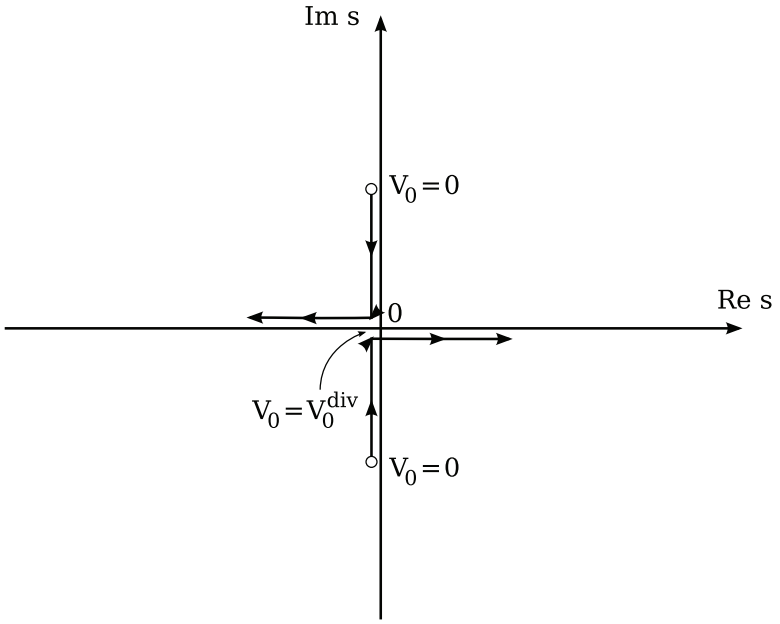

FIGURE 13 Behavior of the stability index s. Divergence, i.e. critical velocity, can be found in the origo.

2.3 Dynamic instability of a membrane

In this section, we have considered the instability of a membrane. Membrane studies are the classical approaches for the problems in moving materials, because the analytical methods are effective in many cases.

First we define the eigenvalue problem. The homogeneous tension force is applied on the boundaries $x = 0$ and $x = \ell$; in order to investigate the dynamic behavior we insert the representation (50) into the equation (47). Because we are studying a membrane, we have omitted the bending rigidity terms from the equation (47). We now have the equation

$$s^2 W + 2sV_0 \frac{\partial W}{\partial x} + \left(V_0^2 - C^2\right) \frac{\partial^2 W}{\partial x^2} = 0 \tag{56}$$

with zero boundary conditions

$$(W)_{x=0,\,\ell} = 0\,, \quad -b \leq y \leq b\,. \tag{57}$$

We multiply the left-hand side of the equation (56) by W and perform integration over the domain

$$\Omega \; = (0 < x < \ell,\; -b < y < b) \tag{58}$$

to obtain

$$s^2 \int_\Omega W^2 \,\mathrm{d}\Omega + 2sV_0 \int_\Omega W \frac{\partial W}{\partial x} \,\mathrm{d}\Omega + \left(V_0^2 - C^2\right) \int_\Omega W \frac{\partial^2 W}{\partial x^2} \,\mathrm{d}\Omega = 0\,. \tag{59}$$

It is worth noting that the problem (59) is not exactly the variational form of the original eigenvalue problem (56). This is because in the equation (59) we only test against W itself, not against an arbitrary test function. However, the eigenvalues of the problem (59) include the eigenvalues of the problem (56), i.e. we may get additional solutions. As we are interested in the behavior of the eigenvalues of the problem (56), it is sufficient to notice they must have the same behavior as the eigenvalues of the problem (59).

The second and third integrals in the equation (59) are evaluated with integration by parts and the boundary conditions (57), e.g.,

$$\begin{aligned}\int_\Omega W\frac{\partial W}{\partial x}\,\mathrm{d}\Omega &= \int_{-b}^{b}\int_0^{\ell} W\frac{\partial W}{\partial x}\,\mathrm{d}x\,\mathrm{d}y \\ &= \int_{-b}^{b}\left[\frac{W^2(\ell,y)}{2}-\frac{W^2(0,y)}{2}\right]\mathrm{d}y, \\ &= 0\end{aligned} \tag{60}$$

and, in a similar manner, by performing integration by parts in the third integral in the equation (59) and again applying the boundary conditions (57), we have

$$\int_\Omega W\frac{\partial^2 W}{\partial x^2}\,\mathrm{d}\Omega = -\int_\Omega\left(\frac{\partial W}{\partial x}\right)^2\,\mathrm{d}\Omega\,. \tag{61}$$

Using the equalities (59) – (61) and performing elementary transformations, we obtain the following expression for the characteristic index:

$$s^2 = \left(V_0^2 - C^2\right)\frac{\displaystyle\int_\Omega\left(\frac{\partial W}{\partial x}\right)^2\mathrm{d}\Omega}{\displaystyle\int_\Omega W^2\,\mathrm{d}\Omega}\,. \tag{62}$$

If s becomes zero, we have a steady state solution (buckling) with frequency $\omega = 0$ at the velocity $V_0 = V_0^{\mathrm{div}}$. The value of this divergence velocity is estimated as

$$V_0^{\mathrm{div}} = C = \sqrt{\frac{T_0}{m}} = \sqrt{\frac{hu_0}{m\ell}E_1}\,, \tag{63}$$

where in the last form the equation (37) has been used.

2.4 Dynamic analysis of small transverse vibrations and elastic instability of an isotropic plate

To investigate the dynamic behavior of the plate, we insert, following the membrane case, the representation (50) into the equation (47). As the object is a plate,

the bending rigidities cannot be omitted this time. Therefore we have the equation

$$s^2W + 2sV_0\frac{\partial W}{\partial x} + (V_0^2 - C^2)\frac{\partial^2 W}{\partial x^2} + \frac{D}{m}\Delta^2 W = 0. \tag{64}$$

Again, following the membrane case, we multiply the left-hand side of the equation (64) by W and perform integration over the domain Ω to obtain

$$s^2\int_\Omega W^2\,\mathrm{d}\Omega + 2sV_0\int_\Omega W\frac{\partial W}{\partial x}\,\mathrm{d}\Omega + (V_0^2 - C^2)\int_\Omega W\frac{\partial^2 W}{\partial x^2}\,\mathrm{d}\Omega + \frac{D}{m}\int_\Omega W\Delta^2 W\,\mathrm{d}\Omega = 0\,. \tag{65}$$

The same argument holds for the variational form as in the membrane case. The equation (65) can be seen as an eigenvalue problem for the pair (s, W) with the parameter V_0, producing a spectrum of complex eigenfrequencies s and eigenmodes W for the chosen value of V_0. Alternatively, (65) can be viewed as an eigenvalue problem for the pair (V_0, W) with the parameter s, when s is fixed to any such value that at least one complex eigenfrequency exists for at least one choice of V_0. For other choices of s, this second eigenvalue problem has no solution.

Previously we have noted the equalities (60) and (61) for the membrane. Our boundary conditions in this problem are

$$(W)_{x=0,\ell} = 0, \qquad \left(\frac{\partial^2 W}{\partial x^2}\right)_{x=0,\ell} = 0\,, \qquad -b \le y \le b\,, \tag{66}$$

$$\left(\frac{\partial^2 W}{\partial y^2} + \beta_1\frac{\partial^2 W}{\partial x^2}\right)_{y=\pm b} = 0\,, \qquad 0 \le x \le \ell\,, \tag{67}$$

$$\left(\frac{\partial^3 W}{\partial y^3} + \beta_2\frac{\partial^3 W}{\partial x^2\partial y}\right)_{y=\pm b} = 0, \qquad 0 \le x \le \ell. \tag{68}$$

The last integral in (65) can be estimated, using Green's 2nd identity, as

$$\int_\Omega W\Delta^2 W\,\mathrm{d}\Omega = \int_\Omega (\Delta W)^2\,\mathrm{d}\Omega + \int_\Gamma \left(W\frac{\partial}{\partial n}\Delta W - \Delta W\frac{\partial W}{\partial n}\right)\mathrm{d}\Gamma, \tag{69}$$

where n is the exterior unit normal to the boundary Γ of the domain Ω.

We divide the boundary Γ into four parts (see Figure 14):

$$\Gamma_- = \{0 \le x \le \ell,\ y = -b\}, \qquad \Gamma_r = \{x = \ell,\ -b \le y \le b\},$$

$$\Gamma_+ = \{0 \le x \le \ell,\ y = b\}, \qquad \Gamma_\ell = \{x = 0,\ -b \le y \le b\}.$$

Admitting counterclockwise integration along Γ, we have

$$I = \int_\Gamma \left(W\frac{\partial}{\partial n}\Delta W - \Delta W\frac{\partial W}{\partial n}\right)\mathrm{d}\Gamma = I_- + I_r + I_+ + I_\ell. \tag{70}$$

Here

$$I_r = I_\ell = 0\,, \tag{71}$$

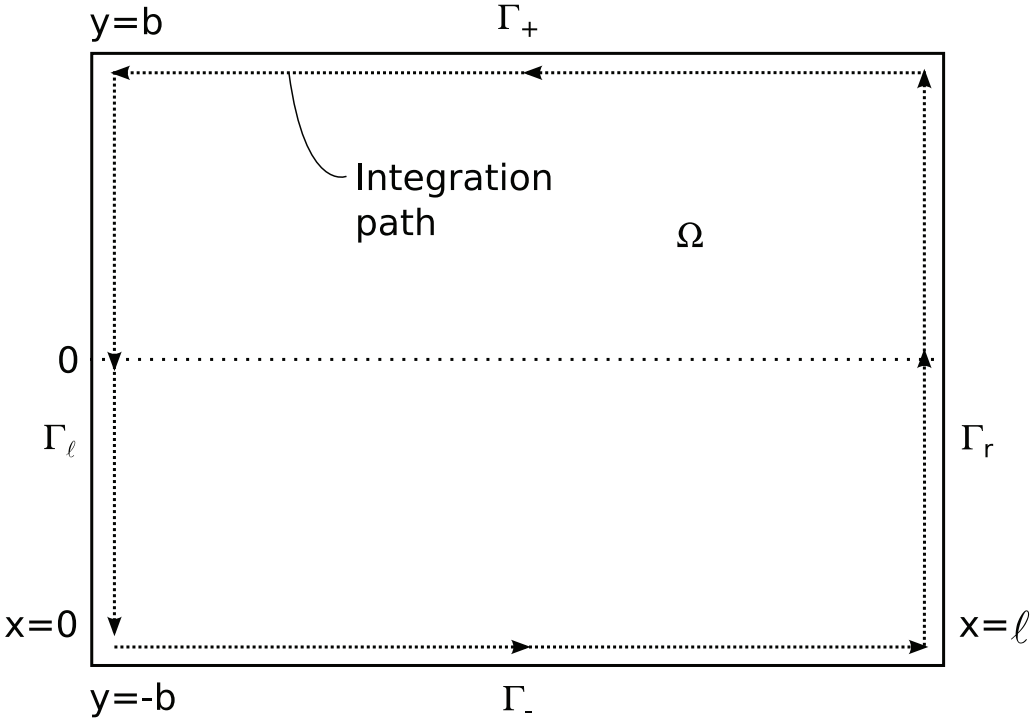

FIGURE 14 Division of the boundary Γ for the investigated contour integral.

$$\begin{aligned} I_- &= \int_{\Gamma_-} \left(W \frac{\partial}{\partial n} \Delta W - \Delta W \frac{\partial W}{\partial n} \right) \mathrm{d}\Gamma \\ &= -\int_0^\ell \left(W \frac{\partial}{\partial y} \Delta W - \Delta W \frac{\partial W}{\partial y} \right)_{y=-b} \mathrm{d}x \,, \end{aligned} \tag{72}$$

$$\begin{aligned} I_+ &= \int_{\Gamma_+} \left(W \frac{\partial}{\partial n} \Delta W - \Delta W \frac{\partial W}{\partial n} \right) \mathrm{d}\Gamma \\ &= -\int_\ell^0 \left(W \frac{\partial}{\partial y} \Delta W - \Delta W \frac{\partial W}{\partial y} \right)_{y=b} \mathrm{d}x \\ &= \int_0^\ell \left(W \frac{\partial}{\partial y} \Delta W - \Delta W \frac{\partial W}{\partial y} \right)_{y=b} \mathrm{d}x \,. \end{aligned} \tag{73}$$

where we have used the relations

$$\mathrm{d}\Gamma = \mathrm{d}x, \quad \frac{\partial}{\partial n} = -\frac{\partial}{\partial y} \quad \text{for } (x,y) \in \Gamma_- \,, \tag{74}$$

$$\mathrm{d}\Gamma = -\mathrm{d}x, \quad \frac{\partial}{\partial n} = \frac{\partial}{\partial y} \quad \text{for } (x,y) \in \Gamma_+ \,, \tag{75}$$

and

$$W = \Delta W = 0 \quad \text{for } (x, y) \ \in \Gamma_\ell + \Gamma_r \, . \tag{76}$$

We obtain

$$I = I_- + I_+ = \int_0^\ell \left(Q(W, W)_{y=b} - Q(W, W)_{y=-b} \right) \mathrm{d}x \, , \tag{77}$$

where

$$Q(w, v) \equiv v \frac{\partial}{\partial y} \Delta w - \Delta w \frac{\partial v}{\partial y} \tag{78}$$

with the arbitrary functions v and w. Using the boundary conditions for an isotropic plate, (67) and (68), we find that

$$Q = \frac{W \dfrac{\partial^3 W}{\partial y^3}}{\left(\dfrac{2 - \nu}{1 - \nu} \right)} + \frac{\dfrac{\partial W}{\partial y} \dfrac{\partial^2 W}{\partial y^2}}{\left(\dfrac{\nu}{1 - \nu} \right)}, \qquad at \ y = \pm b. \tag{79}$$

We can see from the equation (79) that the function Q is antisymmetric with respect to the transformation $y \to -y$ for symmetric and antisymmetric functions W, and consequently,

$$Q(W, W)_{y=b} = -Q(W, W)_{y=-b} \, . \tag{80}$$

We observe that

$$I = 2 \int_0^\ell Q(W, W)_{y=b} \, \mathrm{d}x \, . \tag{81}$$

From equations (69) and (81), we obtain

$$\int_\Omega W \Delta^2 W \, \mathrm{d}\Omega = \int_\Omega (\Delta W)^2 \, \mathrm{d}\Omega + 2 \int_0^\ell Q(W, W)_{y=b} \, \mathrm{d}x \, , \tag{82}$$

and, furthermore, inserting this result in the equation (65), we get the following representation

$$\omega^2 = -s^2$$

$$= \frac{(C^2 - V_0^2) \displaystyle\int_\Omega \left(\frac{\partial W}{\partial x} \right)^2 \mathrm{d}\Omega + \frac{D}{m} \left(\int_\Omega (\Delta W)^2 \, \mathrm{d}\Omega + 2 \int_0^\ell Q_{y=b} \, \mathrm{d}x \right)}{\displaystyle\int_\Omega W^2 \, \mathrm{d}\Omega}. \tag{83}$$

We can now observe from the representation (83) the following equation for the divergence mode:

$$\left(V_0^{\mathrm{div}} \right)^2 = C^2 + \frac{D}{m} \frac{\displaystyle\int_\Omega (\Delta W)^2 \mathrm{d}\Omega + 2 \int_0^\ell Q_{y=b} \, \mathrm{d}x}{\displaystyle\int_\Omega \left(\frac{\partial W}{\partial x} \right)^2 \mathrm{d}\Omega} \, . \tag{84}$$

In particular, it follows from the equation (84) that when the bending rigidity of the plate is negligible, the case reduces to the axially travelling string. This is a known result (see, e.g., Chang and Moretti [21]). From the result, (see the equation (63)) we notice that the same value for the critical velocity also applies to ideal membranes [1]. These observations generalize the analogous results by the author for a cylindrical deformation (see the article by Banichuk et al. [7]), i.e. a flat panel model of an ideal membrane. The trend of the behavior is that if V_0 increases, s becomes real and the displacement grows exponentially with time. However a rigorous analysis should be completed with the aim of the perturbation analysis, but we have excluded this and studied only the behaviour of the system in a numerical manner.

2.5 Divergence instability of an isotropic plate

In this section, we concentrate on an isotropic plate. In many cases it is reasonable to consider equations with this simplification; later in this thesis, we will show numerically that the effect of orthotropicity on the divergence velocity is relatively small.

2.5.1 Statement of the eigenvalue problem

In this section, we will study the divergence (buckling) instability of an isotropic plate**.** This problem is formulated as the eigenvalue problem of the partial differential equation

$$(mV_0^2 - T_0)\frac{\partial^2 W}{\partial x^2} + D\left(\frac{\partial^4 W}{\partial x^4} + 2\frac{\partial^4 W}{\partial x^2 \partial y^2} + \frac{\partial^4 W}{\partial y^4}\right) = 0 \tag{85}$$

with an isotropic version of boundary conditions (66) – (68). Note that time-dependent components are excluded when compared with the equation (47). In order to determine the minimal eigenvalue

$$\lambda = \gamma^2 = \frac{\ell^2}{\pi^2 D}(mV_0^2 - T_0) \tag{86}$$

of the problem (66) – (68), (85), and the corresponding eigenfunction $w = w(x, y)$, we apply the following representation:

$$W = W(x, y) = f\left(\frac{y}{b}\right)\ \sin\left(\frac{\pi x}{\ell}\right), \tag{87}$$

where $f\left(\frac{y}{b}\right)$ is an unknown function. It follows from the equation (87) that the desired buckling form w satisfies the boundary condition (66). The solution, a

[1] Note that the divergence velocity does not depend on W; thus the theory predicts that any combination of modes may occur at the critical velocity for the special case of an ideal membrane under a homogeneous tension.

half-sine in the longitudinal direction, is well-known (see e.g. the article by Lin [46]). Using the dimensionless formulation

$$\eta = \frac{y}{b}, \quad \mu = \frac{\ell}{\pi b}, \tag{88}$$

and the relations (67) – (68) and (85) – (88), we obtain the following eigenvalue problem for the unknown function $f(\eta)$:

$$\mu^4 \frac{\mathrm{d}^4 f}{\mathrm{d}\eta^4} - 2\mu^2 \frac{\mathrm{d}^2 f}{\mathrm{d}\eta^2} + (1-\lambda) f = 0, \quad -1 \le \eta \le 1 \tag{89}$$

$$\mu^2 \frac{\mathrm{d}^2 f}{\mathrm{d}\eta^2} - \nu f = 0, \quad \eta = \pm 1 \tag{90}$$

$$\mu^2 \frac{\mathrm{d}^3 f}{\mathrm{d}\eta^3} - (2-\nu) \frac{\mathrm{d} f}{\mathrm{d}\eta} = 0, \quad \eta = \pm 1. \tag{91}$$

2.5.2 Solution process for the eigenvalue problem

In this section, we will present the theory of the solution process of this eigenvalue problem. We consider the problem as a spectral boundary value problem; see the equations (89) – (91). Note that it is an invariant with respect to the symmetry operation $\eta \to -\eta$, and consequently, all its eigenfunctions can be classified as

$$f^s(\eta) = f^s(-\eta), \quad f^a(\eta) = -f^a(-\eta), \quad 0 \le \eta \le 1\,. \tag{92}$$

Here f^s and f^a are, respectively, functions that are symmetric and antisymmetric (skew-symmetric) with respect to the x-axis. When $\gamma \le 1$, a divergence mode symmetric with respect to the x-axis can be presented in the form

$$W = f^s(\eta)\ \sin\left(\frac{\pi x}{\ell}\right) \tag{93}$$

where

$$f^s(\eta) = A^s \cosh(\kappa_+ \eta) + B^s \cosh(\kappa_- \eta) \tag{94}$$

and

$$\kappa_+ = \sqrt{1+\gamma}\,, \quad \kappa_- = \sqrt{1-\gamma}. \tag{95}$$

The function $f^s(\eta)$ is a symmetric solution of the eigenvalue problem (89), and A^s and B^s are arbitrary constants. At first, we concentrate on the symmetric case and return to the antisymmetric case later.

Using the relations (90) – (94), we can derive the linear algebraic equations for determining the constants A^s and B^s :

$$A^s(\kappa_+^2 - \nu)\ \cosh\left(\frac{\kappa_+}{\mu}\right) + B^s(\kappa_-^2 - \nu)\ \cosh\left(\frac{\kappa_-}{\mu}\right) = 0 \tag{96}$$

$$-A^s\kappa_+(\kappa_-^2-\nu)\ \sinh\left(\frac{\kappa_+}{\mu}\right)-B^s\kappa_-(\kappa_+^2-\nu)\ \sinh\left(\frac{\kappa_-}{\mu}\right)=0\,. \tag{97}$$

The condition for a non-trivial solution to exist in the form (93) – (95) is that the determinant of the system (96) and (97) must vanish. This leads to the transcendental equation

$$\Delta^s(\gamma,\mu)=\kappa_-(\kappa_+^2-\nu)^2\ \cosh\left(\frac{\kappa_+}{\mu}\right)\ \sinh\left(\frac{\kappa_-}{\mu}\right)- \kappa_+(\kappa_-^2-\nu)^2\ \sinh\left(\frac{\kappa_+}{\mu}\right)\ \cosh\left(\frac{\kappa_-}{\mu}\right)=0, \tag{98}$$

which determines the eigenvalues $\lambda=\gamma^2$ as an implicit function. The equation (98) can be transformed into a more convenient form

$$\Phi(\gamma,\mu)-\Psi(\gamma,\nu)=0\,, \tag{99}$$

where

$$\Phi(\gamma,\mu)=\tanh\left(\frac{\sqrt{1-\gamma}}{\mu}\right)\ \coth\left(\frac{\sqrt{1+\gamma}}{\mu}\right) \tag{100}$$

and

$$\Psi(\gamma,\nu)=\frac{\sqrt{1+\gamma}\,(\gamma+\nu-1)^2}{\sqrt{1-\gamma}\,(\gamma-\nu+1)^2}\,. \tag{101}$$

Let us consider the modes of buckling which are antisymmetric with respect to the x-axis:

$$W=f^a(\eta)\ \sin\left(\frac{\pi x}{\ell}\right)\,, \tag{102}$$

where

$$f^a(\eta)=A^a\sinh(\kappa_+\eta)+B^a\sinh(\kappa_-\eta) \tag{103}$$

for $\gamma\leq 1$. Here the values κ_+, κ_- are defined by the expressions (95). Using the expression (103) for f^a and the boundary conditions on the free edges of the plate (see the equations (90) and (91)), we obtain the following transcendental equation for determining the quantity γ:

$$\Phi(\gamma,\mu)-\Psi^{-1}(\gamma,\nu)=0\,. \tag{104}$$

In the equation (104), $\Phi(\gamma,\mu)$ and $\Psi(\gamma,\nu)$ are again defined by the formulas (100) and (101). In the segment $0\leq\gamma\leq 1$ being considered, the equation has two roots,

$$\gamma=\gamma_1\quad\rightarrow\quad\gamma_0<\gamma_1<1 \tag{105}$$

and

$$\gamma=\gamma_2\quad\rightarrow\quad\gamma_2=1, \tag{106}$$

for the arbitrary values of ν and the parameter μ, which characterizes the elongation of the plate. By using the equations (105) and (106) and some properties described in the next section, we are able to define

$$\gamma_*<\gamma_1<\gamma_2\,, \tag{107}$$

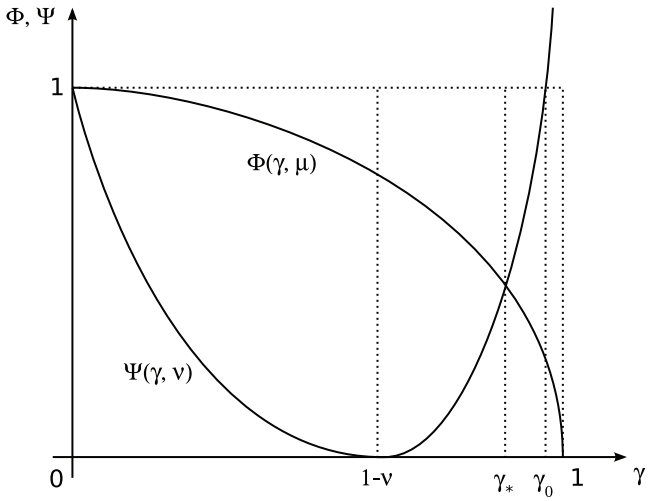

FIGURE 15 Behavior of the functions Φ and Ψ with respect to the parameter γ in the isotropic case. The presentation is qualitative.

and the minimal eigenvalue is γ_*. Thus, the critical buckling mode is symmetric with respect to the x-axis, and corresponds to $\gamma = \gamma_*$, i.e., to the solution of the equation (99).

2.5.3 Analytical details of the solution for the eigenvalue problem

In this section we investigate the properties of the functions $\Phi(\gamma, \mu)$ and $\Psi(\gamma, \nu)$, expressed by (100) and (101), when $0 \leq \gamma \leq 1$. Their schematic illustration is presented in Figure 15. As γ increases from zero to unity, the function $\Phi(\gamma, \mu)$ decreases continuously and monotonically from 1 to 0, i.e.

$$1 \geq \Phi(\gamma, \mu) \geq 0, \quad \frac{\partial \Phi(\gamma, \mu)}{\partial \gamma} < 0, \quad 0 \leq \gamma \leq 1 \tag{108}$$

and

$$\Phi(0, \mu) = \left(\tanh \frac{\sqrt{1-\gamma}}{\mu} \ \coth \frac{\sqrt{1+\gamma}}{\mu} \right)_{\gamma=0} = 1 \tag{109}$$

$$\Phi(1, \mu) = \left(\tanh \frac{\sqrt{1-\gamma}}{\mu} \ \coth \frac{\sqrt{1+\gamma}}{\mu} \right)_{\gamma=1} = 0. \tag{110}$$

We note that the proof of the monotonical decrease of the function Φ is performed in section 2.6 and the result is utilized here as a special case. The function $\Psi(\gamma, \nu)$ decreases from 1 to 0 in the interval $0 < \gamma < 1 - \nu$,

$$1 \geq \Psi(\gamma, \nu) \geq 0, \quad \frac{\partial \Psi(\gamma, \nu)}{\partial \gamma} < 0, \quad 0 < \gamma < 1 - \nu \tag{111}$$

and

$$\Psi(0, \nu) = \left[\frac{\sqrt{1+\gamma}}{\sqrt{1-\gamma}} \frac{(\gamma + \nu - 1)^2}{(\gamma - \nu + 1)^2} \right]_{\gamma=0} = 1 \tag{112}$$

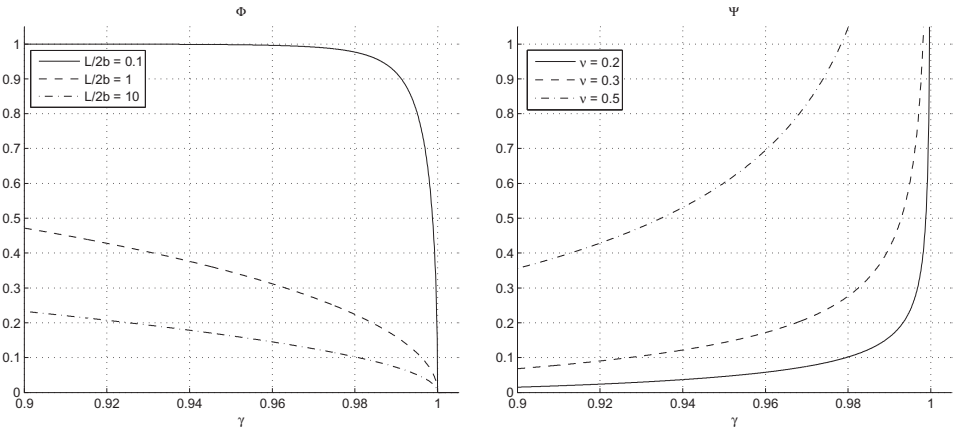

FIGURE 16 Plots of Φ (left) and Ψ (right) for different values of the parameters $\ell/2b$ and ν.

$$\Psi(1-\nu,\nu) = \left[\frac{\sqrt{1+\gamma}}{\sqrt{1-\gamma}}\frac{(\gamma+\nu-1)^2}{(\gamma-\nu+1)^2}\right]_{\gamma=1-\nu} = 0. \tag{113}$$

The function Ψ increases monotonically in the interval $1-\nu < \gamma < 1$ and increases without limit as $\gamma \to 1$, i.e.

$$0 \le \Psi(\gamma,\nu) < \infty, \quad \frac{\partial\Psi(\gamma,\nu)}{\partial\gamma} > 0, \quad 1-\nu < \gamma < 1, \tag{114}$$

where

$$\Psi(1-\nu,\nu) = 0 \tag{115}$$

and

$$\lim_{\gamma\to 1}\Psi(\gamma,\nu) = \infty. \tag{116}$$

Plots of the function $\Phi(\gamma,\mu)$ when the geometric aspect ratio $\frac{\ell}{2b} = 0.1,\ 1,$ and 10 are shown in Figure 16 on the left. The functions $\Psi(\gamma,\nu)$ when $\nu = 0.2$, 0.3 and 0.5 are shown on the right.

The value of $\gamma = \gamma_0$, for which

$$\Psi(\gamma_0,\nu) = 1, \quad \gamma_0 \in [1-\nu, 1] \tag{117}$$

is of special interest. Solving the corresponding equation, we obtain that

$$\gamma_0^2 = (1-\nu)(3\nu - 1 + 2\sqrt{1-2\nu(1-\nu)}). \tag{118}$$

The value of γ_0 turns out to be close to unity.

Assuming that $\ell \gg b$, e.g. a long band span assumption that corresponds to a large μ, we have the approximate expression

$$\Psi = \sqrt{\frac{1-\gamma}{1+\gamma}} \tag{119}$$

and the equation (99) has the solution

$$\lambda_e = \gamma_e^2 = 1 - \nu^2 \ . \tag{120}$$

This solution corresponds to a narrow strip simply supported at its ends; it leads to the Euler value of the force for stability loss (buckling)

$$P = P_e = \lambda_e \frac{\pi^2 D}{\ell^2} = \pi^2 \frac{EI}{\ell^2} \ , \tag{121}$$

where

$$P = mV_0^2 - T_0, \quad D = \frac{Eh^3}{12(1-\nu^2)}, \quad I = \frac{h^3}{12}. \tag{122}$$

Thus, we find that the case of a narrow strip corresponds to the classical one-dimensional case.

It follows from the above treatment and the properties of the functions $\Phi(\gamma, \mu)$ and $\Psi(\gamma, \nu)$ that the roots $\gamma = \gamma_*$ of the equation (99) lie in the interval

$$\gamma_e \leq \gamma_* \leq \gamma_0 \tag{123}$$

for all $0 < \mu < \infty$. Note that this is the property that is needed to complete the analysis of the equation (107).

The corresponding critical velocity of the travelling band is represented as

$$(V_0)_*^2 = \frac{T_0}{m} + \frac{\gamma_*^2}{m} \left(\frac{\pi^2 D}{\ell^2} \right) \ . \tag{124}$$

In the limit of a wide band, we have

$$\gamma_* \to \gamma_0 \neq 1 \quad \text{for } \mu \to 0 \tag{125}$$

and therefore the corresponding mode of stability loss from the equations (93) – (95) does not turn out to be a cylindrical. Thus, the case of a wide band does not reduce to the classical one-dimensional case as assumed.

The largest difference between the critical parameter γ_*, which leads to the loss of stability of an infinitely wide band, and the corresponding value obtained assuming a distribution of the deflections in the form of cylindrical surface, occurs when $\nu = 0.5$, i.e., in the case of an absolutely incompressible material.

2.6 Divergence instability of an orthotropic plate

In many applications, an assumption for isotropic material properties is valid. In this section, we will provide a solid foundation for analyzing the theoretical importance for the orthotropic material in the case of stability of moving plates.

2.6.1 Formulation of the eigenvalue problem

In this section we will extend the results from section 2.5 for orthotropic materials. The problem is formulated similarly to the eigenvalue problem, describing the divergence of orthotropic plate. We have the partial differential equation

$$\left(mV_0^2 - T_0\right)\frac{\partial^2 W}{\partial x^2} + D_0\mathcal{L}_0(w) = 0 \tag{126}$$

with the boundary conditions (66) – (68). To determine the minimal eigenvalue,

$$\lambda = \gamma^2 = \frac{\ell^2}{\pi^2 D_0}\left(mV_0^2 - T_0\right)\,, \tag{127}$$

of the problem (66) – (68) and (126). For the corresponding eigenfunction $w = w(x,y)$, we apply the same representation as before

$$W = W(x,y) = f(\frac{y}{b})\sin(\frac{\pi x}{\ell})\,. \tag{128}$$

The fact that the solution is a half-sine in the longitudinal direction is well-known in the isotropic case. It can be shown that the same form is applicable for the orthotropic plate. What remains to be determined is the unknown cross-section $f\left(\frac{y}{b}\right)$.

It follows from the equation (128) that the desired buckling form W satisfies the boundary condition (66). Using the same dimensionless formulations η and μ as before (see the equation (88)) and the relations (67), (68) and (126) – (128), we obtain the following eigenvalue problem for the unknown function $f(\eta)$:

$$\mu^4 H_2\frac{\mathrm{d}^4 f}{\mathrm{d}\eta^4} - 2\mu^2 H_3\frac{\mathrm{d}^2 f}{\mathrm{d}\eta^2} + (H_1 - \lambda)\,f = 0\,, \qquad -1 \le \eta \le 1\,, \tag{129}$$

$$\left(\mu^2\frac{\mathrm{d}^2 f}{\mathrm{d}\eta^2} - \beta_1 f\right) = 0\,, \qquad -1 \le \eta \le 1\,, \tag{130}$$

$$\left(\mu^2\frac{\mathrm{d}^3 f}{\mathrm{d}\eta^3} - \beta_2\frac{\mathrm{d}f}{\mathrm{d}\eta}\right) = 0\,, \qquad -1 \le \eta \le 1\,,. \tag{131}$$

We denote

$$\mathcal{L}_1(f) = \mu^4 H_2\frac{\mathrm{d}^4 f}{\mathrm{d}\eta^4} - 2\,\mu^2 H_3\frac{\mathrm{d}^2 f}{\mathrm{d}\eta^2} + H_1 f \tag{132}$$

where $H_{1,}H_2$ and H_3 are dimensionless bending rigidities,

$$H_1 = \frac{D_1}{D_0}, \qquad H_2 = \frac{D_2}{D_0}, \qquad H_3 = \frac{D_3}{D_0}\,, \tag{133}$$

and D_0 is the characteristic bending rigidity.

2.6.2 Proof of non-negative eigenvalues for the problem

To show that the eigenvalues λ of $\mathcal{L}_1(f)$ (see the equation (132)) are non-negative, we proceed by using general ideas from Chen et al. [22], who proved a similar result for an isotropic stationary plate. We introduce the bilinear form $a(f,g)$ that corresponds to the strain energy of a plate (see e.g. p. 377 in the book by Timoshenko and Woinowsky–Krieger [79]),

$$a(f,g) = \int_{-1}^{1} \Bigg[H_1 f\, \bar{g} - \mu^2 B_1 f\, \frac{\mathrm{d}^2 \bar{g}}{\mathrm{d}\eta^2} - \mu^2 B_1 \frac{\mathrm{d}^2 f}{\mathrm{d}\eta^2}\, \bar{g} + \mu^4 H_2 \frac{\mathrm{d}^2 f}{\mathrm{d}\eta^2} \frac{\mathrm{d}^2 \bar{g}}{\mathrm{d}\eta^2} + 4\mu^2 B_2 \frac{\mathrm{d}f}{\mathrm{d}\eta} \frac{\mathrm{d}\bar{g}}{\mathrm{d}\eta} \Bigg] \mathrm{d}\eta\,, \tag{134}$$

where

$$B_1 + 2\, B_2 = H_3\,. \tag{135}$$

Performing an integration by parts on the bilinear equation (134) we obtain

$$a(f,g) = \int_{-1}^{1} \left[\mu^4 H_2 \frac{\mathrm{d}^4 f}{\mathrm{d}\eta^4} - 2\,\mu^2 H_3 \frac{\mathrm{d}^2 f}{\mathrm{d}\eta^2} + H_1 f \right] \bar{g}\, \mathrm{d}\eta\,. \tag{136}$$

Thus, the form $a(f,g)$ can alternatively be defined as

$$a(f,g) \;=\; (\mathcal{L}_1(f), g)\,, \tag{137}$$

where the inner product $(\cdot\,,\cdot\,)$ is

$$(u,v) \;=\; \int_{-1}^{1} u\, \bar{v}\, \mathrm{d}\eta \tag{138}$$

and $\bar{v}$ denotes the complex conjugate of v. The operator $\mathcal{L}_1(f)$ is self-adjoint, and the form $a(f,g)$ induces a positive semidefinite norm $a(f,f)$

$$a(f,f) = \int_{-1}^{1} \Bigg[H_1 \left\| f - \mu^2 \nu_{21} \frac{\mathrm{d}^2 f}{\mathrm{d}\eta^2} \right\|^2 + \mu^4 H_2 (1 - \nu_{12}\nu_{21}) \left\| \frac{\mathrm{d}^2 f}{\mathrm{d}\eta^2} \right\|^2 + 4\,\mu^2 B_2 \left\| \frac{\mathrm{d}f}{\mathrm{d}\eta} \right\|^2 \Bigg] \mathrm{d}\eta \;\geq 0\,. \tag{139}$$

This implies that the eigenvalues of $\mathcal{L}_1(f)$ are non-negative. That is,

$$\lambda \geq 0\,, \tag{140}$$

for all eigenvalues λ of the problem (129) – (131), which governs the cross-sectional eigenfunctions $f(y)$ and the corresponding eigenvalues of the buckled, moving orthotropic plate.

2.6.3 The solution process of the eigenvalue problem in the case of the orthotropic plate

The general solutions of the ordinary differential equation (129) have the form

$$f = Ae^{p\eta}, \qquad p = \frac{\kappa}{\mu} \tag{141}$$

where A is an arbitrary constant and κ is a solution of the following biquadratic algebraic characteristic equation:

$$H_2\kappa^4 - 2H_3\kappa^2 + (H_1 - \lambda) = 0 \tag{142}$$

that is written as

$$\kappa_\pm^2 = \frac{H_3}{H_2}\left(1 \pm \sqrt{1 - \frac{H_2(H_1-\lambda)}{H_3^2}}\right) = \frac{H_3}{H_2}\left(1 \pm \sqrt{1 - \frac{H_2(1-\lambda)}{H_3^2}}\right), \tag{143}$$

where the upper, and respectively the lower, signs correspond to each other.

The solutions $\kappa_\pm$ are real-valued if we have the following range for λ:

$$\lambda_{\min} \equiv 1 - \frac{H_3^2}{H_2} \le \lambda \le 1 \equiv \lambda_{\max}\,, \tag{144}$$

corresponding to a real-valued eigenfunction f. The lower limit

$$\lambda_{\min} < 0 \qquad \text{when} \qquad G_{12} \ge G_H. \tag{145}$$

By the equations (140) and (144), we may seek the lowest eigenvalue in the range $0 \le \lambda \le 1$, as was done in the isotropic case in section 2.5.

On the other hand, we can find examples for measurements of $G_{12} < G_H$ for paper materials (see, e.g. the articles of Mann et al. [52], Seo [70], Yokoyama and Nakai [92], and Bonnin et al.[20]). In that case,

$$\lambda_{\min} \ge 0 \qquad \text{when} \qquad G_{12}{<}G_H. \tag{146}$$

This will produce complex solutions $\kappa_\pm$ and complex eigenfunctions if λ is between zero and $\lambda_{\min}$. In practice, based on numerical approximations of the solution, it has been observed that this interval contains no solutions.

From the equations (141) and (143) we obtain that the general solution can be represented in the form

$$f(\eta) = A_1 e^{+\frac{\kappa_+}{\mu}\eta} + A_2 e^{-\frac{\kappa_+}{\mu}\eta} + A_3 e^{+\frac{\kappa_-}{\mu}\eta} + A_4 e^{-\frac{\kappa_-}{\mu}\eta} \tag{147}$$

with unknown constants A_1, A_2, A_3 and A_4.

The eigenvalue boundary value problem (129) – (131) is an invariant under the symmetry operation $\eta \to -\eta$, and consequently the eigenforms can be classified into functions that are symmetric f^s, or antisymmetric f^a, based on the

origin. Using the relations (129) – (131) and (147), we obtain a general representation for the function $f^s(\eta)$ and linear algebraic equations for determining the constants A^s and B^s:

$$f^s(\eta) = A^s \cosh\frac{\kappa_+\eta}{\mu} + B^s \cosh\frac{\kappa_-\eta}{\mu} \tag{148}$$

$$A^s\left(\kappa_+^2 - \beta_1\right)\cosh\frac{\kappa_+}{\mu} + B^s\left(\kappa_-^2 - \beta_1\right)\cosh\frac{\kappa_-}{\mu} = 0 \tag{149}$$

$$A^s\kappa_+\left(\kappa_+^2 - \beta_2\right)\sinh\frac{\kappa_+}{\mu} + B^s\kappa_-\left(\kappa_-^2 - \beta_2\right)\sinh\frac{\kappa_-}{\mu} = 0\,, \tag{150}$$

where A^s and B^s are unknown constants. Due to the symmetry or antisymmetry of the solution f, we have only two independent unknown constants, instead of the four as in the general representation (147), where the symmetry considerations had not yet been applied.

The conditions for a non-trivial solution to exist in the form of the equations (148) – (150) reduce to the requirement that the determinant of the homogeneous system (149) and (150) vanishes. The zero determinant condition can be expressed as

$$\Phi(\gamma, \mu, \nu_{12}, E_1, E_2, G_{12}) - \Psi(\gamma, \nu_{12}, E_1, E_2, G_{12}) = 0\,, \tag{151}$$

where

$$\Phi(\gamma, \mu, \nu_{12}, E_1, E_2, G_{12}) = \tanh\frac{\kappa_-}{\mu}\coth\frac{\kappa_+}{\mu}\,, \tag{152}$$

$$\Psi(\gamma, \nu_{12}, E_1, E_2, G_{12}) = \frac{\kappa_+(\kappa_+^2 - \beta_2)(\kappa_-^2 - \beta_1)}{\kappa_-(\kappa_+^2 - \beta_1)(\kappa_-^2 - \beta_2)}, \tag{153}$$

and where

$$\kappa_+ = \kappa_+(\gamma, \nu_{12}, E_1, E_2, G_{12}), \qquad \kappa_- = \kappa_-(\gamma, \nu_{12}, E_1, E_2, G_{12})\,. \tag{154}$$

This equation (151) can be used to determine the eigenvalues $\lambda = \gamma^2$ corresponding to symmetric eigenfunctions with different values of the parameters μ, ν_{12}, E_1, E_2 and G_{12}. Note that there is no dependence on the parameter ν_{21} since it depends on ν_{12}, E_1 and E_2 via Maxwell's relation (36). Similarly, using the relations (130) and (131), we can obtain a representation for antisymmetric eigenfunctions $f^a(\eta)$, the equation for determining the corresponding constants A^a and B^a, and the transcendental equation

$$\Phi - \frac{1}{\Psi} = 0\,, \tag{155}$$

where Φ and Ψ are the functions defined in the equations (152) – (153). These equations can be used for determining the eigenvalues corresponding to antisymmetric eigenforms. The representations differ from the equations (148) – (150) through the replacements

$$\cosh \to \sinh \quad \text{and} \quad \sinh \to \cosh\,. \tag{156}$$

2.6.4 Analytical details of the transcendental and algebraic parts of the eigenvalue problem

In the following section, we will investigate the properties of the functions Φ and Ψ, when λ is in the range $0 \leq \lambda \leq 1$. Unlike in the isotropic case described in section 2.5.3, the decoupling between the geometric and material parameters is very minimal. The function Ψ does not depend on the aspect ratio μ (geometry), but both Φ and Ψ depend on all the independent material parameters (ν_{12}, E_1, E_2 and G_{12}).

We start our examination by noting that (by direct calculation)

$$\Phi(\lambda_{\min}) = 1 \tag{157}$$

$$\Psi(\lambda_{\min}) = 1 \tag{158}$$

and

$$\Phi(1) = 0 \tag{159}$$

regardless of the problem parameters. We defer the evaluation of the

$$\lim \Psi(\lambda \to \lambda_{\max}) \tag{160}$$

to the subsection on the algebraic part below. It is trivial to see that Ψ has a singularity

$$\lim_{\lambda \to \lambda_{\max}} \kappa_- \to 0^+ \tag{161}$$

and in order to deduce its signs we need to know the sign of each of the terms in the equation (153). Let us assume values of ν_{12}, E_1, E_2 and G_{12} to be given and that they correspond to some orthotropic material. The qualitative behavior of the functions Φ and Ψ is illustrated in Figure 17. One can compare the difference between orthotropic and isotropic plates by looking at Figure 15 on page 51. The range for γ, which is defined in the equation (127), is obtained by taking the square root of the equation (144). Note that the x-axis of the figure starts at $\gamma_{\min}$. In the isotropic case, we had $\gamma_{\min} = 0$, which does not hold for the general orthotropic case.

Figure 18 shows some examples of Φ and Ψ plotted for some typical orthotropic materials. Note that, as discussed above, only Φ depends on the aspect ratio $\ell/2b$. We see that the case $G_{12} = G_H$ behaves like the isotropic case, as expected (compare to section 2.5.3). When the value of G_{12} deviates from the Huber quantity, it is seen that when $G_{12} < G_H$, the curvature of Φ becomes more pronounced, especially for a large aspect ratio (i.e. a long, narrow strip). If $G_{12} > G_H$, the value of both functions at

$$\gamma = \max(0, \gamma_{\min}) \tag{162}$$

decreases, again especially for a large aspect ratio in the case of Φ.

When γ increases

$$\gamma_{\min} \to \gamma_{\max} \tag{163}$$

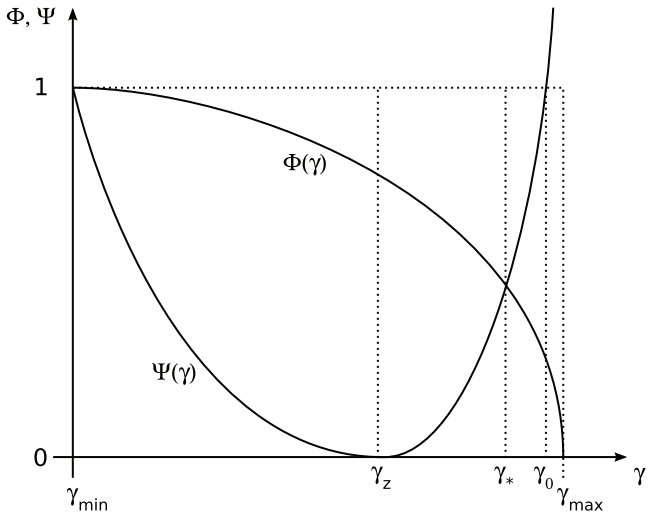

FIGURE 17 Behavior of Φ and Ψ as a function of γ when the parameters D_1, D_2, D_3, μ, β_1 and β_2 are fixed. This is a qualitative drawing. The main difference between this figure and Figure 15 on page 51 is that in the x-axis, graphs begin at $\gamma_{\min}$ instead of 0 and γ_z is the minimal value of the function Ψ, instead of ν.

the function $\Phi(\gamma, \mu)$ decreases continuously and monotonically from 1 to 0, i.e.

$$1 \geq \Phi(\gamma, \mu) \geq 0, \quad \frac{\partial \Phi(\gamma, \mu)}{\partial \gamma} < 0, \quad \gamma_{\min} \leq \gamma \leq \gamma_{\max}. \tag{164}$$

The critical values of the function Φ in that interval are

$$\Phi(\gamma_{\min}, \mu) = \left(\tanh \frac{\kappa -}{\mu} \coth \frac{\kappa_+}{\mu} \right)_{\gamma = \gamma_{\min}} = 1 \tag{165}$$

and

$$\Phi(\gamma_{\max}, \mu) = \left(\tanh \frac{\kappa -}{\mu} \coth \frac{\kappa_+}{\mu} \right)_{\gamma = \gamma_{\max}} = 0. \tag{166}$$

The function $\Psi(\gamma)$ decreases monotonically from 1 to 0 in the interval $\gamma_{\min} < \gamma < \gamma_z$, i.e.,

$$1 \geq \Psi(\gamma) \geq 0, \quad \frac{\partial \Psi(\gamma)}{\partial \gamma} < 0, \quad \gamma_{\min} < \gamma < \gamma_z. \tag{167}$$

The critical values of the function Ψ in that interval are

$$\Psi(\gamma_{\min}) = 1 \tag{168}$$

and

$$\Psi(\gamma_z) = 0. \tag{169}$$

The function Ψ increases monotonically in the interval $\gamma_z < \gamma < \gamma_{\max}$ and it increases without limit when $\gamma \to \gamma_{\max}$, i.e.

$$0 \leq \Psi(\gamma) < \infty, \quad \frac{\partial \Psi(\gamma)}{\partial \gamma} > 0, \quad \gamma_z < \gamma < 1. \tag{170}$$

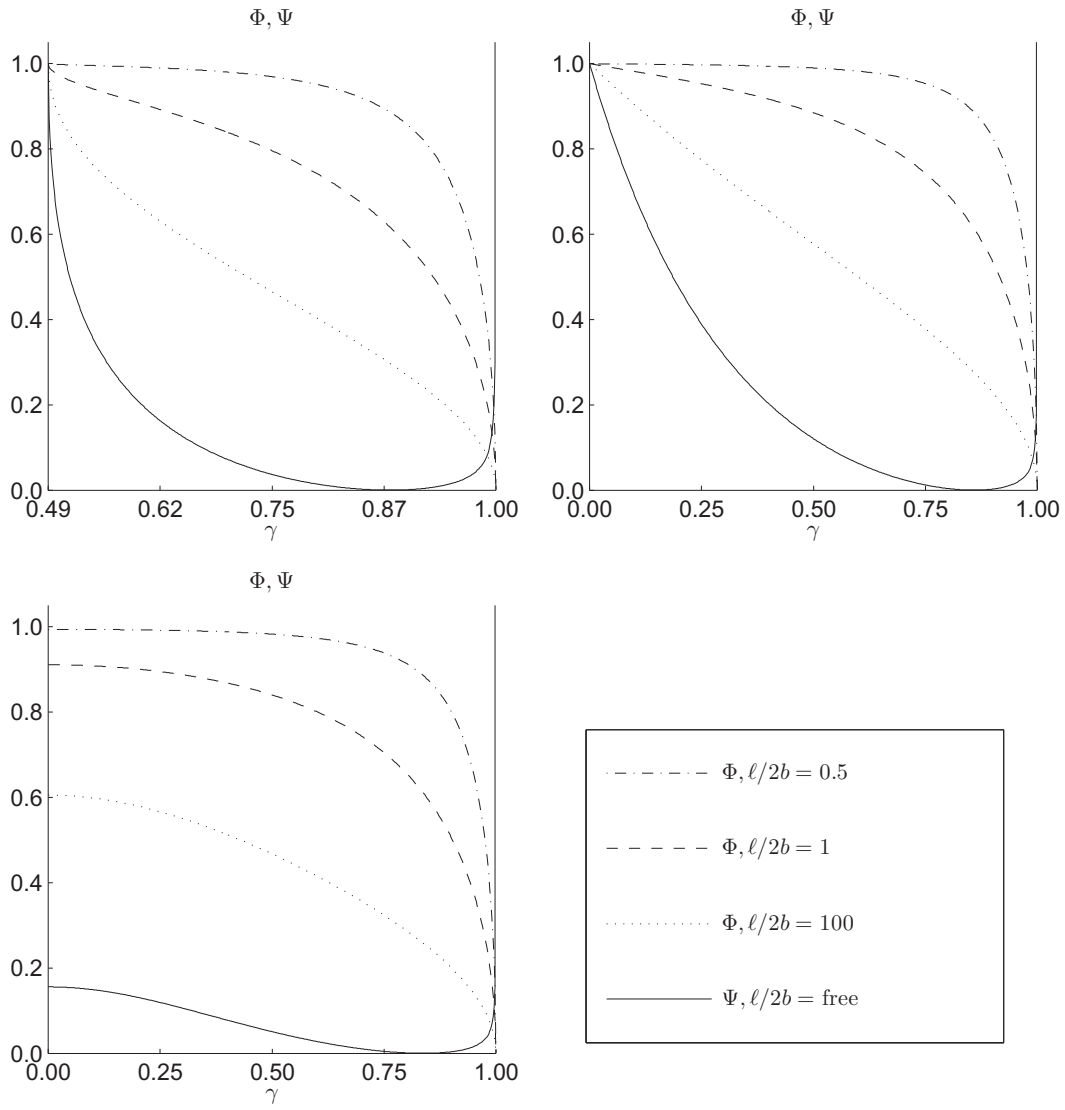

FIGURE 18 Behavior of the functions Φ and Ψ for some orthotropic materials, at different aspect ratios $\ell/2b$ and different values for the in-plane shear modulus G_{12}. For all cases, the other material parameters are $E_1 = 6.8$ GPa, $E_2 = 3.4$ GPa and $\nu_{12} = 0.2, \nu_{21} = 0.1$. Note that only Φ depends on the aspect ratio. Upper left: $G_{12} = 0.85\ G_H$ (note the scale for γ). Upper right: $G_{12} = G_H$. Lower left: $G_{12} = 1.15\ G_H$, where G_H is the value given by the Huber quantity. The range of γ is $\max(0, \gamma_{\min}) \leq \gamma \leq \gamma_{\max}$, based on the equations (127), (140) and (144), and evaluated separately for each subfigure.

The values of Ψ are thus

$$\Psi(\gamma_z) = 0,$$

and

$$\lim_{\gamma \to \gamma_{\max}} \Psi(\gamma) = \infty \, .$$

The function touches zero at the point

$$\gamma_z = \sqrt{\beta_j^2 H_2 - 2\beta_j H_3 + H_1} \, , \tag{171}$$

where $j = 1, 2$. It will be shown below that γ_z is unique. Thus both choices for j result in the same γ_z.

Because

$$0 \leq \Phi \leq 1 \qquad \forall \qquad \gamma_{\min} \leq \gamma \leq \gamma_{\max} \tag{172}$$

the symmetric solution in the equation (151) is only possible in the range where $\Psi \leq 1$. Likewise, the antisymmetric solution in the equation (155) is only possible in the range where

$$1/\Psi \leq 1 \Leftrightarrow \Psi \geq 1. \tag{173}$$

Note that the value of $\gamma = \gamma_0$ for which $\Psi = 1$, is of special interest; at this point we also have $\Psi = 1/\Psi$, and thus

$$\Phi - \Psi = \Phi - \frac{1}{\Psi}. \tag{174}$$

The functions defined by the left-hand sides of the equations (151) and (155) will therefore cross at the value $\gamma = \gamma_0$.

Note that the equation (167), combined with the consideration in the previous paragraph, implies that the eigenvalue γ_* corresponding to the symmetric solution is always lower than the eigenvalues γ_1 and γ_2 corresponding to the antisymmetric solution. Additionally, since

$$\Phi(\gamma_{\max}, \mu) = 0 \qquad \text{and} \qquad \lim_{\gamma \to \gamma_{\max}} \Psi(\gamma) = \infty, \tag{175}$$

the second antisymmetric eigenvalue is $\gamma_2 = \gamma_{\max}$. For the various values of γ defined above, we have the ordering

$$\gamma_{\min} < \gamma_z < \gamma_* < \gamma_0 < \gamma_1 < \gamma_2 = \gamma_{\max}. \tag{176}$$

An analytical expression for γ_0 can be found by using the definitions (152) and (153) and solving $\Psi^2(\gamma) = 1$ for γ. Let us define the auxiliary expression

$$\alpha \equiv \sqrt{8\,\beta_1\,H_2\,H_3 + \left({\beta_1}^2 - 6\,\beta_1\,\beta_2 + {\beta_2}^2\right)\,{H_2}^2} \, . \tag{177}$$

Then, for the root γ_0 that interests us, the following expression holds:

$$\gamma_0^2 = \frac{1}{2}\left((\beta_2 - \beta_1)\;\alpha + 2\,H_1 - \left({\beta_1}^2 - 4\,\beta_1\,\beta_2 + {\beta_2}^2\right)\,H_2 - 4\,\beta_1\,H_3\right) \, . \tag{178}$$

Using the theory presented, it is possible, by first solving γ_* from the equation (151), to find the critical velocity numerically from the equation (127) and the corresponding buckling form; see the equations (128), (143), and (148) – (150).

2.6.5 Analytical considerations of the behaviour of the transcendental equation

Let us show that the transcendental part Φ is monotonically decreasing in the open interval $(\lambda_{\min}, \lambda_{\max})$. First, we define

$$g(\lambda) \equiv \sqrt{1 - \frac{H_2(H_1 - \lambda)}{H_3^2}} \,, \tag{179}$$

i.e. the square root expression in $\kappa_\pm^2$ in the equation (143). We see that $g(\lambda_{\min}) = 0$ and $g(\lambda_{\max}) = 1$. Between these extreme values, $g(\lambda)$ increases monotonously as λ increases.

We write the equation (143) in the form

$$\kappa_\pm^2 = \frac{1}{cH_3} \left(1 \pm \sqrt{1 - c(1-\lambda)} \right) \,, \tag{180}$$

where we have defined the auxiliary constant

$$c \equiv H_2 / H_3^2 \,.$$

Differentiating the equation (180), we have

$$\frac{\partial(\kappa_\pm^2)}{\partial\lambda} = \frac{\pm 1}{2H_3\sqrt{1 - c(1-\lambda)}} \,, \tag{181}$$

where the upper and lower signs correspond to each other. Note that the square root expression in the denominator is $g(\lambda)$ in the equation (179), and as discussed above, it takes values in the range $(0, 1)$ as $\lambda \in (\lambda_{\min}, \lambda_{\max})$, and especially is positive in our range of interest. Thus, the equation (181) is always positive for κ_+^2 and always negative for κ_-^2.

On the other hand, by the rules of differentiation,

$$\frac{\partial(\kappa_\pm^2)}{\partial\lambda} = 2\kappa_\pm \frac{\partial\kappa_\pm}{\partial\lambda} \,, \tag{182}$$

and thus

$$\frac{\partial\kappa_\pm}{\partial\lambda} = \frac{\partial(\kappa_\pm^2)}{\partial\lambda} / 2\kappa_\pm \,. \tag{183}$$

Noting that $\kappa_\pm > 0$, we can conclude that the signs match:

$$\operatorname{sign} \frac{\partial\kappa_\pm}{\partial\lambda} = \operatorname{sign} \frac{\partial(\kappa_\pm^2)}{\partial\lambda} \,. \tag{184}$$

In the special case of $\lambda = \lambda_{\max}$, we have $\kappa_- = 0$, but this point is not in our open interval. Now we turn our attention to the function Φ. Differentiating the definition in the equation (152) with respect to λ, we have

$$\begin{aligned} \frac{\partial\Phi}{\partial\lambda} &= \frac{\partial}{\partial\lambda}\left(\tanh\frac{\kappa_-}{\mu}\right)\coth\frac{\kappa_+}{\mu} + \left(\tanh\frac{\kappa_-}{\mu}\right)\frac{\partial}{\partial\lambda}\left(\coth\frac{\kappa_+}{\mu}\right) \\ &= \frac{1}{\cosh^2\frac{\kappa_-}{\mu}} \cdot \frac{1}{\mu} \cdot \frac{\partial\kappa_-}{\partial\lambda}\coth\frac{\kappa_+}{\mu} + \tanh\frac{\kappa_-}{\mu}\left(-\frac{1}{\sinh^2\frac{\kappa_+}{\mu}}\right) \cdot \frac{1}{\mu} \cdot \frac{\partial\kappa_+}{\partial\lambda} \,. \end{aligned} \tag{185}$$

In the first term on the right-hand side,

$$\frac{\partial \kappa_-}{\partial \lambda} < 0, \tag{186}$$

by the equations (181) and (184), while the other factors are all positive, and in the second term,

$$\frac{-1}{\sinh^2 \frac{\kappa_+}{\mu}} < 0 \tag{187}$$

while all the other factors are positive. Thus, both terms on the right side are negative and we conclude that

$$\frac{\partial \Phi}{\partial \lambda} < 0 \quad \forall\, \lambda \in (\lambda_{\min}, \lambda_{\max})\,. \tag{188}$$

2.6.6 Analytical considerations of the behaviour of the algebraic equation

The second part is the algebraic function Ψ. We prove the following results:

1. The function Ψ has exactly one zero at λ_z.
2. The function Ψ has exactly one singularity located at $\lambda = \lambda_{\max}$, and its sign is positive:
$$\lim_{\lambda \to \lambda_{\max}} \Psi(\lambda) = +\infty.$$
3. If the root $\lambda_z \in (\lambda_{\min}, \lambda_{\max})$, then the function Ψ is monotonically decreasing in the interval $\lambda \in (\lambda_{\min}, \lambda_z)$, and monotonically increasing in the interval $\lambda \in (\lambda_z, \lambda_{\max})$.

Again, we begin with the equation (143). We note that the coefficient in front of the expression can be written as

$$\frac{H_3}{H_2} = \frac{D_3}{D_2} = \nu_{12} + 2\frac{G_{12}}{E_2}(1 - \nu_{12}\nu_{21})\,. \tag{189}$$

By defining the constants

$$A \equiv \frac{H_3}{H_2} = \nu_{12} + 2\frac{G_{12}}{E_2}(1 - \nu_{12}\nu_{21})\,, \quad B \equiv 2\frac{G_{12}}{E_2}(1 - \nu_{12}\nu_{21})\,, \tag{190}$$

we see that

$$\beta_1 = A - B\,, \qquad \beta_2 = A + B\,. \tag{191}$$

Using equations (190) and (179), the definition (143) reduces to a more convenient form,

$$\kappa_\pm^2 = A(1 \pm g(\lambda))\,. \tag{192}$$

Inserting the equations (191) and (192) into the definition (153), we have

$$\Psi = \frac{\sqrt{A(1 + g(\lambda))}(A\, g(\lambda) - B)^2}{\sqrt{A(1 - g(\lambda))}(A\, g(\lambda) + B)^2}\,. \tag{193}$$

All factors in the representation (193) are always positive, except the second one in the numerator. Thus, the function can only have one zero, which is located at such λ_z that

$$A g(\lambda_z) - B = 0. \tag{194}$$

The first result is therefore established.

To prove the second result, we note that there is exactly one singularity, caused by the first term in the denominator as $g(\lambda) \to 1$, i.e. as $\lambda \to \lambda_{\max}$. The function Ψ is continuous outside its singularities. Furthermore, from the equation (193) we have that $\Psi \geq 0$ for all λ for which the function is nonsingular. Because Ψ is continuous, the singularity must have a positive sign.

To prove the last result we consider the derivative of the function Ψ with regard to λ. We assume that

$$\lambda_z \in (\lambda_{\min}, \lambda_{\max}). \tag{195}$$

We obtain from the equation (193)

$$\frac{\partial \Psi}{\partial \lambda} = \tag{196}$$
$$\frac{\partial g}{\partial \lambda} \frac{(B - A\, g(\lambda))}{(B + A\, g(\lambda))} \frac{\sqrt{A(1 - g(\lambda))}}{\sqrt{A(1 + g(\lambda))}} \frac{\left(B^2 - A^2 g(\lambda)^2 + 4\, A\, B(g(\lambda)^2 - 1)\right)}{(1 - g(\lambda)^2)}.$$

Note that the special case $A = B$ does not happen as long as $\nu_{12} \neq 0$ and $\nu_{21} \neq 0$. This assumption holds for nearly all reasonable materials except cork. Because all other terms are positive, we have for the sign of the derivative the expression

$$\text{sign } \frac{\partial \Psi}{\partial \lambda} = \text{sign } \left[(B - A\, g(\lambda)) \left(B^2 - A^2 g(\lambda)^2 + 4\, A\, B(g(\lambda)^2 - 1) \right) \right] . \tag{197}$$

Because $g(\lambda)$ is monotonically increasing and therefore $\partial g / \partial \lambda > 0$, and the zero of the function Ψ is located at $A\, g(\lambda_z) = B$, we see that

$$\text{sign } [A\, g(\lambda) - B] = \text{sign } [\lambda - \lambda_z] , \tag{198}$$

i.e. the sign of the expression $A\, g(\lambda) - B$ corresponds to whether λ is smaller or larger than λ_z.

We can write the expression on the right-hand side of the equation (197) as

$$(B - A\, g(\lambda)) \left[(B - A\, g(\lambda))\, (B + A\, g(\lambda)) + 4\, A\, B \left(g(\lambda)^2 - 1 \right) \right] . \tag{199}$$

If

$$B - A\, g(\lambda) < 0 \Longleftrightarrow \lambda > \lambda_z, \tag{200}$$

the expression in the parenthesis on the right is negative. The last term is always negative because $g(\lambda) < 1$. In this case we have

$$\frac{\partial \Psi}{\partial \lambda}|_{\lambda > \lambda_z} > 0 . \tag{201}$$

The other case,

$$B - A\,g(\lambda) > 0 \Longleftrightarrow \lambda < \lambda_z, \tag{202}$$

is trickier because then the expression in the parenthesis on the right in the equation (199) will have one positive and one negative term. The expression represents a parabola with the variable $g(\lambda)$, and has zeroes at

$$g(\lambda) = \pm\sqrt{\frac{4AB - B^2}{4AB - A^2}} \equiv g_0^{\pm}\ . \tag{203}$$

Because $g(\lambda) > 0$, we may discard the negative solution g_0^- in the equation (203). The expression is negative until $g(\lambda)$ becomes larger than the positive solution g_0^+.

The last question remaining is whether this solution lies within our range. We calculate (numerator) − (denominator) from the right side of the equation (203), looking again at the definitions (190), and recall that $\nu_{12} > 0$:

$$(4AB - B^2) - (4AB - A^2) = A^2 - B^2 > 0\ ,$$

i.e. the numerator is always larger than the denominator. Thus $g_0^+ > 1$ and the parabola remains negative in our entire range. The total sign is negative and thus

$$\frac{\partial \Psi}{\partial \lambda}|_{\lambda<\lambda_z} < 0\ .$$

This completes the proof.

2.7 Divergence instability of an isotropic plate with a non-homogeneous tension profile

From a practical point of view, the tension profile is one of the major causes for the runnability problems of a paper web. The profile can be adjusted with various rollers, moisture content, mass concentration etc. The connections between out-of-plane displacement and stability and, for example, crack propagation, have not so far been studied. In this section we have presented the fundamentals of divergence instability in the case of a linear non-homogeneous tension profile. Combining this study with the crack propagation models is subject to ongoing research in our group and the results are excluded from this thesis.

2.7.1 Dynamic analysis

To investigate the dynamic behavior of the isotropic plate with a non-homogeneous tension profile, we insert (as in the previous sections 2.3 and 2.4) the representation (50) into the equation (47). We now take into account the non-homogeneous

tension profile from the equation (3):

$$s^2 W + 2sV_0 \frac{\partial W}{\partial x} + \left(V_0^2 - C^2\right) \frac{\partial^2 W}{\partial x^2} - \frac{\alpha}{m} y \frac{\partial^2 W}{\partial x^2} + \frac{D}{m} \Delta^2 W = 0\,. \tag{204}$$

We multiply the left-hand side of the equation (204) by W and perform integration over the domain Ω to obtain

$$s^2 \int_\Omega W^2 \,\mathrm{d}\Omega + 2sV_0 \int_\Omega W \frac{\partial W}{\partial x} \,\mathrm{d}\Omega + (V_0^2 - C^2) \int_\Omega W \frac{\partial^2 W}{\partial x^2} \,\mathrm{d}\Omega$$

$$- \frac{\alpha}{m} y \int_\Omega W \frac{\partial^2 W}{\partial x^2} \,\mathrm{d}\Omega + \frac{D}{m} \int_\Omega W \Delta^2 W \,\mathrm{d}\Omega = 0.\,. \tag{205}$$

Using the boundary conditions for the isotropic plate (66) – (68) and performing integration by parts as before, we find the equations (60) and (61) and the following representation for the non-homogeneous tension-related integral

$$\int_\Omega y W \frac{\partial^2 W}{\partial x^2} \,\mathrm{d}\Omega = - \int_\Omega y \left(\frac{\partial W}{\partial x}\right)^2 \,\mathrm{d}\Omega, \tag{206}$$

We get the form

$$s^2 \int_\Omega W^2 \,\mathrm{d}\Omega + (C^2 - V_0^2) \int_\Omega \left(\frac{\partial W}{\partial x}\right)^2 \,\mathrm{d}\Omega +$$

$$+ \frac{\alpha}{m} \int_\Omega y \left(\frac{\partial W}{\partial x}\right)^2 \,\mathrm{d}\Omega + \frac{D}{m} \int_\Omega W \Delta^2 W \,\mathrm{d}\Omega = 0 \tag{207}$$

For any such $W \not\equiv 0$ that satisfies the equation (207), we have

$$\omega^2 = -s^2 =$$

$$\frac{(C^2 - V_0^2) \int_\Omega \left(\frac{\partial W}{\partial x}\right)^2 \mathrm{d}\Omega + \frac{\alpha}{m} \int_\Omega y \left(\frac{\partial W}{\partial x}\right)^2 \mathrm{d}\Omega + \frac{D}{m} \int_\Omega W \,\Delta^2 W \,\mathrm{d}\Omega}{\int_\Omega W^2 \,\mathrm{d}\Omega} \tag{208}$$

All quantities on the right side of the equation (208) are real-valued; thus s^2 is always real, and s is either pure imaginary, pure real, or zero. Consider the situation at an arbitrary fixed value of V_0. Choose W as one of the eigenmodes of the equation (207) for this V_0. The characteristic parameter s is continuous with respect to small changes of V_0 and W around the original solution point (V_0, W). Because this holds for any V_0, we conclude that s may only change between imaginary and real values by passing through the origin; see route of the arrows in Figure 13 on page 43. As a conclusion, if the system in the equation (207) has any

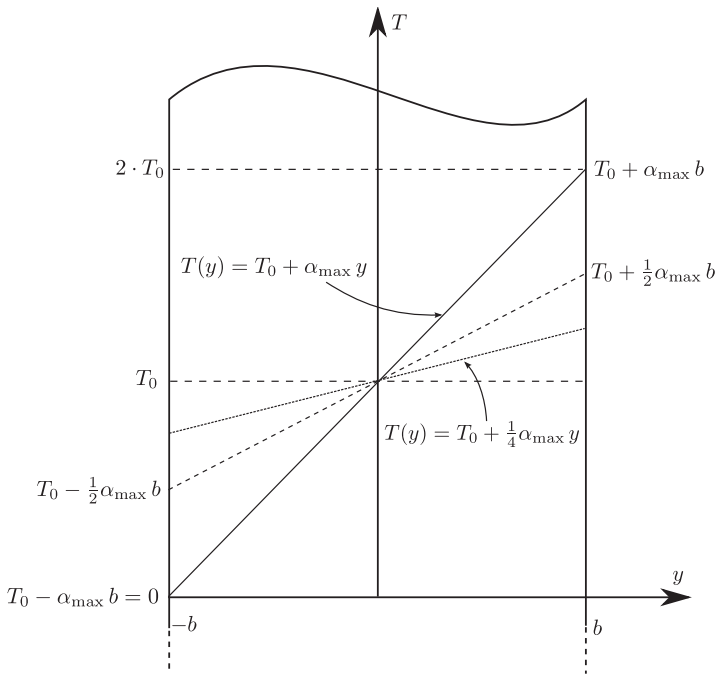

FIGURE 19 The definition of α_{max}

instabilities, i.e. velocities V_0 where Re s becomes positive, they must be of the static type (Im $s = 0$), and can be captured by a static analysis.

According to the above considerations, all eigenvalues of the equation (207) exhibit this behavior. This holds especially for the critical, i.e. the lowest, instability. We must note that the equation (205) correctly describes the physical system only up to the critical instability; after that point, non-linear considerations become necessary. This is known to occur for a family of related problems; see, e.g., the book by Paidoussis [67]. Thus, this analysis does not rule out dynamic instability behaviour of the physical system at post-critical velocities, but it is sufficient for conclusions about the critical instability.

This general argument cannot predict the stability of the system at $V_0 = 0$ because the signs of the last two integrals in the numerator of the equation (208) are not known in the general case. Therefore, we conclude that for the problem of an axially moving elastic plate, simply supported at two opposite edges and free at the other two, with homogeneous or linearly distributed in-plane tension, the critical instability (if any) is of the static type.

Let us consider a special case, where the bending rigidity of the axially moving plate is negligibly small, and the in-plane tension in the x-direction is positive. For this assumption we will avoid the consideration of compression and wrinkling. The setup for the parameters is illustrated in Figure 12 on page 35 and Figure 19.

That is, we assume that

$$D = 0\,, \quad T_0 > \alpha\, b\,, \tag{209}$$

where the latter condition follows from the constraints

$$T_{xx}(x, y) = T_0 + \alpha\, y > 0 \tag{210}$$

and $y \geq -b$. In this case, the characteristic parameter s is evaluated as

$$\omega^2 = -s^2 = \frac{(C^2 - V_0^2) \int_\Omega \left(\dfrac{\partial W}{\partial x}\right)^2 \mathrm{d}\Omega + \dfrac{\alpha}{m} \int_\Omega y \left(\dfrac{\partial W}{\partial x}\right)^2 \mathrm{d}\Omega}{\displaystyle\int_\Omega W^2 \,\mathrm{d}\Omega} \tag{211}$$

We obtain the steady-state solution (divergence) at a velocity

$$\left(V_0^{\mathrm{div}}\right)^2 = C^2 + \frac{\alpha}{m} \frac{\displaystyle\int_\Omega y \left(\frac{\partial W}{\partial x}\right)^2 \mathrm{d}\Omega}{\displaystyle\int_\Omega \left(\frac{\partial W}{\partial x}\right)^2 \mathrm{d}\Omega}\,. \tag{212}$$

Taking into account the expression in the equation (212) and the inequalities in (209), we estimate the divergence velocity as

$$\left(V_0^{\mathrm{div}}\right)^2 \geq C^2 - \frac{\alpha b}{m} = \frac{T_0 - \alpha b}{m}\,. \tag{213}$$

We see from the equation (213) that as long as the condition for T_0 in the statement (209) is fulfilled, we have

$$(V_0^{\mathrm{div}})^2 \geq 0, \tag{214}$$

and therefore the value of V_0^{div} is physically meaningful.

By applying again the same estimate for the second integral in the numerator of the equation (211), and using the conditions (209), we see that s is initially ($V_0 = 0$) purely imaginary. As V_0 is increased, the numerator decreases and, at some point, the numerator vanishes and the characteristic parameter s becomes zero.

2.7.2 Transformation into an ordinary differential equation

The stationary eigenvalue problem of elastic instability consists of finding a nontrivial solution (mode) and the corresponding minimal eigenvalue of the following boundary-value problem. Consider the static equation corresponding to the original problem in the equation (204),

$$(V_0^2 - C^2)\frac{\partial^2 W}{\partial x^2} - \frac{\alpha y}{m}\frac{\partial^2 W}{\partial x^2} + \\ + \frac{D}{m}\left(\frac{\partial^4 W}{\partial x^4} + 2\frac{\partial^4 W}{\partial x^2 \partial y^2} + \frac{\partial^4 W}{\partial y^4}\right) = 0\,, \quad (x, y) \in \Omega \tag{215}$$

with the boundary conditions for W that follow from the equations (66) – (68). From the latter condition in the equation (209), we obtain a constraint for α:

$$\alpha < T_0/b \, . \tag{216}$$

To determine the minimal eigenvalue λ (see the equation (86) on page 48) of the problem (66) – (68) and (215), and the corresponding eigenfunction, we apply the same representation as before:

$$W = W(x,y) = f\left(\frac{y}{b}\right) \sin\left(\frac{\pi x}{\ell}\right) \, , \tag{217}$$

where $f\left(\frac{y}{b}\right)$ is an unknown function.

It follows from the equation (217) that the desired divergence form W satisfies the boundary conditions (66). Using dimensionless variables, η and μ, defined in the equation (88) on page 49, and the free-of-traction boundary conditions (67) and (68) on page 45, with relations (86), (215) and (217), we obtain the following eigenvalue problem for the unknown function $f(\eta)$:

$$\mu^4 \frac{\mathrm{d}^4 f}{\mathrm{d}\eta^4} - 2\mu^2 \frac{\mathrm{d}^2 f}{\mathrm{d}\eta^2} + (1 - \lambda + \tilde{\alpha}\eta) f = 0, \quad -1 \leq \eta \leq 1 \, , \tag{218}$$

where

$$\tilde{\alpha} = \frac{b\ell^2}{\pi^2 D}\alpha = \frac{b^3\mu^2}{D}\alpha \, . \tag{219}$$

The equation (218) is considered with the boundary conditions

$$\mu^2 \frac{\mathrm{d}^2 f}{\mathrm{d}\eta^2} - \nu f = 0, \quad \eta = \pm 1 \quad \text{and} \tag{220}$$

$$\mu^2 \frac{\mathrm{d}^3 f}{\mathrm{d}\eta^3} - (2 - \nu) \frac{\mathrm{d} f}{\mathrm{d}\eta} = 0, \quad \eta = \pm 1 \, . \tag{221}$$

The equation (218) with the boundary conditions (220) and (221) constitutes a linear eigenvalue problem for f with polynomial coefficients.

2.8 Divergence instability of an orthotropic plate with a non-homogeneous tension profile

The last study of this thesis combines all information described before and produces the equations for handling the onset of instability of an axially moving orthotropic plate with a non-homogeneous tension profile. The process follows the procedure in the previous sections directly; the equations are presented here briefly as reminders for the reader. One must also note that it is possible to extend the previous results to orthotropic materials in a more straightforward way by using the Huber quantities. However, in this study we assume that the Huber

quantity is not used because several shear moduli are observed in the application area.

We have the following partial differential equation:

$$\left(mV_0^2 - T_0\right)\frac{\partial^2 W}{\partial x^2} - \frac{\alpha y}{m}\frac{\partial^2 W}{\partial x^2} + D_0\mathcal{L}_0(w) = 0 \tag{222}$$

The boundary conditions for W, which follow from the equations (66) – (68), are from the latter condition in the equation (209). We obtain a constraint for α:

$$\alpha < T_0/b\ . \tag{223}$$

To determine the minimal eigenvalue λ (see the equation (86)) of the problem (215), (66) – (68), and the corresponding eigenfunction, we apply the same representation as before:

$$W = W(x,y) = f\left(\frac{y}{b}\right)\sin\left(\frac{\pi x}{\ell}\right), \tag{224}$$

where $f\left(\frac{y}{b}\right)$ is an unknown function.

It follows from the equation (217) that the desired divergence form W satisfies the boundary conditions (66). Using dimensionless variables η and μ defined by the formula (88) and the free-of-traction boundary conditions (67) and (68) (68), with relations (86), (215), and (217), we obtain the following eigenvalue problem for the unknown function $f(\eta)$:

$$\mu^4 H_2\frac{\partial^4 f}{\partial\eta^4} - 2\mu^2 H_3\frac{\partial^2 f}{\partial\eta^2} + (H_1 - \lambda - \bar{\alpha}\eta)\,f = 0, \tag{225}$$

where

$$\bar{\alpha} = \frac{\alpha\mu^2 b}{D_0}. \tag{226}$$

The solution of the equation (225) is subjected to the boundary conditions (220) and (221). The equation (225) with the boundary conditions (220) and (221) constitutes the linear eigenvalue problem in f with polynomial coefficients.

3 NUMERICAL SOLUTIONS FOR THE WEB MODELS

In this section, we present numerical solutions based on the models developed above. While the theory predicts a certain general behavior, many characteristics must be numerically computed. The implementation of the solution process is one of the key factors in numerical analysis; on the other hand, a reliable analysis requires a solid numerical basis. We note that in the following computations, we use E_1, E_2 and ν_{12} as independent parameters and calculate ν_{21} from the equation (36).

3.1 The numerical solution process for the problem of instability of a moving orthotropic plate

In this section we present the solution process for the case of a moving orthotropic plate. The analysis of the isotropic plate was performed previously by the author (see Banichuk et al. **[6]**) in order to avoid redundancy we have presented only the general approach.

The root $\gamma = \gamma_*$ of the equation (151) was searched numerically in the interval

$$[\gamma_{\min} + \varepsilon_1,\ \gamma_{\max} - \varepsilon_2] \qquad \text{where} \qquad \varepsilon_j,\ j = 1, 2. \tag{227}$$

This interval (227) was used to avoid singularities; the values of ε were small and determined adaptively based on the sign of $\Phi - \Psi$. The values were initialized as $\varepsilon_j = 10^{-8}$ for both $j = 1, 2$, and each parameter ε_j was halved until the sign of $\Phi - \Psi$ was positive at the left end, and negative at the right end. Then a bisection search was used to locate the root. It was found that this search for a suitable ε_j's was necessary, especially in the cases where $G_{12} < G_H$, because a fixed-size epsilon would skip over the root in some parts of the parameter space, particularly when the ratio of the Young's modulus and ν_{12} were both small.

When $G_{12} < G_H$, it was verified that no roots existed in the tested cases in

the interval $\gamma \in [0, \gamma_{\min})$. This was done by minimizing

$$||f(\lambda)||^2 = f(\lambda) \cdot \overline{f(\lambda)}\,, \tag{228}$$

where

$$f(\lambda) = \Phi(\lambda) - \Psi(\lambda)\,. \tag{229}$$

Here $\overline{z}$ denotes the complex conjugate of z. Local minima larger than ε were discarded, as were also any duplicates, and any solutions $\gamma \geq \gamma_{\min}$. Note that $\gamma = \gamma_{\min}$ is always a root, corresponding to the trivial solution.

The critical value γ_0 was evaluated from the analytical expression (178), and the root corresponding to the antisymmetric case, $\gamma = \gamma_1$, was found numerically from the equation (155) using the interval (227). Once the eigenvalue γ_* of the symmetric case was found, the corresponding eigenfunction was constructed by inserting the eigenvalue into the equations (143), (149) and (150). It is possible to eliminate either A^s or B^s from one of the equations of the system. Either equation, (149) or (150), can be chosen. Note that the other equation is implicitly used by the zero determinant condition (see the equation (151)).

A numerically stable approach for choosing the constant to be eliminated is to test both possibilities, assigning $A^s = 1$ and calculating B^s from the equation system. Respectively, choosing $B^s = 1$ and calculate A^s. The choice that gives a result that is smaller than or equal to 1 is then kept. This is necessary because, depending on the problem parameters and this choice, the other constant may be very large, which affects numerical accuracy.

We evaluated $w^s(x, y)$ using this choice, and normalized the final result by scaling the maximum value of w^s to unity.

3.2 The numerical solution process for the non-homogeneous tension profile case

We will proceed to the numerical solution to the problem (218), (220) – (221). Note that the boundary conditions (220) and (221) are not natural in the sense that they are not generated by deriving the variational form of the equation (218) and applying integration by parts.

We discretized the strong form of the equations (218), (220) – (221) directly, with classical central differences of second-order asymptotic accuracy. To account for the boundary conditions, we used the method of virtual points.

As the problem is linear in f, the discretization leads to a standard discrete linear eigenvalue problem presented in the equation (218):

$$Af = \lambda f\,. \tag{230}$$

The boundary conditions (220) – (221) have not been applied so far. Because the boundary conditions are homogeneous, it is possible to add them to the discrete

system by rewriting the original discrete problem (230) as a generalized linear eigenvalue problem

$$Af = \lambda Bf \ , \tag{231}$$

where B is an identity matrix with the first two and the last two rows zeroed out. In the equation (231), the first two and the last two rows of A contain the discretized boundary conditions.

To sum up, in order to solve the original problem, we compute the solution of the equation (231), discard eigenvalues of an infinite magnitude, and then extract the smallest eigenvalue and its corresponding eigenvector. Note that the first two and the last two components of the eigenvector should be discarded because they represent the function values at virtual points that were generated from the boundary conditions. Finally, the divergence mode $W(x, y)$ is constructed by the equation (217).

3.3 Numerical results for the web models

In this section, the numerical results are presented. We have divided the studies into two categories with respect to the tension profile. At first, we present the isotropic and orthotropic studies on homogeneous tension. After that, the non-homogeneous tension profile in both the isotropic and orthotropic cases, is in focus. The parameters in use have been chosen for the sake of illustration, and have not been measured in practice. However, the basic values are close to the real values of paper.

3.3.1 Homogeneous tension profile studies

In this section, the homogeneous tension profile studies are presented. They are arranged as follows: In Figure 20 on page 76 we present the case of one isotropic material similar to those presented in Banichuk et al. **[6]**, and including some orthotropic variants based on the Huber quantity (see the parameter values in Table 1). The left part of Figure 20 on page 76 shows the complete buckling shape, while the right part displays a slice of the shape at the center of the open draw that corresponds to the bold line on the left side of the figure. It is observed that when the Huber quantity is used, the qualitative behaviour agrees with the isotropic case as expected. Quantitatively, we see the effect of the Young modulus ratio E_1/E_2. The smaller the ratio, the more the shape is localized near the free edges.

Figure 21 on page 77 shows the effect of the in-plane shear modulus G_{12} for general orthotropic materials. In this case, the shear modulus is represented as a fraction of the Huber quantity (see detailed parameters in Table 2 on page 75). The left column displays complete buckling shapes, while the right column shows the strength of the localization effect that was discussed in Banichuk et al. **[6]**. We see that according to the numerical tests the ratio of the Young moduli E_1 and

TABLE 1 The parameter values for the study presented in Figure 20.

Parameter	Case 1	Case 2 (Isotropic)	Case 3	Case 4
E		5 GPa		
E_1	5 GPa		5 GPa	5 GPa
E_2	10 GPa		7.5 GPa	2.5 GPa
ν		0.2		
ν_{12}	0.2		0.2	0.2
ν_{21}	0.4		0.13	0.10
$\ell/2b$	0.01	0.01	0.01	0.01
h	10^{-4} m	10^{-4} m	10^{-4} m	10^{-4} m
m	0.08 kg/m^2	0.08 kg/m^2	0.08 kg/m^2	0.08 kg/m^2
ℓ	0.1 m	0.1 m	0.1 m	0.1 m
T_0	500 N/m	500 N/m	500 N/m	500 N/m
G_{12}	G_H	G_H	G_H	G_H

E_2 is the significant factor affecting the buckling shape, regardless of the absolute magnitudes of E_1 and E_2. Note that when the material parameters E_1, E_2, and ν_{12} are given, the other Poisson ratio ν_{21} can be found from the compatibility condition (the Maxwell relation (36)). In addition to the material parameters, we have one geometric parameter, $\ell/2b$, which describes the ratio of the plate's length to its width. The effect of the problem geometry on the displacement localization phenomenon was investigated in the same article **[6]** . It was observed that when the plate is short and wide (i.e., when $\ell/2b$ is small), the localization is more pronounced, that is, most of the displacement occurs near the free edges.

Briefly, the degree of localization represents the variation of the displacement in the width (y) direction. When the localization is high (in the relative sense), the maximal displacement and strains occur near the free edges. When the localization approaches zero, so does the y dependence, and the displacement profile approaches a cylindrical one. The degree of localization is computed from a numerical approximation of the integral

$$\int_{-b}^{b} [1 - f(y)] \, \mathrm{d}y \,, \tag{232}$$

where $f(y)$ is the cross-section. As a conclusion, the problem parameters affecting the localization effect are the aspect ratio $\ell/2b$, the Young modulus ratio E_1/E_2, the Poisson ratio ν_{12}, and the in-plane shear modulus G_{12}.

As can be seen in Figure 21 on page 77, the result qualitatively matches the earlier one from the isotropic case, in that the degree of localization increases as the Poisson ratios increase and therefore incompressibility increases. As a new result, we see that the zone where the relative strength of localization rapidly increases shifts to the right towards the larger values of ν_{12} when the ratio G_{12}/G_H is increased.

By solving the equation (127) for V_0 and inserting these values, we obtain $V_0 \approx 79.11$ m/s. We solved two different isotropic limit cases, with $E = 8$ GPa

TABLE 2 The parameter values for the study presented in Figure 21.

Parameter	Case 1	Case 2	Case 3
E_1	6.8 GPa	6.8 GPa	6.8 GPa
E_2	3.4 GPa	3.4 GPa	3.4 GPa
ν_{12}	0.2	0.2	0.2
ν_{21}	0.1	0.1	0.1
$\ell/2b$	0.01	0.01	0.01
h	10^{-4} m	10^{-4} m	10^{-4} m
m	0.08 kg/m^2	0.08 kg/m^2	0.08 kg/m^2
ℓ	0.1 m	0.1 m	0.1 m
T_0	500 N/m	500 N/m	500 N/m
G_{12}	0.7 G_H	G_H	1.3 G_H

TABLE 3 The parameter values and the results for the study of critical velocity V_0 .

Parameter	Case 1	Case 2	Case 3
E_1	8 GPa	8 GPa	0.8 GPa
E_2	0.8 GPa	8 GPa	0.8 GPa
ν_{12}	0.8	0.4	0.4
ν_{21}	0.08	0.4	0.4
m	0.08 kg/m^2	0.08 kg/m^2	0.08 kg/m^2
ℓ	0.1 m	0.1 m	0.1 m
b	0.5 m	0.05 m	0.05 m
$\ell/2b$	0.1	0.01	0.01
T_0	500 N/m	500 N/m	500 N/m
h	10^{-4} m	10^{-4} m	10^{-4} m
$\mathbf{V_0}$	$\approx$ 79.11 m/s	$\approx$ 79.12 m/s	$\approx$ 79.06 m/s

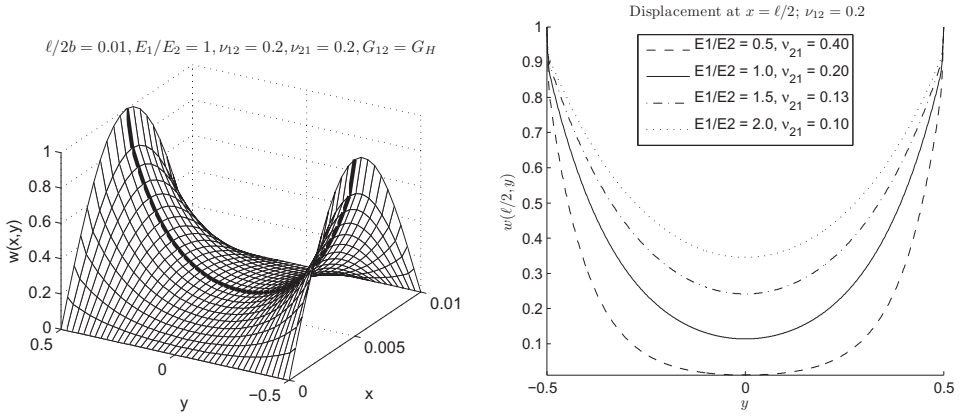

FIGURE 20 Left: The symmetric buckling shape for the isotropic material, $E = 5$ GPa and $\nu = 0.2$. The aspect ratio $\ell/2b = 0.01$. Right: The shape of the profile on the bold line of the left picture. The solid line corresponds to the picture on the left. The dotted lines show the shape of the resulting profile if the isotropic material is replaced with an orthotropic one, while keeping $E_1 = 5$ GPa and $\nu_{12} = 0.2$. The other Poisson ratio ν_{21} is calculated from Maxwell's relation (36), and for G_{12} the Huber quantity is used. All parameters of this study are collected in Table 1.

and $E = 0.8$ GPa. The other parameters were kept the same (see Table 3 on the previous page), and for the Poisson ratio the geometric average $\nu = \overline{\nu} = \sqrt{\nu_{12}\nu_{21}} = 0.4$ was used. The critical velocities were for the first case $V_0 \approx 79.12$ m/s, and for the second case, $V_0 \approx 79.06$ m/s.

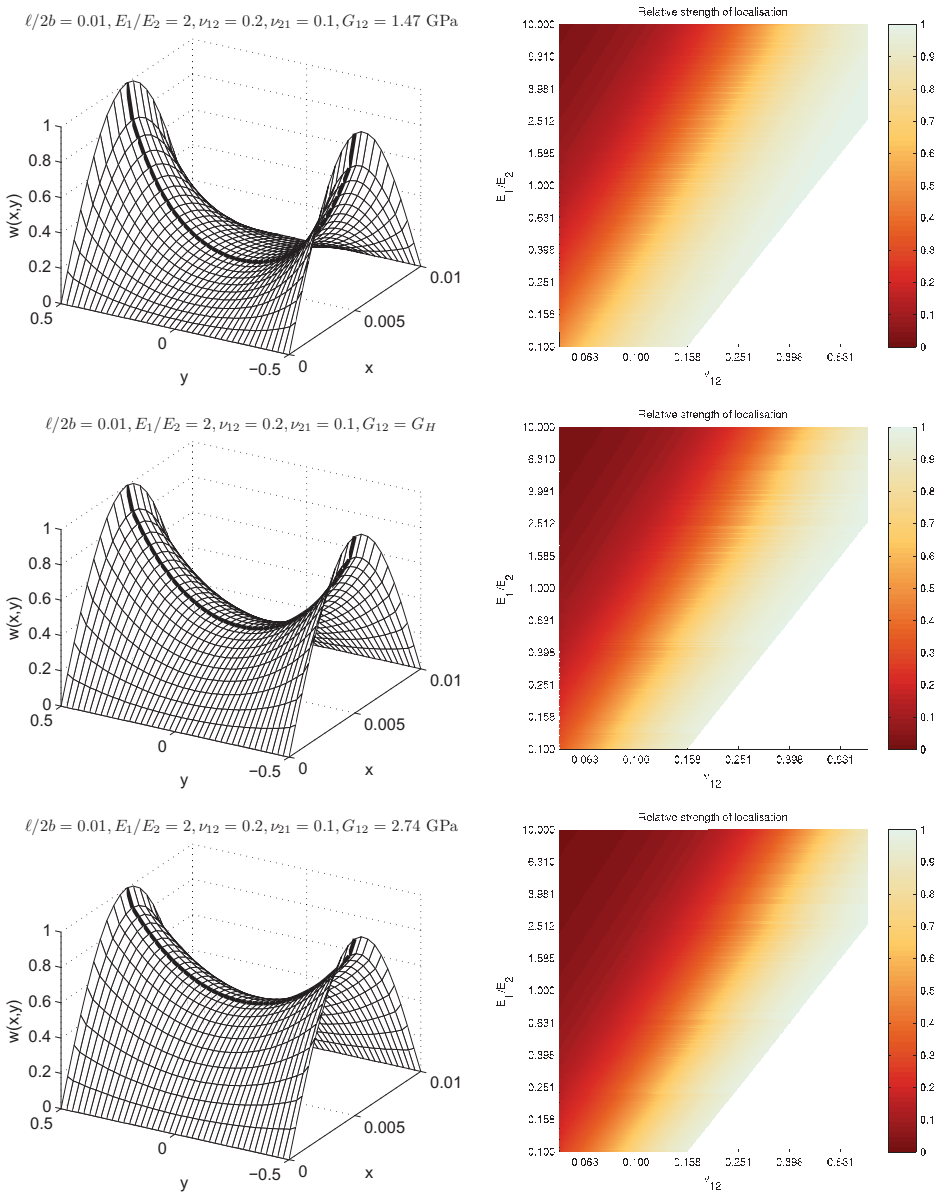

FIGURE 21 The studied case. The effect of the in-plane shear modulus G_{12}. The Poisson ratio ν_{21} is calculated from Maxwell's relation (36). Case 1, the top row; Case 2, the middle row; and Case 3, the bottom row. The left column: the symmetric buckling shape. The right column: the relative strength of the localization effect as a function of the Young modulus ratio E_1/E_2 and the Poisson ratio ν_{12}. The effect has been plotted in the area where $\sqrt{\nu_{12}\nu_{21}} \leq 0.5$. The maximum localization value is normalized to 1 for each subfigure separately, and the reference value G_H is evaluated separately for each point in each plot. For the detailed parameter values, see Table 2 on page 75.

3.3.2 Non-homogeneous tension profile studies

In this section, the studies where tension is considered non-homogeneous, are presented. In the case of the isotropic non-linear tension profile, the numerical results were computed for some practically interesting choices of problem parameters (see Table 4).

In the study of critical divergence shapes, various values of the Poisson ratio ν and the tension profile skew parameter $\tilde{\alpha}$ were considered. Note that when we consider the ratio $\alpha/\alpha_{\max}$, this ratio is the same as $\tilde{\alpha}/\tilde{\alpha}_{\max}$. Thus, tildes can be omitted below in the cases where this ratio is considered. Note also that the ratio $\alpha/\alpha_{\max}$ (or $\tilde{\alpha}/\tilde{\alpha}_{\max}$) directly gives the relative deflection of the average tension T_0 at the edges $y = \pm b$ (see Figure 22 on the facing page). For the Poisson ratio, the values 0, 0.1, 0.3 and 0.5 were used (see all the parameters in Table 4). The values of $\alpha/\alpha_{\max}$ (or $\tilde{\alpha}/\tilde{\alpha}_{\max}$) were 0, 10^{-6}, 10^{-4} and 10^{-2}, where $\alpha_{\max}$ corresponds to the upper limit imposed by the constraint (216) and

$$\tilde{\alpha}_{\max} = \frac{\ell^3}{\pi^3 D}\alpha_{max} = \mu\frac{\ell^2 T_0}{\pi^2 D}. \tag{233}$$

Note that $\tilde{\alpha}_{\max}$ depends on ν, via D. In Table 5 on the facing page, the critical divergence velocities are presented for these cases. We see that the analytical solution for $\tilde{\alpha} = 0$ for the same geometric and material parameters matches the values in the first column of the table.

TABLE 4 The parameters of the study of divergence velocity of the non-linear tension profile. Results can be observed in Table 5.

	Case 1	Case 2	Case 3	Case 4
E	1 GPa	1 GPa	1 GPa	1 GPa
ν	0	0.1	0.3	0.5
$T_0 \mid_{y=0}$	500 N/m	500 N/m	500 N/m	500 N/m
h	10^{-4} m	10^{-4} m	10^{-4} m	10^{-4} m
m	0.08 kg/m^2	0.08 kg/m^2	0.08 kg/m^2	0.08 kg/m^2
ℓ	0.1 m	0.1 m	0.1 m	0.1 m
b	0.5 m	0.5 m	0.5 m	0.5 m
$\ell/2b$	0.1	0.1	0.1	0.1
$\approx \tilde{\alpha}_{\max}$	387, 02	383, 12	352, 19	290, 26

TABLE 5 Critical divergence velocities V_0^{div} for the cases studied. Note that $\tilde{\alpha}_{\max}$ is different for each value of ν. See the approximated values in Table 4 on the preceding page.

	$\nu \setminus \tilde{\alpha}$	0	$10^{-6}\tilde{\alpha}_{\max}$	$10^{-4}\tilde{\alpha}_{\max}$	$10^{-2}\tilde{\alpha}_{\max}$
Case 1	0	79.0634	79.0634	79.0604	78.6891
Case 2	0.1	79.0635	79.0635	79.0605	78.6885
Case 3	0.3	79.0640	79.0640	79.0608	78.6876
Case 4	0.5	79.0652	79.0652	79.0618	78.6869

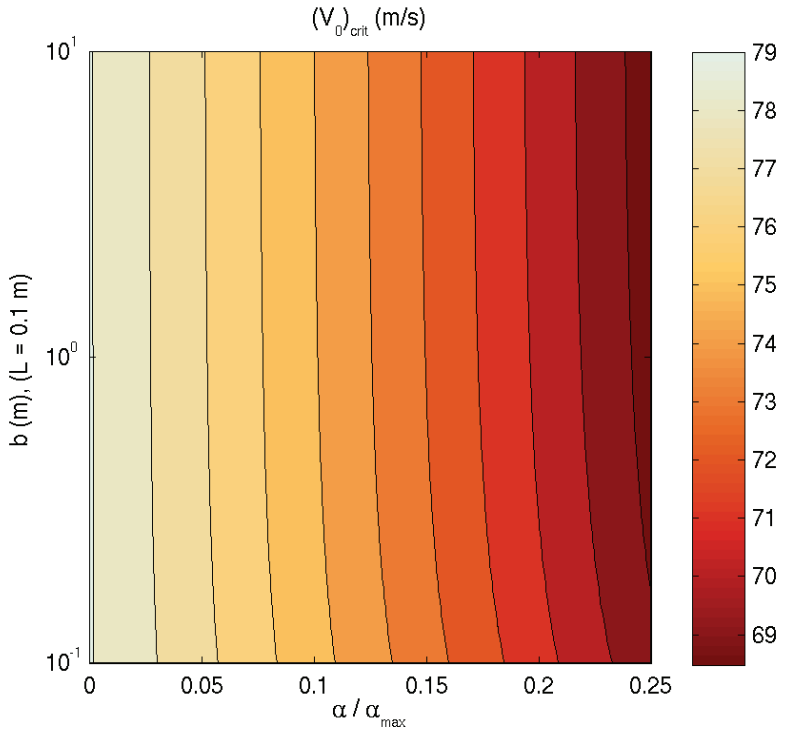

FIGURE 22 The critical web velocity with respect to the tension profile skew parameter α and half a web width b. Note the logarithmic scale of b. The web length is constant ($\ell = 0.1$ m).

In the study of critical (divergence) velocities, the values of $\alpha/\alpha_{\max}$ were $0 - 0.25$ (in the equation (216)) and the values of b (half a web width) were $0.1 - 10$ m. Thus, the web width was $0.2 - 20$ m. The web length was again $\ell = 0.1$ m. The results for the critical velocities with respect to the relative tension profile skew parameters $\alpha/\alpha_{\max}$ and b are shown in Figure 22.

The results for the transverse displacement are shown in Figures 24 – 26 on page 84. In each figure, ν is fixed. Figure 24 on page 82 is divided into two parts. Both parts of the figure are further divided into four subfigures. Each subfigure

shows the results for a different value of the skew parameter $\tilde{\alpha}$. In the upper four subfigures, $f(\eta)$ is plotted, showing a slice of the out-of-plane displacement from one free edge to the other at $x = \ell/2$. The tension increases towards a positive η. The total out-of-plane displacement in the whole domain $\Omega = [0, \ell] \times [-b, b]$, from the equation (217), is shown in the lower four subfigures. Note the orientation of the axes. In Figures 25 on page 83 and 26 on page 84, the four subfigures show the slices of the out-of-plane displacement at $x = \ell/2$ for the limiting cases $\nu = 0$ and $\nu = 0.5$, in an analogous order.

In the following, we have computed critical divergence velocities for the non-homogeneous tension profile in isotropic materials. The results were computed for some practically interesting choices of problem parameters. Detailed parameter values are listed in Table 4 on page 78. These parameter values approximately correspond to some paper materials, within the limitations of the isotropic model.

From Figures 22 – 26 on page 84 and Table 5 on the previous page, four apparent conclusions can be drawn. First of all, in the study of critical velocities, it was seen that inhomogeneities in the tension profile may significantly decrease the critical velocities. For up to a 20 % tension inhomogeneity between the midpoint and the edges, the decrease in the critical velocity is found to be 10 %. Secondly, it is also seen that the wider the web is, the more sensitive it is for tension inhomogeneities. Thirdly, by comparing Figures 24 on page 82, 25 on page 83 and 26 on page 84, we conclude that materials with a larger Poisson ratio tend to exhibit a higher degree of sensitivity to inhomogeneities in the tension profile. Lastly, we can draw the conclusion that in all the cases investigated, the critical velocity is not significantly affected by slight inhomogeneities in the tension profile.

Various values of the Poisson ratio ν and the tension profile skew parameter $\tilde{\alpha}$ were considered. For the Poisson ratio the values 0, 0.1, 0.3, and 0.5 were used. The values of $\tilde{\alpha}$ were 0, $10^{-6}\tilde{\alpha}_{\max}$, $10^{-4}\tilde{\alpha}_{\max}$, and $10^{-2}\tilde{\alpha}_{\max}$, where $\tilde{\alpha}_{\max}$ corresponds to the upper limit imposed by the constraint (216). From the formulation (233) we can see that the $\tilde{\alpha}_{\max}$ depends on ν, via D. In Table 5, critical divergence velocities are presented for these cases. We can see that the analytical solution for $\tilde{\alpha} = 0$ with the same geometric and material parameters (see Banichuk et al. **[6]**: note that $\ell/2b = 0.1$) matches the values in the first result column of the table.

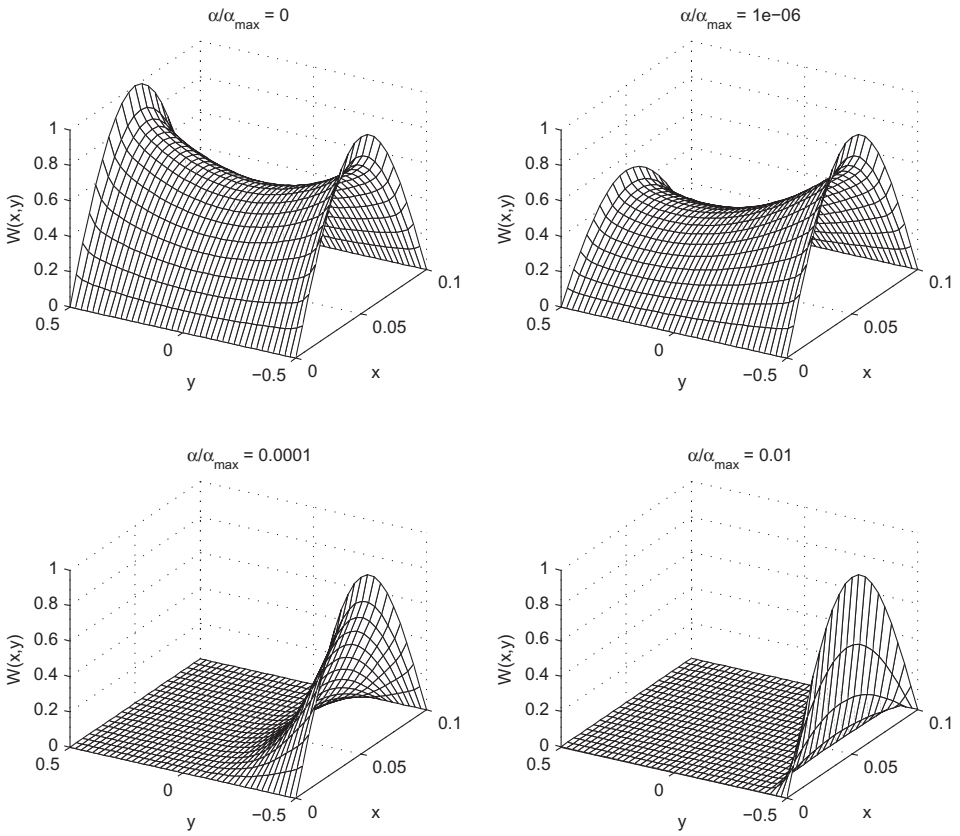

FIGURE 23 The out-of-plane displacement of an axially travelling pinned-free plate with dimensions $L = 0.1$ m, $2b = 1$ m, $h = 10^{-4}$ m. The Poisson ratio $\nu = 0.3$. The tension profile skew parameter $\tilde{\alpha} = 0$, $10^{-6}\tilde{\alpha}_{\max}$, $10^{-4}\tilde{\alpha}_{\max}$, and $10^{-2}\tilde{\alpha}_{\max}$.

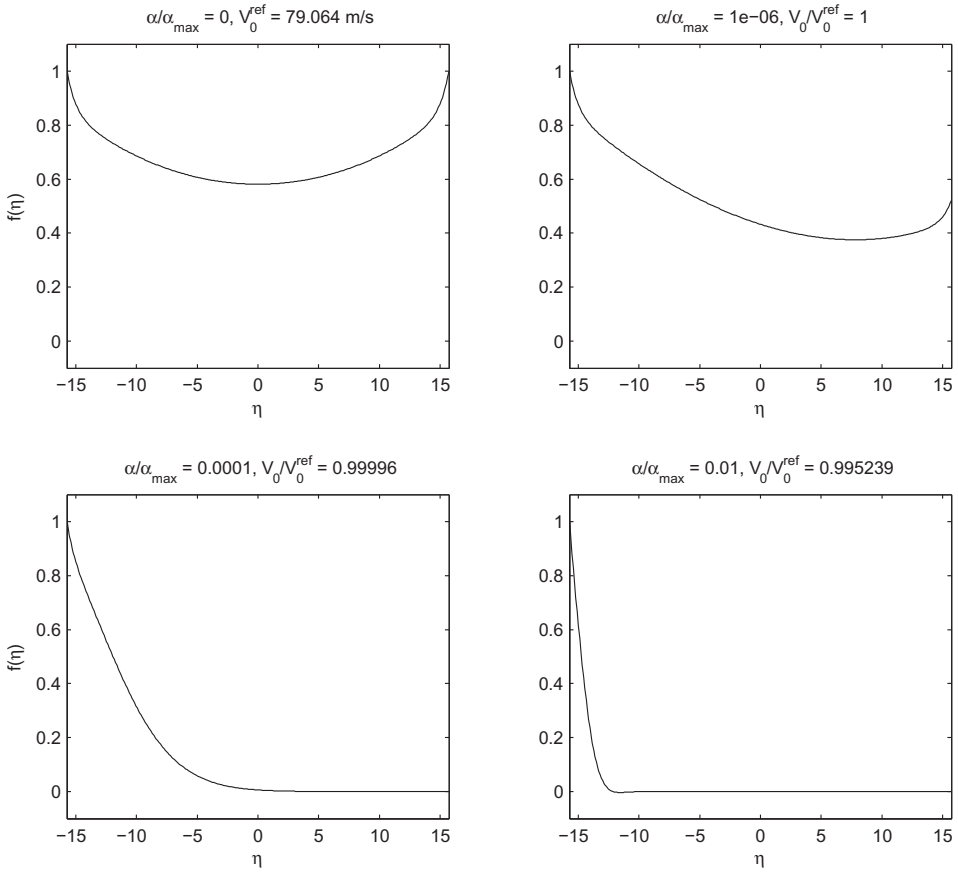

FIGURE 24 The out-of-plane displacement of an axially travelling pinned-free plate with dimensions $L = 0.1$ m, $2b = 1$ m, $h = 10^{-4}$ m. The Poisson ratio $\nu = 0.3$. The tension profile skew parameter $\tilde{\alpha} = 0$, $10^{-6}\tilde{\alpha}_{\max}$, $10^{-4}\tilde{\alpha}_{\max}$, and $10^{-2}\tilde{\alpha}_{\max}$.

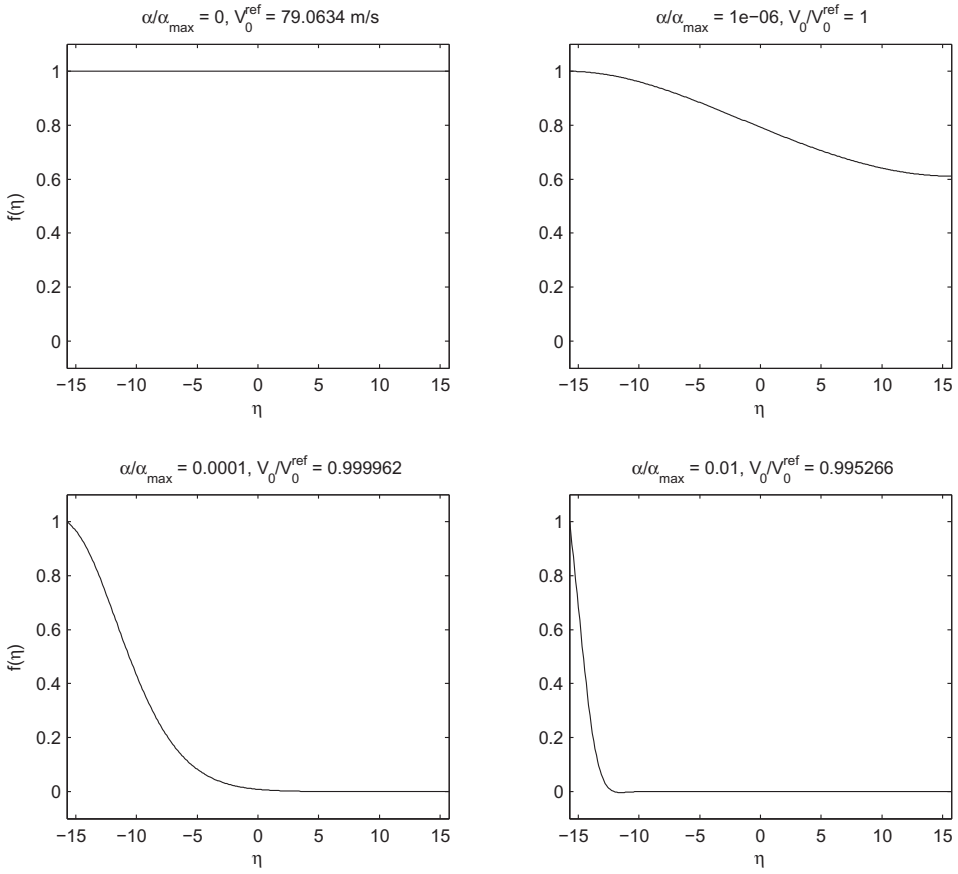

FIGURE 25 The out-of-plane displacement of an axially travelling pinned-free plate at $x = \ell/2$ with dimensions $L = 0.1$ m, $2b = 1$ m, $h = 10^{-4}$ m. The Poisson ratio $\nu = 0$. The tension profile skew parameter $\tilde{\alpha} = 0$, $10^{-6}\tilde{\alpha}_{\max}$, $10^{-4}\tilde{\alpha}_{\max}$, and $10^{-2}\tilde{\alpha}_{\max}$.

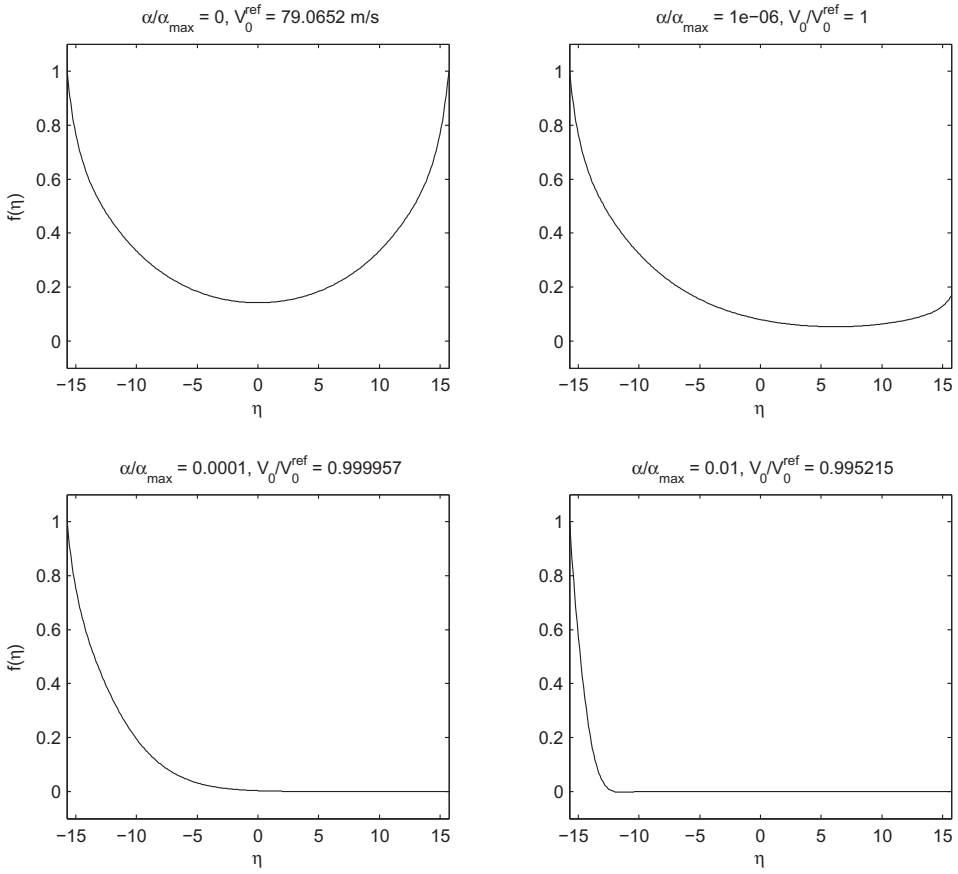

FIGURE 26 The out-of-plane displacement of an axially travelling pinned-free plate at $x = \ell/2$ with dimensions $L = 0.1$ m, $2b = 1$ m, $h = 10^{-4}$ m. Poisson ratio $\nu = 0.5$. Tension profile skew parameter $\tilde{\alpha} = 0$, $10^{-6}\tilde{\alpha}_{\max}$, $10^{-4}\tilde{\alpha}_{\max}$, and $10^{-2}\tilde{\alpha}_{\max}$.

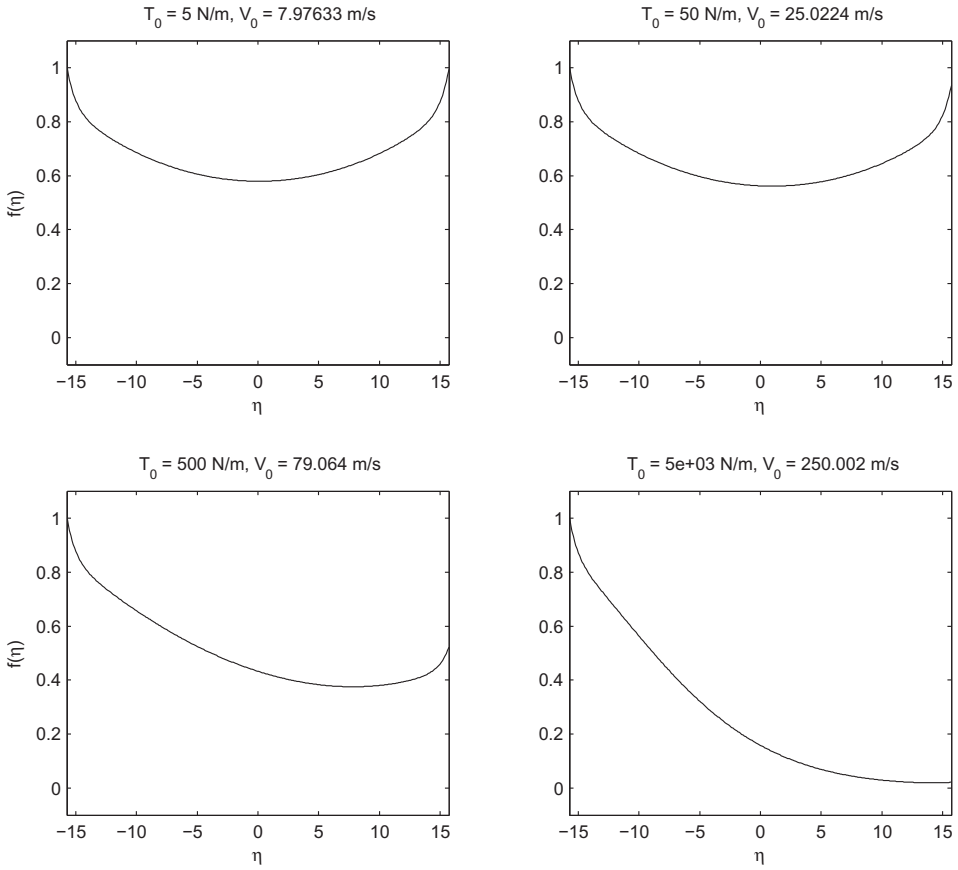

FIGURE 27 The out-of-plane displacement of an axially travelling pinned-free plate at $x = \ell/2$ with dimensions $L = 0.1$ m, $2b = 1$ m, $h = 10^{-4}$ m. The Poisson ratio $\nu = 0.3$. The tension profile skew parameter $\tilde{\alpha} = 10^{-6}\tilde{\alpha}_{\max}$. Midpoint tension $T_0 = 5$, 50, 500, and 5000 N/m.

We can see that even for the smallest inhomogeneity tested, one part in 10^6, the divergence (buckling) mode changes completely for these problem parameters. Thus, from a practical point of view, although studies of the homogeneous tension case can relatively accurately predict the critical velocity, the analysis indicates that the predictions of the divergence shape may be completely inaccurate.

The sensitivity for the inhomogeneity was found to be affected also by the tension at the midpoint T_0. The higher the tension, the more sensitive the system is for small inhomogeneities. This effect is shown in Figure 27. The subfigure on the bottom left of Figure 27 corresponds to the subfigure at the top right of Figure 24 on page 82. We can see that with $\nu = 0.3$, $\tilde{\alpha} = 10^{-6}\tilde{\alpha}_{\max}$, and the values of the other parameters fixed to those given at the beginning of this section, the sensitivity is very high already at $T_0 = 500$ N/m, which is realistic in paper production.

It should be noted that as far as geometric parameters are concerned, the divergence shape is a function of not only the aspect ratio $\ell/2b$ but also of the overall scale. Even for the same aspect ratio, scaling ℓ (and also b to keep the same aspect ratio) changes the divergence shape. This effect occurs even if h is scaled by the same amount as ℓ and b. Thus, it should be emphasized that the results in Figures 23–27 only represent the specific case of plates with the dimensions $\ell \times 2b \times h = 0.1 \text{ m} \times 1 \text{ m} \times 10^{-4} \text{ m}$.

The last case in the study is concerned with the stability of the moving orthotropic plate with the non-homogeneous tension profile. We have chosen a set of parameters (see Table 6 and Table 7 on page 88), which differ from each other in the orientation of the orthotropicity. As assumed, the main results are the same as in the previous studies: the value of the tension does not affect the shape, the orthotropicity has a slight effect and it increases the localization on the edges and the skewness in the tension profile is very important from the critical velocity point of view in major changes between the edges. The reader can compare the results in Figure 28 on the next page and 29 on page 88 to the subfigure 3 in Figure 24 on page 82 and conclude that there are no dramatic differences between the illustrations. We noticed that the curvature has been increased slightly for the sake of orthotropicity; the orientation of the orthotropicity has only a minimal effect on the critical velocity.

TABLE 6 The parameter values of Figures 28 and 29.

	Case 1	Case 2	Case 3	Case 4
E_1	$0.5\ GPa$	$0.5\ GPa$	$0.5\ GPa$	$0.5\ GPa$
E_2	$1\ GPa$	$1\ GPa$	$1\ GPa$	$1\ GPa$
ν_{12}	0.3	0.3	0.3	0.3
G_{12} *Rate*	0.7	0.7	0.7	0.7
$T_0 \mid_{y=0}$	500 N/m	500 N/m	500 N/m	500 N/m
h	10^{-4} m	10^{-4} m	10^{-4} m	10^{-4} m
m	0.08 kg/m^2	0.08 kg/m^2	0.08 kg/m^2	0.08 kg/m^2
ℓ	0.1 m	0.1 m	0.1 m	0.1 m
b	0.5 m	0.5 m	0.5 m	0.5 m
$\ell/2b$	0.1	0.1	0.1	0.1
α	$1e-6 \cdot amax$	$1e-4 \cdot amax$	$0.1 \cdot amax$	$0.2 \cdot amax$
V_0 *Crit*	$79.0608\ m/s$	$79.05765\ m/s$	$75.1112\ m/s$	$70.90514\ m/s$

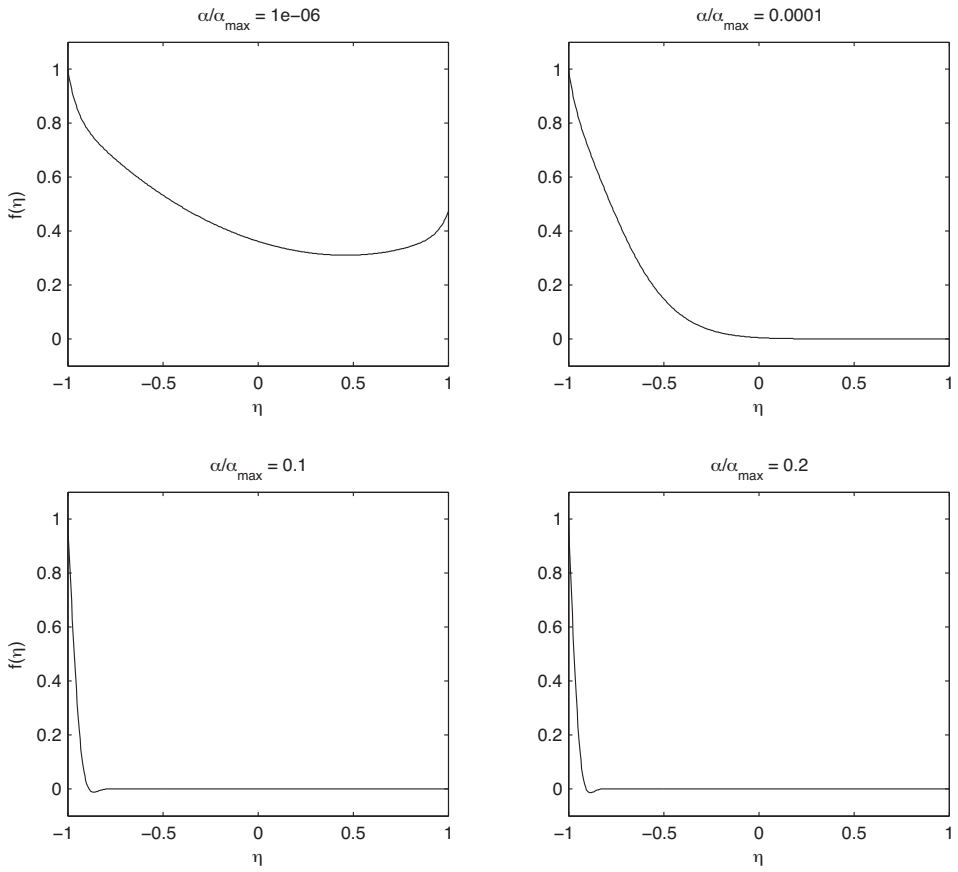

FIGURE 28 The out-of-plane displacement in the orthotropic plate with the non-linear tension profile. The effect of skewness on the tension (see the parameters from Table 6 on the facing page).

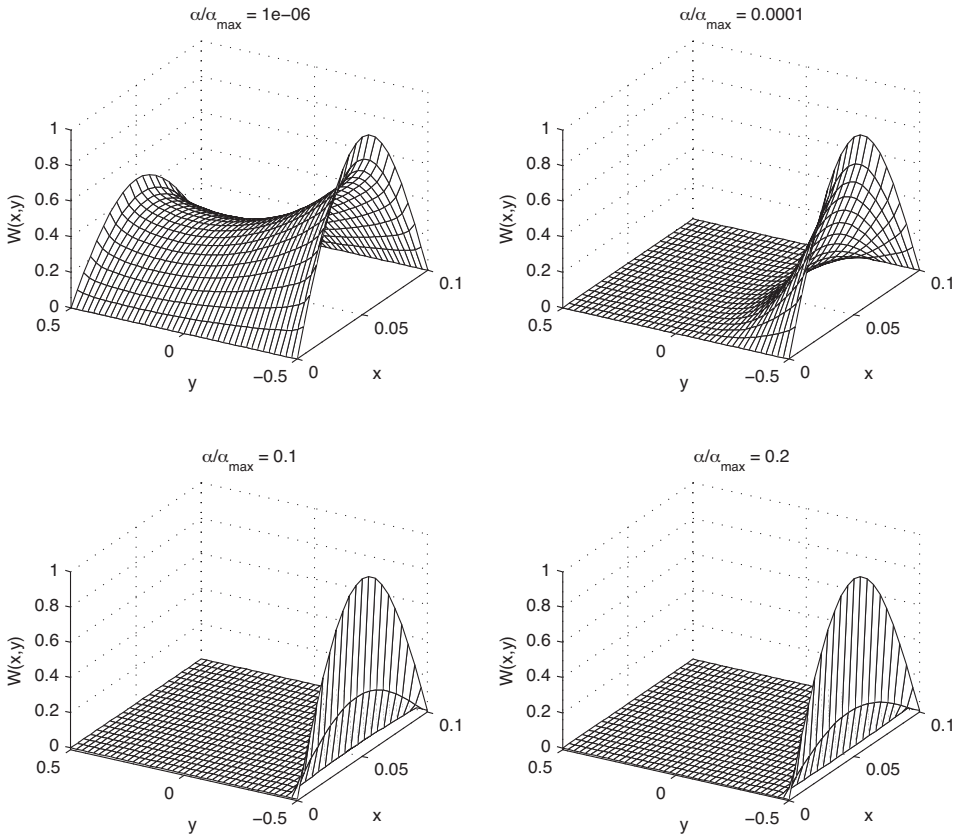

FIGURE 29 The out-of-plane displacement in the orthotropic plate with the non-linear tension profile. The effect of skewness on the tension (see the parameters from Table 6 on page 86).

TABLE 7 The parameter values of Figures 30 and 31.

	Case 1	Case 2	Case 3	Case 4
E_1	1 GPa	1 GPa	1 GPa	1 GPa
E_2	0.5 GPa	0.5 GPa	0.5 GPa	0.5 GPa
ν_{12}	0.3	0.3	0.3	0.3
G_{12} $Rate$	0.7	0.7	0.7	0.7
$T_0 \ \|_{y=0}$	500 N/m	500 N/m	500 N/m	500 N/m
h	10^{-4} m	10^{-4} m	10^{-4} m	10^{-4} m
m	0.08 kg/m^2	0.08 kg/m^2	0.08 kg/m^2	0.08 kg/m^2
ℓ	0.1 m	0.1 m	0.1 m	0.1 m
b	0.5 m	0.5 m	0.5 m	0.5 m
$\ell/2b$	0.1	0.1	0.1	0.1
α	$1e-6 \cdot$ amax	$1e-4 \cdot$ amax	$0.1 \cdot$ amax	$0.2 \cdot$ amax
V_0 $Crit$	79.06372 m/s	79.060578 m/s	75.104355 m/s	70.88857 m/s

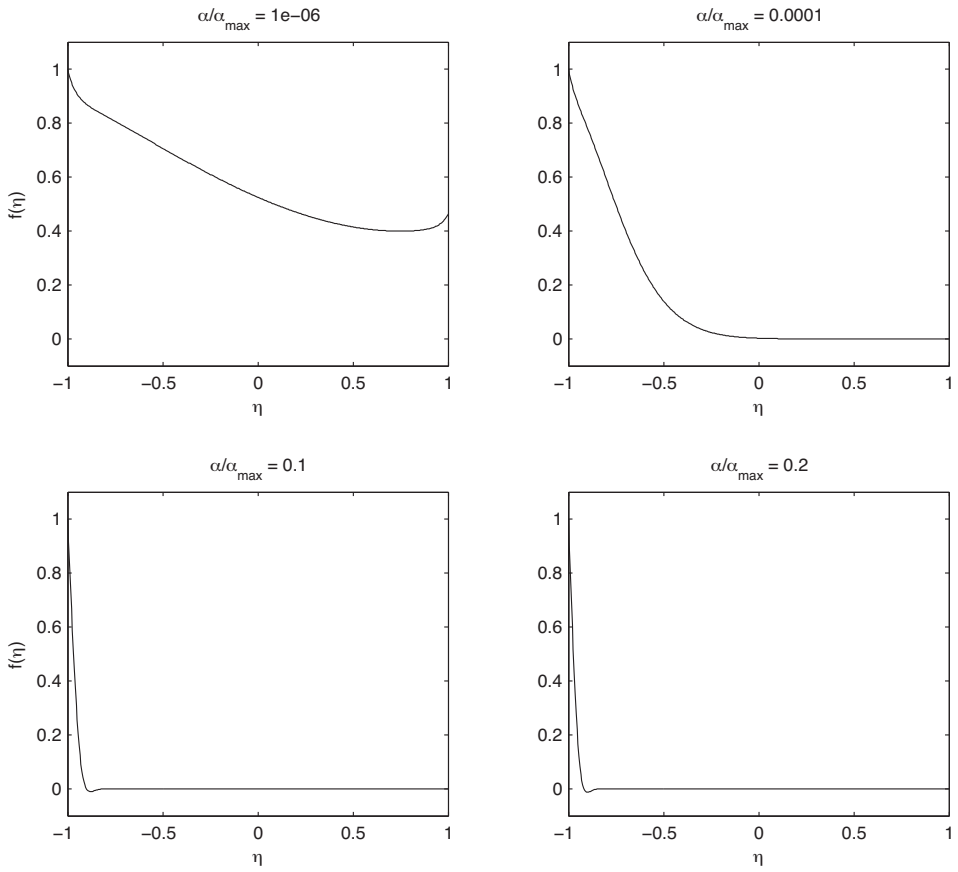

FIGURE 30 The out-of-plane displacement in the orthotropic plate with the non-linear tension profile. The effect of skewness on the tension (see the parameters from Table 7 on the facing page).

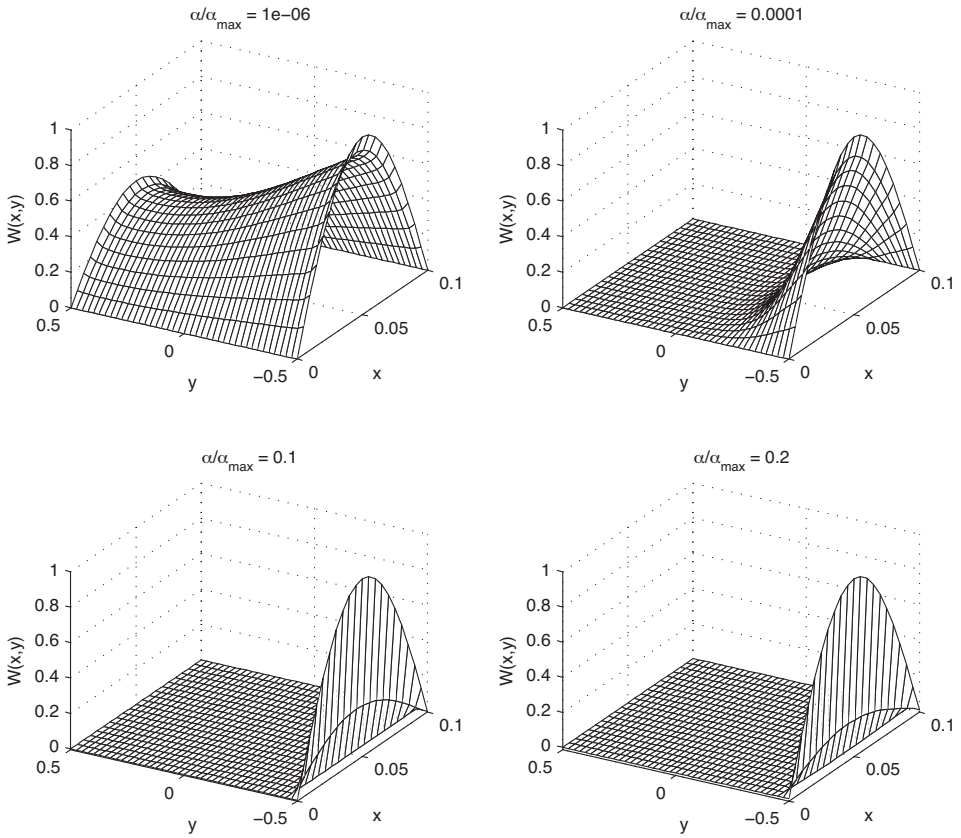

FIGURE 31 The out-of-plane displacement in the orthotropic plate with the non-linear tension profile. The effect of skewness on the tension (see the parameters from Table 7 on page 88).

4 CONCLUSIONS AND NOTES CONCERNING FUTURE PLANS AND DIRECTIONS FOR THE RESEARCH RELATED TO MOVING MATERIALS

In this section, we draw conclusions from the studies in this thesis. The reader will note that this thesis is a part of a more extensive research project related to moving materials and web handling. We have chosen a rather general approach because, by looking at the mathematical basis of the behavior of materials, it is possible to gain a better understanding of complex processes and to focus the future studies on appropriate subjects. The main result of this thesis is that the non-homogenenous tension profile of moving webs is a critical parameter when analyzing their stability.

4.1 Conclusions

We studied the model of an axially moving thin elastic plate subjected to in-plane loads (tensions) and out-of-plane actions (centrifugal forces and bending moments). A general dynamic analysis of small out-of-plane vibrations was performed, and some qualitative results describing the onset of instability were obtained. In particular, it was shown that under certain constraints the loss of stability of an axially moving elastic plate can be expressed in the static form. Equalities and inequalities for the critical velocities, in terms of the problem parameters, were derived and discussed.

The loss of the stability of axially moving plates was investigated in a two-dimensional formulation, taking into account their bending resistance and in-plane tension. The studies were mainly based on an analytical approach, and the basic relation characterizing the behavior of the plate at the onset of instability was found in an analytical form. A detailed analysis was performed for the static modes of instability. The critical divergence velocity and the corresponding buckling shapes were studied as functions of geometric and mechanical problem

parameters. It was proved that the buckled plate shape is symmetrical, i.e., the antisymmetric shapes correspond to higher values of the transport velocity. It was shown that the meaningful elastic deflections become localized in the vicinity of the free edges of the plate, and that the degree of localization depends only on the Poisson and aspect ratios of the plate.

It is necessary to note that for some buckling problems of plates with a large ratio of width to length, b/ℓ, a one-dimensional panel model is used. In this model, the critical parameter is equal to one ($\gamma_* = 1$). However, as was seen in our studies of the two-dimensional buckling problem, the limit of γ_* as the

$$\frac{b}{\ell} \to \infty \tag{234}$$

(this is the panel limit), the behaviour depends on the Poisson ratio and $\gamma_* < 1$. For any meaningful Poisson ratio ($\nu > 0$), this difference is small but significant. The largest difference is obtained when the Poisson ratio is equal to 0.5 and the material is fully compressible. This unusual conclusion is important for rigorous estimation.

The analytical solution originally developed for isotropic axially moving plates, as reported in the article by Banichuk et al. **[6]**, was extended to the general orthotropic case. The case was general in the sense that the in-plane shear modulus G_{12} was assumed to be an independent material parameter. The analytical approach allows for a fast solver, which can then be used for applications such as statistical uncertainty and sensitivity analysis, real-time parameter space exploration, and finding optimal values for design parameters.

As a result of applying the analytical approach developed, an explicit expression for the limit velocity of stable axial motion was found, and the limit velocity was computed for an example case. The critical regime was studied as a function of the moduli of orthotropicity. Localized modes of the instability of the axially moving orthotropic plate were found for a range of the problem parameters, and the localization effect was demonstrated with the help of numerical examples. It was shown analytically that the eigenvalues of the problem determining the shape of the buckled cross-section are non-negative. The transcendental and algebraic parts of the analytical solution were analyzed in detail, and certain properties were shown to hold. These properties apply not only to the general orthotropic case but also to the earlier isotropic one. Thus, the present study adds details to the analysis in the article by Banichuk et al. **[6]**.

It was shown that in the limit of the isotropic case, the present results reduce to the earlier ones presented in the above article. It was seen that the orthotropicity of the plate causes a quantitative change in the buckling behaviour, and it increases the critical velocity only slightly. The buckling shapes were found to depend significantly on the in-plane shear modulus G_{12}. It was observed that if the ratio G_{12}/G_H, where G_H is the geometric average shear modulus, is increased, the degree of localization of the deformation close to the free boundaries decreases. However, the orthotropicity of the material was found to have a negligible effect on the estimation of the critical velocity. Thus, if one only aims at estimating the

critical velocity, the isotropic model is sufficiently accurate. The orthotropic and isotropic buckling shapes were confirmed to be qualitatively similar. The main difference was found in the expressions of the condition that the boundary conditions are fulfilled.

The effects of problem parameters on the critical divergence mode were investigated by a numerical analysis. It was found that inhomogeneities in the tension profile may significantly decrease the critical velocities, and that even slight inhomogeneities have a very dramatic effect on the divergence shapes. Specifically, an inhomogeneity of one part in a million is sufficient to create a significant effect, and the divergence will have changed completely by the time a 1% inhomogeneity is reached. As no tension profile is completely homogeneous in practice, these results suggest that in order to predict the divergence shape accurately, tension inhomogeneities must be accounted for.

Note that we only considered linear distributions of the applied boundary tensions in this thesis. Other distributions of boundary tensions, such as piecewise linear or parabolic distributions, can also be considered in the framework of the described approach by means of a generalization of the solution for a more complex in-plane stress function. The analytical investigation was performed for the case of an isotropic elastic web, modelled as an isotropic membrane or an isotropic elastic plate. We have studied small vibrations and instability modes of orthotropic membranes and plates moving axially with constant velocities in the same manner. It is very important to realize this because many materials — especially in papermaking processes — are orthotropic.

Two further assumptions were used in this thesis. First of all, it was assumed that there are no gravity forces or forces from the interaction of the web with external media. In many applications, the gravity effects are indeed negligible as we have shown in our article **[11]**. However, for the interaction of the moving elastic web with surrounding fluid, corresponding studies are very important. These effects have been shown to be significant in published studies (see e.g., Banichuk et al., Kulachenko et al., Frondelius et al. and Pramila [4, 5, 7, 40, 68, 27, 8]). Secondly, in many conditions, such as the dynamics of a wet paper web, the plate must be considered as viscoelastic. However, the field of viscoelastic studies is very broad and requires special attention and another thesis to complete. Finally, some brief observations were made. It was noted that although a prescribed tension value was assumed, the analysis easily generalizes to the case where the x-direction displacement at one of the rollers is prescribed instead. It was also briefly stated that the classical reduction technique, i.e. bringing the equations to an isotropic form in the case where the geometric average in-plane shear modulus is used, works also for the dynamic case of an axially moving orthotropic plate, despite the Coriolis effect present in this setting.

In conclusion, we note that the investigation of ideal models provides a solid foundation for more complex multiphysics problems and a thorough understanding of certain technological processes.

4.2 Notes

In this section, we present some future plans and extensions discussed in the group about the topic of this thesis. The main direction of the future research is to concentrate on more efficient and more realistic models for moving materials. There are three branches where studies have already begun:

- Efficient methods for solving fluid flow around the web.
- Uncertainty of the models and parameters, crack propagation and fatigue analysis of the paper web.
- Viscoelastic models for moving webs.

Why the following directions? At first, it is known that fluid-structure problems involving slender structures lead to very non-linear and time-consuming numerical solutions in practical situations. In this thesis, we have simplified the problem in many ways, mainly by excluding the fluid from the equations. In the future, our aim is to form more realistic models and simulations. First of all, we plan to take the effect of fluid flow into account. The first results in that area have already been published in the articles by Banichuk et al. [7] and [8]. The next step is to try to improve the efficiency of the used numerical methods by including a hybrid meshless approach.

Our literature survey shows that the meshless methods are becoming a potential numerical technique for the analysis of this application. Traditionally, one difficulty with meshless methods has been their lack of efficiency compared to traditional mesh methods. One way to take advantage of both mesh and meshless methods is to hybridize them. In the article by Ma [50], hybrid mesh/meshless methods are shown to be accurate, flexible, and efficient. Compared with the pure meshless methods, the efficiency of the hybrid methods is improved to the level of mesh methods when the most part of the computational flow domain is covered with grid cells. Moreover, the hybrid methods are still flexible in dealing with complex configurations, as clouds of points are used to cover the region close to the aerodynamical geometries. Promising results have been obtained in solving two dimensional Euler equations with hybrid methods (see e.g. the article by Wang et al. [84]). A fast dynamic cloud method named Delaunay Graph Mapping has been introduced to ensure that clouds of points can automatically follow the moving rigid boundaries (see e.g. the article by Wang et al. [83]). It makes use of algebraic mapping principles, and therefore points can be accurately redistributed in the flow field without any iteration. In this way, the structure of the meshless clouds is not necessarily changed and therefore it avoids regenerations of the cloud during the movement of the aerodynamic geometry.

Moreover, ongoing research aims at investigating Euler and Navier-Stokes flows using hybrid mesh/meshless methods. In the future, we plan to consider a field method to simulate the movement of the membrane and the plate according to the external speed of the moving web, allowing more realistic modeling of the fluid/structure interaction problem. Introducing the meshless methods can

be advantageous for accuracy since they have demonstrated great flexibility in controlling the cloud node distribution in the vicinity of the moving obstacle.

The second approach of the future research looks at the imperfections of the paper web. We have done some preliminary work on modeling the effect of cracking of the moving paper web by using the linear fracture mechanics. By combining the results with the critical tension and velocity, we are able to optimize the productivity with respect to line breaks. Some of the methods that will be used are described in the book by Banichuk and Neittaanmäki [17] and we have already published the articles [13] and [12] as a preliminary steps of this research. The reader should note that the process, driven by the tension of the web, competes directly for the safety and fracture of the material. The solution derived from the process in use has been low tension on the edges and higher, nearly homogeneous tension in the middle of the web. The main question is: What is the optimal profile with respect to sensibility and production? We are also interested in other uncertainties of the models from a statical point of view.

The third and last area for the future visions is the viscoelastic properties of paper. The known fact is that paper as a material changes completely in the process. At the very beginning, the paper is in almost a liquid form, characterized by a high moisture level and fiber content. During the process, the paper will dry and acquire all its elastic properties, and at the very end it looks and feels like solid material. In our group, we have introduced a new model for taking the viscoelastic properties of the paper web into account and this model will be combined with our numerical analysis codes. From mathematical and numerical points of view, there are still many interesting problems that have not yet been addressed.

YHTEENVETO (FINNISH SUMMARY)

Tässä väitöskirjassa, jonka otsikko on: *Liikkuvan ortotrooppisen kalvon ja laatan stabiilisuusanalyysi lineaarisen ja epähomogeenisenjännitysprofiilin tukemana*, tutkitaan, liikkuvan materiaalin stabiilisuutta sekä ominaismuotoja kriittisessä nopeudessa. Tutkimuksessa käytetään kalvo- ja laattateoriaa iso- ja ortotrooppiselle materiaalimallille. Lisäksi tutkitaan sekä homogeenisen että epähomogeenisen jännitysprofiilin vaikutusta kriittiseen nopeuteen. Motivaatio tutkimukselle tulee paperin tuotannosta, erityisesti ajettavuudesta paperikoneissa. Paperi on viskoelastinen, melkein plastinen materiaali, jota tuotetaan paperikoneissa yli 1800 m/min. Suuri ajonopeus on keskeinen vaikuttaja mitattaessa paperikoneen tuottavuutta, mutta samalla se vaatii suurempia jännityksiä, että rata pysyy stabiilina. Kokeellinen mittaaminen paperikoneissa on hankalaa ja kallista, usein jopa mahdotonta, joten matemaattisen mallintamisen ja numeerisen analyysin avulla tästä monimutkaisesta ilmiöstä pyritään havaitsemaan keskeiset radan käytökseen vaikuttavat komponentit.

Tavoitteena tutkimuksessa on määrittää suurin mahdollinen rainan nopeus, jolla teoreettisesti rataa voidaan ajaa. Todellisuudessa tämä raja on luonnollisesti huomattavasti matalampi, johtuen mm. ilmavirtauksien vaikutuksesta ja materiaalin ominaisuuksista. Mallintamalla saavutettua tietoa radan käyttäytymisestä ja kriittisistä nopeuksista pystytään hyödyntämään esimerkiksi radan jännitysprofiilin säätämisessä. Yhdistämällä säröteoria jännitysprofiilin käyttäytymisestä saatuun tietoon mahdollistetaan ajettavuuden ja tuotannon optimointi suhteessa ratakatkojen herkkyyteen. Tässä väitöskirjassa luodaan perusta esitellylle optimointitehtävälle, mutta yhdistäminen säröteoriaan ei kuitenkaan kuulu tässä väitöskirjassa käsiteltäviin aihealueisiin.

Väitöskirjassa tutkitaan lineaarisen ja epähomogeenisen jännitysprofiilin vaikutusta sekä isotrooppiseen että ortotrooppiseen materiaaliin sen liikkuessa eteenpäin. Analyysissa sovelletaan Bolotinin esittelemää menetelmää, jossa klassisista liikkuvan laatan (ja kalvon) yhtälöistä muodostetaan ominaisarvotehtävä, josta ratkaistaan alimmat ominaisarvot ja -muodot. Menetelmällä voidaan tutkia vain staattisia epästabiiliustiloja, joten tutkimus ei ota kantaa dynaamisiin epästabiilisuuksiin.

Väitöskirjan keskeinen tulos on, että jopa äärimmäisen pienet muutokset jännitysprofiilissa vaikuttavat liikkuvan laatan ominaismuotoihin ja suuremmilla muutoksilla on merkittävä vaikutus myös liikkuvan laatan kriittiseen nopeuteen. Lisäksi tutkimuksesta havaitaan, että ortotrooppisen materiaalimallin vaikutus laatan stabiilisuusanalyysissä on heikko. Stabiilisuusanalyysi on suoritettu numeerisesti ja teoreettiset yksityiskohdat käydään läpi tässä väitöstyössä. Väitöskirjassa ei ole huomioitu ilman vaikutusta liikkuvaan laattaan, paperin viskoelastisuutta, adheesiovoimia tai kontaktia teloihin.

REFERENCES

[1] F. R. Archibald, A. G. Emslie, The vibration of a string having a uniform motion along its length, ASME Journal of Applied Mechanics 25 (1958) 347–348.

[2] N. Banichuk, J. Jeronen, M. Kurki, P. Neittaanmäki, T. Saksa, T. Tuovinen, On the limit velocity and buckling phenomena of axially moving orthotropic membranes and plates, International Journal of Solids and Structures 48 (13) (2011) 2015–2025.
URL http://dx.doi.org/10.1016/j.ijsolstr.2011.03.010

[3] N. Banichuk, J. Jeronen, P. Neittaanmäki, T. Tuovinen, Instability analysis for traveling membranes and plates interacting with surrounding ideal fluid, Tech. Rep. 13, University of Jyväskylä (2008).

[4] N. Banichuk, J. Jeronen, P. Neittaanmäki, T. Tuovinen, Nonstationary dynamics of travelling membranes and plates interacting with axially moving ideal fluid. part i: Theory, Tech. Rep. 11, University of Jyväskylä (2008).

[5] N. Banichuk, J. Jeronen, P. Neittaanmäki, T. Tuovinen, Nonstationary dynamics of travelling membranes and plates interacting with axially moving ideal fluid. part ii: Numerical results, Tech. Rep. 12, University of Jyväskylä (2008).

[6] N. Banichuk, J. Jeronen, P. Neittaanmäki, T. Tuovinen, On the instability of an axially moving elastic plate, International Journal of Solids and Structures 47 (1) (2010) 91–99.
URL http://dx.doi.org/10.1016/j.ijsolstr.2009.09.020

[7] N. Banichuk, J. Jeronen, P. Neittaanmäki, T. Tuovinen, Static instability analysis for travelling membranes and plates interacting with axially moving ideal fluid, Journal of Fluids and Structures 26 (2) (2010) 274–291.
URL http://dx.doi.org/10.1016/j.jfluidstructs.2009.09.006

[8] N. Banichuk, J. Jeronen, P. Neittaanmäki, T. Tuovinen, Dynamic behaviour of an axially moving plate undergoing small cylindrical deformation submerged in axially flowing ideal fluid, Journal of Fluids and Structures 27 (7) (2011) 986–1005.
URL http://dx.doi.org/10.1016/j.jfluidstructs.2011.07.004

[9] N. Banichuk, J. Jeronen, P. Neittaanmäki, T. Tuovinen, T. Saksa, Theoretical study on travelling web dynamics and instability under a linear tension distribution, Tech. Rep. 1, University of Jyväskylä (2010).

[10] N. Banichuk, J. Jeronen, T. Saksa, T. Tuovinen, On the instability of elastic web axially moving in the gravitational field, Tech. Rep. 2, University of Jyväskylä (2011).

[11] N. Banichuk, J. Jeronen, T. Saksa, T. Tuovinen, Static instability analysis of an elastic band travelling in the gravitational field, Rakenteiden mekaniikka (Journal of Structural Mechanics) 44 (3) (2011) 172–185.

[12] N. Banichuk, M. Kurki, P. Neittaanmäki, T. Saksa, M. Tirronen, T. Tuovinen, Optimization of axially moving webs subjected to instability and fracture, Tech. Rep. 9, University of Jyväskylä (2011).

[13] N. Banichuk, M. Kurki, P. Neittaanmäki, T. Saksa, T. Tuovinen, On axially moving webs under fracture and instability constraints, Tech. Rep. 8, University of Jyväskylä (2011).

[14] N. Banichuk, P. Neittaanmäki, Instability analysis for traveling paper web interacting with surrounding air, Tech. Rep. 4, University of Jyväskylä (2008).

[15] N. Banichuk, P. Neittaanmäki, On application of the galerkin method and perturbation techniques for vibration analysis of a moving web submerged into ideal fluid, Tech. Rep. 3, University of Jyväskylä (2008).

[16] N. Banichuk, P. Neittaanmäki, On the transverse vibrations analysis of traveling membranes and plates submerged into ideal fluid, Tech. Rep. 2, University of Jyväskylä (2008).

[17] N. V. Banichuk, P. J. Neittaanmäki, Structural Optimization with Uncertainties, Springer-Verlag, 2010, ISBN 978-90-481-2517-3.

[18] M. E. Biancolini, C. Brutti, L. Reccia, Approximate solution for free vibrations of thin orthotropic rectangular plates, Journal of Sound and Vibration 288 (1–2) (2005) 321 – 344, dOI: 10.1016/j.jsv.2005.01.005.

[19] V. V. Bolotin, Nonconservative Problems of the Theory of Elastic Stability, Pergamon Press, New York, 1963.

[20] A. Bonnin, R. Huchon, M. Deschamps, Ultrasonic waves propagation in absorbing thin plates: Application to paper characterization, Ultrasonics 37 (8) (2000) 555–563.
URL http://dx.doi.org/10.1016/S0041-624X(99)00106-7

[21] Y. B. Chang, P. M. Moretti, Interaction of fluttering webs with surrounding air, TAPPI Journal 74 (3) (1991) 231–236.

[22] G. Chen, M. P. Coleman, Z. Ding, Some corner effects on the loss of selfadjointness and the non-excitation of vibration for thin plates and shells, The Quarterly Journal of Mechanics and Applied Mathematics 51 (2) (1998) 213–240, doi:10.1093/qjmam/51.2.213.

[23] L.-Q. Chen, H. Ding, Steady-state transverse response in coupled planar vibration of axially moving viscoelastic beams, ASME Journal of Vibrations and Acoustics 132 (2010) 011009–1–9, http://dx.doi.org/10.1115/1.4000468.

[24] L.-Q. Chen, X.-D. Yang, Vibration and stability of an axially moving viscoelastic beam with hybrid supports, European Journal of Mechanics - A/Solids 25 (6) (2006) 996 – 1008, dOI: 10.1016/j.euromechsol.2005.11.010.

[25] L.-Q. Chen, W.-J. Zhao, A numerical method for simulating transverse vibrations of an axially moving string, Applied Mathematics and Computation 160 (2) (2005) 411 – 422, dOI: 10.1016/j.amc.2003.11.012.

[26] S. Chonan, Steady state response of an axially moving strip subjected to a stationary lateral load, Journal of Sound and Vibration 107 (1986) 155–165.

[27] T. Frondelius, H. Koivurova, A. Pramila, Interaction of an axially moving band and surrounding fluid by boundary layer theory, Journal of Fluids and Structures 22 (8) (2006) 1047–1056.

[28] R.-F. Fung, J.-S. Huang, Y.-C. Chen, The transient amplitude of the viscoelastic travelling string: An integral constitutive law, Journal of Sound and Vibration 201 (2) (1997) 153 – 167, dOI: 10.1006/jsvi.1996.0776.

[29] R.-F. Fung, J.-S. Huang, Y.-C. Chen, C.-M. Yao, Nonlinear dynamic analysis of the viscoelastic string with a harmonically varying transport speed, Computers & Structures 66 (6) (1998) 777 – 784, dOI: 10.1016/S0045-7949(98)00001-7.

[30] D. J. Gorman, Free Vibration Analysis of Rectangular Plates, Elsevier North Holland, Inc., 1982, ISBN 0-444-00601-X.

[31] L. Göttsching, H. L. Baumgarten, Triaxial deformation of paper under tensile load, in: The Fundamental Properties of Paper Related to Its Uses, Vol. 1, Technical Division of the British Paper and Board Industry Federation, 1976, pp. 227–252.

[32] S. Hatami, M. Azhari, M. M. Saadatpour, P. Memarzadeh, Exact free vibration of webs moving axially at high speed, in: AMATH'09: Proceedings of the 15th american conference on Applied mathematics, World Scientific and Engineering Academy and Society (WSEAS), Stevens Point, Wisconsin, USA, 2009, pp. 134–139, Houston, USA.

[33] M. T. Huber, Die theorie des kreuzweise bewehrten eisenbetonplatten, Der Bauingenieur 4 (1923) 354–392.

[34] J. Jeronen, N. Banichuk, P. Neittaanmäki, T. Tuovinen, On the effects of bending rigidity on the stability of an axially moving orthotropic plate, in: Proceedings of the 10th Finnish Mechanics Days — X Suomen Mekaniikkapäivät, University of Jyväskylä, 2009, pp. 510–521, ISBN 978-951-39-3738-6.

[35] J. Jeronen, T. Saksa, T. Tuovinen, N. Banichuk, P. Neittaanmäki, On the moving web dynamics under stability considerations including interaction with

surrounding fluid, in: K. J. Bathe (ed.), Compilation of Abstracts for the Sixth M.I.T. Conference on Computational Fluid and Solid Mechanics – Focus: Advances in Solids & Structures, Massachusetts Institute of Technology, Cambridge, MA 02139 U.S.A., 2011, p. 64.

[36] J. Jeronen, T. Tuovinen, P. Neittaanmäki, N. Banichuk, Instability analysis of axially travelling membranes and plates interacting with axially moving ideal fluid, in: Proceedings of the Twenty Second Nordic Seminar on Computational Mechanics, No. 11, Aalborg University, 2009, pp. 101–104.

[37] M. Karlsson (ed.), Papermaking, Part 2 Drying, vol. 9 of Papermaking Science and Technology, Paperi ja Puu Oy, 2009, ISBN 978-952-5216-37-0 (book 9).

[38] N. Kikuchi, Finite Element Methods in Mechanics, Cambridge University Press, Cambridge, UK, 1986, ISBN 0 521 33972 3.

[39] S. Kshirsagar, K. Bhaskar, Accurate and elegant free vibration and buckling studies of orthotropic rectangular plates using untruncated infinite series, Journal of Sound and Vibration 314 (3–5) (2008) 837 – 850, dOI: 10.1016/j.jsv.2008.01.013.

[40] A. Kulachenko, P. Gradin, H. Koivurova, Modelling the dynamical behaviour of a paper web. Part I, Computers & Structures 85 (2007) 131–147.

[41] A. Kulachenko, P. Gradin, H. Koivurova, Modelling the dynamical behaviour of a paper web. Part II, Computers & Structures 85 (2007) 148–157.

[42] M. Kurki, Modeling of kinematical and rheological web line behavior in a papermaking environment, Licentiate thesis, Lappeenranta University of Technology, Department of Mechanical Engineering, lappeenranta, Finland (2005).

[43] M. Kurki, J. Jeronen, T. Saksa, T. Tuovinen, P. Neittaanmäki, Liikkuvan paperiradan kriittinen rajanopeus ja stabiilisuusanalyysi paperi- ja kartonkikoneen eri osaprosesseissa (2011).

[44] J. Kuula, P. Neittaanmäki, I. Pölönen, T. Tuovinen, Mathematical model based IT tools for supporting the open value forming and pricing of biomass at the renewable energy sector, in: Proceedings of NORDIC BIOENERGY 2011 Conference, 2011.

[45] U. Lee, H. Oh, Dynamics of an axially moving viscoelastic beam subject to axial tension, International Journal of Solids and Structures 42 (8) (2005) 2381 – 2398, dOI: 10.1016/j.ijsolstr.2004.09.026.

[46] C. C. Lin, Stability and vibration characteristics of axially moving plates, International Journal of Solids and Structures 34 (24) (1997) 3179–3190.

[47] C. C. Lin, C. D. Mote, Equilibrium displacement and stress distribution in a two-dimensional, axially moving web under transverse loading, ASME Journal of Applied Mechanics 62 (1995) 772–779.

[48] C. C. Lin, C. D. Mote, Eigenvalue solutions predicting the wrinkling of rectangular webs under non-linearly distributed edge loading, Journal of Sound and Vibration 197 (2) (1996) 179–189.

[49] H. Linna, M. Parola, J. Virtanen, Better productivity by measuring web tension profile, in: 55th APPITA Annual Conference, Hobart, Australia 30 April-2 May 2001: Proceedings, Appita Inc., Carlton, Vic., 2001, pp. 305–311, ISBN 0958554838.

[50] Z. H. Ma, H. Chen, X. J. Wu, A gridless-finite volume hybrid algorithm for euler equations., Chinese Journal of Aeronautics 19 (4) (2006) 286–294.

[51] O. Mali, Analysis of errors caused by incomplete knowledge of material data in mathematical models of elastic media, Jyväskylä studies in computing 132, Department of Mathematical Information Technology, University of Jyväskylä, ISBN 978-951-39-4393-6 (2011).

[52] R. W. Mann, G. A. Baum, C. C. Habeger, Determination of all nine orthotropic elastic constants for machine-made paper, TAPPI Journal 63 (2) (1980) 163–166.

[53] K. Marynowski, Non-linear vibrations of an axially moving viscoelastic web with time-dependent tension, Chaos, Solitons & Fractals 21 (2) (2004) 481 – 490, dOI: 10.1016/j.chaos.2003.12.020.

[54] K. Marynowski, Two-dimensional rheological element in modelling of axially moving viscoelastic web, European Journal of Mechanics - A/Solids 25 (5) (2006) 729 – 744, dOI: 10.1016/j.euromechsol.2005.10.005.

[55] K. Marynowski, Dynamics of the Axially Moving Orthotropic Web, vol. 38 of Lecture Notes in Applied and Computational Mechanics, Springer–Verlag, Germany, 2008.

[56] K. Marynowski, Non-linear vibrations of the axially moving paper web, Journal of Theoretical and Applied Mechanics 46 (3) (2008) 565 – 580.

[57] K. Marynowski, Free vibration analysis of the axially moving levy-type viscoelastic plate, European Journal of Mechanics - A/Solids 29 (5) (2010) 879 – 886, dOI: 10.1016/j.euromechsol.2010.03.010.

[58] K. Marynowski, T. Kapitaniak, Kelvin-voigt versus bürgers internal damping in modeling of axially moving viscoelastic web, International Journal of Non-Linear Mechanics 37 (7) (2002) 1147 – 1161, dOI: 10.1016/S0020-7462(01)00142-1.

[59] K. Marynowski, T. Kapitaniak, Zener internal damping in modelling of axially moving viscoelastic beam with time-dependent tension, International Journal of Non-Linear Mechanics 42 (1) (2007) 118 – 131, dOI: 10.1016/j.ijnonlinmec.2006.09.006.

[60] W. L. Miranker, The wave equation in a medium in motion, IBM Journal of Research and Development 4 (1960) 36–42.

[61] S. Mönkölä, T. Airaksinen, P. Makkonen, T. Tuovinen, P. Neittaanmäki, Prospectives to tractor cabin design with computational acoustics tools, Tech. Rep. 49 (2011).

[62] C. D. Mote, Dynamic stability of axially moving materials, Shock and Vibration Digest 4 (4) (1972) 2–11.

[63] A. S. Mujumdar, W. J. M. Douglas, Analytical modelling of sheet flutter, Svensk Papperstidning 79 (1976) 187–192.

[64] P. Neittaanmäki, S. I. Repin, Reliable methods for computer simulation: error control and a posteriori estimates, Studies in mathematics and its applications, Elsevier, 2004, ISBN 9780444513762.
URL http://books.google.co.uk/books?id=OEX7XWJ1g1EC

[65] J. Niemi, A. Pramila, Vibration analysis of an axially moving membrane immersed into ideal fluid by fem, Tech. rep., Tampere (1986).

[66] H. Oh, J. Cho, U. Lee, Spectral element analysis for an axially moving viscoelastic beam, Journal of Mechanical Science and Technology 18 (7) (2004) 1159–1168, dOI: 10.1007/BF02983290.
URL http://dx.doi.org/10.1007/BF02983290

[67] M. P. Païdoussis, Some unresolved issues in fluid-structure interactions, Journal of Fluids and Structures 20 (6) (2005) 871–890.

[68] A. Pramila, Sheet flutter and the interaction between sheet and air, TAPPI Journal 69 (7) (1986) 70–74.

[69] H. Sagan, Boundary and Eigenvalue Problems in Mathematical Physics, John Wiley & Sons, Inc., 1961, slightly corrected reprint by Dover Publications, Inc., 1989.

[70] Y. B. Seo, Determination of in-plane shear properties by an off-axis tension method and laser speckle photography, Journal of Pulp and Paper Sciences 25 (9) (1999) 321–325.

[71] J. Y. Shen, L. Sharpe, W. M. McGinley, Identification of dynamic properties of plate-like structures by using a continuum model, Mechanics Research Communications 22 (1) (1995) 67–78.

[72] C. Shin, J. Chung, W. Kim, Dynamic characteristics of the out-of-plane vibration for an axially moving membrane, Journal of Sound and Vibration 286 (4-5) (2005) 1019–1031.

[73] A. Simpson, Transverse modes and frequencies of beams translating between fixed end supports, Journal of Mechanical Engineering Science 15 (1973) 159–164.

[74] J. Skowronski, A. A. Robertson, A phenomenological study of the tensile deformation properties of paper, Journal of Pulp and Paper Sciences 11 (1) (1985) J21–J28.

[75] R. Sygulski, Stability of membrane in low subsonic flow, International Journal of Non-Linear Mechanics 42 (1) (2007) 196–202.

[76] J. L. Thorpe, Paper as an orthotropic thin plate, TAPPI Journal 64 (3) (1981) 119–121.

[77] A. Thurman, C. J. Mote, Free, periodic, nonlinear oscillation of an axially moving strip, J. Appl. Mech. 36.

[78] S. P. Timoshenko, J. M. Gere, Theory of Elastic Stability, Dover Publications, 2009, ISBN 9780486472072.
URL http://books.google.com/books?id=C8CoPwAACAAJ

[79] S. P. Timoshenko, S. Woinowsky-Krieger, Theory of plates and shells, 2nd ed., New York : Tokyo : McGraw-Hill, 1959, ISBN 0-07-085820-9.

[80] T. Tuovinen, J. Jeronen, P. Neittaanmäki, N. Banichuk, On the instability of an axially moving elastic plate, in: Proceedings of the Twenty Second Nordic Seminar on Computational Mechanics, No. 11, Aalborg University, 2009, pp. 95–99.

[81] T. Tuovinen, S. Mönkölä, Two different approaches for fluid-structure interaction (FSI) based flutter problems in paper machine, Tech. Rep. 5, University of Jyväskylä (2008).

[82] A. G. Ulsoy, C. D. Mote, Vibration of wide band saw blades, ASME Journal of Engineering for Industry 104 (1982) 71–78.

[83] H. Wang, H. Q. Chen, J. Periaux, A study of gridless method with dynamic clouds of points for solving unsteady cfd problems in aerodynamics, International Journal for Numerical Methods in Fluids 64 (1) (2010) 98–118.

[84] H. Wang, D. S. Lee, J. Periaux, H. Q. Chen, Cfd inverse problems solved by hybrid mesh/mesless methods using eas and nash games on multi-element airfoils in aerodynamics.

[85] X. Wang, Instability analysis of some fluid-structure interaction problems, Computers & Fluids 32 (1) (2003) 121–138.

[86] R. Weinstock, Calculus of Variations — With Applications to Physics and Engineering, Weinstock Press, 2008 (reprint), ISBN 978-1443728812.

[87] J. A. Wickert, Non-linear vibration of a traveling tensioned beam, International Journal of Non-Linear Mechanics 27 (3) (1992) 503–517.

[88] J. A. Wickert, C. D. Mote, Classical vibration analysis of axially moving continua, ASME Journal of Applied Mechanics 57 (1990) 738–744.

[89] Y. Xing, B. Liu, New exact solutions for free vibrations of rectangular thin plates by symplectic dual method, Acta Mech Sinica 25 (2009) 265–270.

[90] X.-D. Yang, L.-Q. Chen, Dynamic stability of axially moving viscoelastic beams with pulsating speed, Applied Mathematics and Mechanics 26 (8) (2005) 905–910.

[91] X.-D. Yang, L.-Q. Chen, Dynamic stability of axially moving viscoelastic beams with pulsating speed, Acta Mechanica Solida Sinica 19 (4) (2006) 365–373.

[92] T. Yokoyama, K. Nakai, Evaluation of in-plane orthotropic elastic constants of paper and paperboard, in: 2007 SEM Annual Conference & Exposition on Experimental and Applied Mechanics, 2007.

[93] N.-H. Zhang, L.-Q. Chen, Nonlinear dynamical analysis of axially moving viscoelastic strings, Chaos, Solitons & Fractals 24 (4) (2005) 1065 – 1074, dOI: 10.1016/j.chaos.2004.09.113.

JYVÄSKYLÄ STUDIES IN COMPUTING

1 Ropponen, Janne, Software risk management - foundations, principles and empirical findings. 273 p. Yhteenveto 1 p. 1999.
2 Kuzmin, Dmitri, Numerical simulation of reactive bubbly flows. 110 p. Yhteenveto 1 p. 1999.
3 Karsten, Helena, Weaving tapestry: collaborative information technology and organisational change. 266 p. Yhteenveto 3 p. 2000.
4 Koskinen, Jussi, Automated transient hypertext support for software maintenance. 98 p. (250 p.) Yhteenveto 1 p. 2000.
5 Ristaniemi, Tapani, Synchronization and blind signal processing in CDMA systems. - Synkronointi ja sokea signaalinkäsittely CDMA järjestelmässä. 112 p. Yhteenveto 1 p. 2000.
6 Laitinen, Mika, Mathematical modelling of conductive-radiative heat transfer. 20 p. (108 p.) Yhteenveto 1 p. 2000.
7 Koskinen, Minna, Process metamodelling. Conceptual foundations and application. 213 p. Yhteenveto 1 p. 2000.
8 Smolianski, Anton, Numerical modeling of two-fluid interfacial flows. 109 p. Yhteenveto 1 p. 2001.
9 Nahar, Nazmun, Information technology supported technology transfer process. A multi-site case study of high-tech enterprises. 377 p. Yhteenveto 3 p. 2001.
10 Fomin, Vladislav V., The process of standard making. The case of cellular mobile telephony. - Standardin kehittämisen prosessi. Tapaustutkimus solukkoverkkoon perustuvasta matkapuhelintekniikasta. 107 p. (208 p.) Yhteenveto 1 p. 2001.
11 Päivärinta, Tero, A genre-based approach to developing electronic document management in the organization. 190 p. Yhteenveto 1 p. 2001.
12 Häkkinen, Erkki, Design, implementation and evaluation of neural data analysis environment. 229 p. Yhteenveto 1 p. 2001.
13 Hirvonen, Kullervo, Towards better employment using adaptive control of labour costs of an enterprise. 118 p. Yhteenveto 4 p. 2001.
14 Majava, Kirsi, Optimization-based techniques for image restoration. 27 p. (142 p.) Yhteenveto 1 p. 2001.
15 Saarinen, Kari, Near infra-red measurement based control system for thermo-mechanical refiners. 84 p. (186 p.) Yhteenveto 1 p. 2001.
16 Forsell, Marko, Improving component reuse in software development. 169 p. Yhteenveto 1 p. 2002.
17 Virtanen, Pauli, Neuro-fuzzy expert systems in financial and control engineering. 245 p. Yhteenveto 1 p. 2002.
18 Kovalainen, Mikko, Computer mediated organizational memory for process control. Moving CSCW research from an idea to a product. 57 p. (146 p.) Yhteenveto 4 p. 2002.
19 Hämäläinen, Timo, Broadband network quality of service and pricing. 140 p. Yhteenveto 1 p. 2002.
20 Martikainen, Janne, Efficient solvers for discretized elliptic vector-valued problems. 25 p. (109 p.) Yhteenveto 1 p. 2002.
21 Mursu, Anja, Information systems development in developing countries. Risk management and sustainability analysis in Nigerian software companies. 296 p. Yhteenveto 3 p. 2002.
22 Seleznyov, Alexandr, An anomaly intrusion detection system based on intelligent user recognition. 186 p. Yhteenveto 3 p. 2002.
23 Lensu, Anssi, Computationally intelligent methods for qualitative data analysis. 57 p. (180 p.) Yhteenveto 1 p. 2002.
24 Ryabov, Vladimir, Handling imperfect temporal relations. 75 p. (145 p.) Yhteenveto 2 p. 2002.
25 Tsymbal, Alexey, Dynamic integration of data mining methods in knowledge discovery systems. 69 p. (170 p.) Yhteenveto 2 p. 2002.
26 Akimov, Vladimir, Domain decomposition methods for the problems with boundary layers. 30 p. (84 p.). Yhteenveto 1 p. 2002.
27 Seyukova-Rivkind, Ludmila, Mathematical and numerical analysis of boundary value problems for fluid flow. 30 p. (126 p.) Yhteenveto 1 p. 2002.
28 Hämäläinen, Seppo, WCDMA Radio network performance. 235 p. Yhteenveto 2 p. 2003.
29 Pekkola, Samuli, Multiple media in group work. Emphasising individual users in distributed and real-time CSCW systems. 210 p. Yhteenveto 2 p. 2003.
30 Markkula, Jouni, Geographic personal data, its privacy protection and prospects in a location-based service environment. 109 p. Yhteenveto 2 p. 2003.
31 Honkaranta, Anne, From genres to content analysis. Experiences from four case organizations. 90 p. (154 p.) Yhteenveto 1 p. 2003.
32 Raitamäki, Jouni, An approach to linguistic pattern recognition using fuzzy systems. 169 p. Yhteenveto 1 p. 2003.
33 Saalasti, Sami, Neural networks for heart rate time series analysis. 192 p. Yhteenveto 5 p. 2003.
34 Niemelä, Marketta, Visual search in graphical interfaces: a user psychological approach. 61 p. (148 p.) Yhteenveto 1 p. 2003.
35 You, Yu, Situation Awareness on the world wide web. 171 p. Yhteenveto 2 p. 2004.
36 Taatila, Vesa, The concept of organizational competence – A foundational analysis. - Perusteanalyysi organisaation kompetenssin käsitteestä. 111 p. Yhteenveto 2 p. 2004.

37 LYYTIKÄINEN, VIRPI, Contextual and structural metadata in enterprise document management. - Konteksti- ja rakennemetatieto organisaation dokumenttien hallinnassa. 73 p. (143 p.) Yhteenveto 1 p. 2004.
38 KAARIO, KIMMO, Resource allocation and load balancing mechanisms for providing quality of service in the Internet. 171 p. Yhteenveto 1 p. 2004.
39 ZHANG, ZHEYING, Model component reuse. Conceptual foundations and application in the metamodeling-based systems analysis and design environment. 76 p. (214 p.) Yhteenveto 1 p. 2004.
40 HAARALA, MARJO, Large-scale nonsmooth optimization variable metric bundle method with limited memory. 107 p. Yhteenveto 1 p. 2004.
41 KALVINE, VIKTOR, Scattering and point spectra for elliptic systems in domains with cylindrical ends. 82 p. 2004.
42 DEMENTIEVA, MARIA, Regularization in multistage cooperative games. 78 p. 2004.
43 MAARANEN, HEIKKI, On heuristic hybrid methods and structured point sets in global continuous optimization. 42 p. (168 p.) Yhteenveto 1 p. 2004.
44 FROLOV, MAXIM, Reliable control over approximation errors by functional type a posteriori estimates. 39 p. (112 p.) 2004.
45 ZHANG, JIAN, Qos- and revenue-aware resource allocation mechanisms in multiclass IP networks. 85 p. (224 p.) 2004.
46 KUJALA, JANNE, On computation in statistical models with a psychophysical application. 40 p. (104 p.) 2004.,
47 SOLBAKOV, VIATCHESLAV, Application of mathematical modeling for water environment problems. 66 p. (118 p.) 2004.
48 HIRVONEN, ARI P., Enterprise architecture planning in practice. The Perspectives of information and communication technology service provider and end-user. 44 p. (135 p.) Yhteenveto 2 p. 2005.
49 VARTIAINEN, TERO, Moral conflicts in a project course in information systems education. 320 p. Yhteenveto 1p. 2005.
50 HUOTARI, JOUNI, Integrating graphical information system models with visualization techniques. - Graafisten tietojärjestelmäkuvausten integrointi visualisointitekniikoilla. 56 p. (157 p.) Yhteenveto 1p. 2005.
51 WALLENIUS, EERO R., Control and management of multi-access wireless networks. 91 p. (192 p.) Yhteenveto 3 p. 2005.
52 LEPPÄNEN, MAURI, An ontological framework and a methodical skeleton for method engineering – A contextual approach. 702 p. Yhteenveto 2 p. 2005.
53 MATYUKEVICH, SERGEY, The nonstationary Maxwell system in domains with edges and conical points. 131 p. Yhteenveto 1 p. 2005.
54 SAYENKO, ALEXANDER, Adaptive scheduling for the QoS supported networks. 120 p. (217 p.) 2005.
55 KURJENNIEMI, JANNE, A study of TD-CDMA and WCDMA radio network enhancements. 144 p. (230 p.) Yhteenveto 1 p. 2005.
56 PECHENIZKIY, MYKOLA, Feature extraction for supervised learning in knowledge discovery systems. 86 p. (174 p.) Yhteenveto 2 p. 2005.
57 IKONEN, SAMULI, Efficient numerical methods for pricing American options. 43 p. (155 p.) Yhteenveto 1 p. 2005.
58 KÄRKKÄINEN, KARI, Shape sensitivity analysis for numerical solution of free boundary problems. 83 p. (119 p.) Yhteenveto 1 p. 2005.
59 HELFENSTEIN, SACHA, Transfer. Review, reconstruction, and resolution. 114 p. (206 p.) Yhteenveto 2 p. 2005.
60 NEVALA, KALEVI, Content-based design engineering thinking. In the search for approach. 64 p. (126 p.) Yhteenveto 1 p. 2005.
61 KATASONOV, ARTEM, Dependability aspects in the development and provision of location-based services. 157 p. Yhteenveto 1 p. 2006.
62 SARKKINEN, JARMO, Design as discourse: Representation, representational practice, and social practice. 86 p. (189 p.) Yhteenveto 1 p. 2006.
63 ÄYRÄMÖ, SAMI, Knowledge mining using robust clustering. 296 p. Yhteenveto 1 p. 2006.
64 IFINEDO, PRINCELY EMILI, Enterprise resource planning systems success assessment: An integrative framework. 133 p. (366 p.) Yhteenveto 3 p. 2006.
65 VIINIKAINEN, ARI, Quality of service and pricingin future multiple service class networks. 61 p. (196 p.) Yhteenveto 1 p. 2006.
66 WU, RUI, Methods for space-time parameter estimation in DS-CDMA arrays. 73 p. (121 p.) 2006.
67 PARKKOLA, HANNA, Designing ICT for mothers. User psychological approach. – Tieto- ja viestintätekniikoiden suunnittelu äideille. Käyttäjäpsykologinen näkökulma. 77 p. (173 p.) Yhteenveto 3 p. 2006.
68 HAKANEN, JUSSI, On potential of interactive multiobjective optimization in chemical process design. 75 p. (160 p.) Yhteenveto 2 p. 2006.
69 PUTTONEN, JANI, Mobility management in wireless networks. 112 p. (215 p.) Yhteenveto 1 p. 2006.
70 LUOSTARINEN, KARI, Resource , management methods for QoS supported networks. 60 p. (131 p.) 2006.
71 TURCHYN, PAVLO, Adaptive meshes in computer graphics and model-based simulation. 27 p. (79 p.) Yhteenveto 1 p.
72 ZHOVTOBRYUKH, DMYTRO, Context-aware web service composition. 290 p. Yhteenveto 2 p. 2006.

73 KOHVAKKO, NATALIYA, Context modeling and utilization in heterogeneous networks. 154 p. Yhteenveto 1 p. 2006.
74 MAZHELIS, OLEKSIY, Masquerader detection in mobile context based on behaviour and environment monitoring. 74 p. (179 p). Yhteenveto 1 p. 2007.
75 SILTANEN, JARMO, Quality of service and dynamic scheduling for traffic engineering in next generation networks. 88 p. (155 p.) 2007.
76 KUUVA, SARI, Content-based approach to experiencing visual art. - Sisältöperustainen lähestymistapa visuaalisen taiteen kokemiseen. 203 p. Yhteenveto 3 p. 2007.
77 RUOHONEN, TONI, Improving the operation of an emergency department by using a simulation model. 164 p. 2007.
78 NAUMENKO, ANTON, Semantics-based access control in business networks. 72 p. (215 p.) Yhteenveto 1 p. 2007.
79 WAHLSTEDT, ARI, Stakeholders' conceptions of learning in learning management systems development. - Osallistujien käsitykset oppimisesta oppimisympäristöjen kehittämisessä. 83 p. (130 p.) Yhteenveto 1 p. 2007.
80 ALANEN, OLLI, Quality of service for triple play services in heterogeneous networks. 88 p. (180 p.) Yhteenveto 1 p. 2007.
81 NERI, FERRANTE, Fitness diversity adaptation in memetic algorithms. 80 p. (185 p.) Yhteenveto 1 p. 2007.
82 KURHINEN, JANI, Information delivery in mobile peer-to-peer networks. 46 p. (106 p.) Yhteenveto 1 p. 2007.
83 KILPELÄINEN, TURO, Genre and ontology based business information architecture framework (GOBIAF). 74 p. (153 p.) Yhteenveto 1 p. 2007.
84 YEVSEYEVA, IRYNA, Solving classification problems with multicriteria decision aiding approaches. 182 p. Yhteenveto 1 p. 2007.
85 KANNISTO, ISTO, Optimized pricing, QoS and segmentation of managed ICT services. 45 p. (111 p.) Yhteenveto 1 p. 2007.
86 GORSHKOVA, ELENA, A posteriori error estimates and adaptive methods for incompressible viscous flow problems. 72 p. (129 p.) Yhteenveto 1 p. 2007.
87 LEGRAND, STEVE, Use of background real-world knowledge in ontologies for word sense disambiguation in the semantic web. 73 p. (144 p.) Yhteenveto 1 p. 2008.
88 HÄMÄLÄINEN, NIINA, Evaluation and measurement in enterprise and software architecture management. - Arviointi ja mittaaminen kokonais- ja ohjelmistoarkkitehtuurien hallinnassa. 91 p. (175 p.) Yhteenveto 1 p. 2008.
89 OJALA, ARTO, Internationalization of software firms: Finnish small and medium-sized software firms in Japan. 57 p. (180 p.) Yhteenveto 2 p. 2008.
90 LAITILA, ERKKI, Symbolic Analysis and Atomistic Model as a Basis for a Program Comprehension Methodology. 321 p. Yhteenveto 3 p. 2008.
91 NIHTILÄ, TIMO, Performance of Advanced Transmission and Reception Algorithms for High Speed Downlink Packet Access. 93 p. (186 p.) Yhteenveto 1 p. 2008.
92 SETÄMAA-KÄRKKÄINEN, ANNE, Network connection selection-solving a new multiobjective optimization problem. 52 p. (111p.) Yhteenveto 1 p. 2008.
93 PULKKINEN, MIRJA, Enterprise architecture as a collaboration tool. Discursive process for enterprise architecture management, planning and development. 130 p. (215 p.) Yhteenveto 2 p. 2008.
94 PAVLOVA, YULIA, Multistage coalition formation game of a self-enforcing international environmental agreement. 127 p. Yhteenveto 1 p. 2008.
95 NOUSIAINEN, TUULA, Children's involvement in the design of game-based learning environments. 297 p. Yhteenveto 2 p. 2008.
96 KUZNETSOV, NIKOLAY V., Stability and oscillations of dynamical systems. Theory and applications. 116 p. Yhteenveto 1 p. 2008.
97 KHRIYENKO, OLEKSIY, Adaptive semantic Web based environment for web resources. 193 p. Yhteenveto 1 p. 2008.
98 TIRRONEN, VILLE, Global optimization using memetic differential evolution with applications to low level machine vision. 98 p. (248 p.) Yhteenveto 1 p. 2008.
99 VALKONEN, TUOMO, Diff-convex combinations of Euclidean distances: A search for optima. 148 p. Yhteenveto 1 p. 2008.
100 SARAFANOV, OLEG, Asymptotic theory of resonant tunneling in quantum waveguides of variable cross-section. 69 p. Yhteenveto 1 p. 2008.
101 POZHARSKIY, ALEXEY, On the electron and phonon transport in locally periodical waveguides. 81 p. Yhteenveto 1 p. 2008.
102 AITTOKOSKI, TIMO, On challenges of simulation-based globaland multiobjective optimization. 80 p. (204 p.) Yhteenveto 1 p. 2009.
103 YALAHO, ANICET, Managing offshore outsourcing of software development using the ICT-supported unified process model: A cross-case analysis. 91 p. (307 p.) Yhteenveto 4 p. 2009.
104 KOLLANUS, SAMI, Tarkastuskäytänteiden kehittäminen ohjelmistoja tuottavissa organisaatioissa. - Improvement of inspection practices in software organizations. 179 p. Summary 4 p. 2009.
105 LEIKAS, JAANA, Life-Based Design. 'Form of life' as a foundation for ICT design for older adults. - Elämälähtöinen suunnittelu. Elämänmuoto ikääntyville tarkoitettujen ICT tuotteiden ja palvelujen suunnittelun lähtökohtana. 218 p. (318 p.) Yhteenveto 4 p. 2009.

106 Vasilyeva, Ekaterina, Tailoring of feedback in web-based learning systems: Certitude-based assessment with online multiple choice questions. 124 p. (184 p.) Yhteenveto 2 p. 2009.

107 Kudryashova, ElenaV., Cycles in continuous and discrete dynamical systems. Computations, computer assisted proofs, and computer experiments. 79 p. (152 p.) Yhteenveto 1 p. 2009.

108 Blackledge, Jonathan, Electromagnetic scattering and inverse scattering solutions for the analysis and processing of digital signals and images. 297 p. Yhteenveto 1 p. 2009.

109 Ivannikov, Andriy, Extraction of event-related potentials from electroencephalography data. - Herätepotentiaalien laskennallinen eristäminen EEG-havaintoaineistosta. 108 p. (150 p.) Yhteenveto 1 p. 2009.

110 kalyakin, Igor, Extraction of mismatch negativity from electroencephalography data. - Poikkeavuusnegatiivisuuden erottaminen EEG-signaalista. 47 p. (156 p.) Yhteenveto 1 p. 2010.

111 Heikkilä, Marikka, Coordination of complex operations over organisational boundaries. 265 p. Yhteenveto 3 p. 2010.

112 Fekete, Gábor, Network interface management in mobile and multihomed nodes. 94 p. (175 p.) Yhteenveto 1 p. 2010.

113 Kujala, Tuomo, Capacity, workload and mental contents - Exploring the foundations of driver distraction. 146 p. (253 p.) Yhteenveto 2 p. 2010.

114 Lugano, Giuseppe, Digital community design - Exploring the role of mobile social software in the process of digital convergence. 253 p. (316 p.) Yhteenveto 4 p. 2010.

115 Kampylis, Panagiotis, Fostering creative thinking. The role of primary teachers. - Luovaa ajattelua kehittämässä. Alakoulun opettajien rooli. 136 p. (268 p.) Yhteenveto 2 p. 2010.

116 Toivanen, Jukka, Shape optimization utilizing consistent sensitivities. - Muodon optimointi käyttäen konsistentteja herkkyyksiä. 55 p. (130p.) Yhteenveto 1 p. 2010.

117 Mattila, Keijo, Implementation techniques for the lattice Boltzmann method. - Virtausdynamiikan tietokonesimulaatioita Hila-Boltzmann -menetelmällä: implementointi ja reunaehdot. 177 p. (233 p.) Yhteenveto 1 p. 2010.

118 Cong, Fengyu, Evaluation and extraction of mismatch negativity through exploiting temporal, spectral, time-frequency, and spatial features. - Poikkeavuusnegatiivisuuden (MMN) erottaminen aivosähkönauhoituksista käyttäen ajallisia, spektraalisia, aikataajuus - ja tilapiirteitä. 57 p. (173 p.) Yhteenveto 1 p. 2010.

119 Liu, Shenghua, Interacting with intelligent agents. Key issues in agent-based decision support system design. 90 p. (143 p.) Yhteenveto 2 p. 2010.

120 Airaksinen, Tuomas, Numerical methods for acoustics and noise control. - Laskennallisia menetelmiä akustisiin ongelmiin ja melunvaimennukseen. 58 p. (133 p.) Yhteenveto 2 p. 2010.

121 Weber, Matthieu, Parallel global optimization Structuring populations in differential evolution. - Rinnakkainen globaalioptimointi. Populaation rakenteen määrittäminen differentiaalievoluutiossa. 70 p. (185 p.) Yhteenveto 2 p. 2010.

122 Väärämäki, Tapio, Next generation networks, mobility management and appliances in intelligent transport systems. - Seuraavan sukupolven tietoverkot, liikkuvuuden hallinta ja sovellutukset älykkäässä liikenteessä. 50 p. (111 p.) Yhteenveto 1 p. 2010.

123 Viukari, Leena, Tieto- ja viestintätekniikka-välitteisen palvelun kehittämisen kolme diskurssia. - Three discourses for an ICT-service development . 304 p. Summary 5 p. 2010.

124 Puurtinen, Tuomas, Numerical simulation of low temperature thermal conductance of corrugated nanofibers. - Poimutettujen nanokuitujen lämmönjohtavuuden numeerinen simulointi matalissa lämpötiloissa . 114 p. Yhteenveto 1 p. 2010.

125 Hiltunen, Leena, Enhancing web course design using action research . - Verkko-opetuksen suunnittelun kehittäminen toimintatutkimuksen keinoin . 192 p. Yhteenveto 2 p. 2010.

126 Aho, Kari, Enhancing system level performance of third generation cellular networks through VoIP and MBMS services. 121 p. (221 p.). Yhteenveto 2 p. 2010.

127 Häkkinen, Markku, Why alarms fail. A cognitive explanatory model. 102 p. (210 p.). Yhteenveto 1 p. 2010.

128 Pennanen, Anssi, A graph-based multigrid with applications. - Graafipohjainen monihilamenetelmä sovelluksineen. 52 p. (128 p.). Yhteenveto 2 p. 2010.

129 Ahlgren, Riikka, Software patterns, organizational learning and software process improvement. 70 p. (137 p.). Yhteenveto 1 p. 2011.

130 Nikitin, Sergiy, Dynamic aspects of industrial middleware architectures 52 p. (114 p.). Yhteenveto 1 p. 2011.

131 Sindhya, Karthik, Hybrid Evolutionary Multi-Objective Optimization with Enhanced Convergence and Diversity. 64 p. (160 p.). Yhteenveto 1 p. 2011.